UTRECHT UNIVERSITY

Integrating ATES and surface water thermal energy in the optimization approach for 5GDHC

MASTER THESIS

October 14, 2021

Utrecht University

Anko Smit (6658911)
a.j.h.smit@students.uu.nl

Supervisor: Dr. ir. Jesús Rosales Carreón
Second reader: Dr. Wen Liu

Master Thesis Energy Science (GEO4-2510)
Wordcount: 25.893

Abstract

An important role in the decarbonisation of the Dutch urban heating and cooling supply is projected for fifth generation district heating and cooling (5GDHC) systems which include aquifer thermal energy storage (ATES) and surface water thermal energy (SWTE) in their configuration (CE Delft, 2018). Existing 5GDHC optimization approaches are unsuitable for optimizing the design and operation of these systems (Wirtz et al., 2020a; Wirtz et al., 2021). This research aims to fill this gap, by proposing a novel mixed-integer linear programming (MILP) model.

The proposed MILP model is suited for determining the optimal design and operation of the ATES and SWTE systems and the energy conversion units installed in buildings with respect to minimizing total annualized costs. It was created by using the model presented by Wirtz et al. (2021) as starting point. The structure of this model comprises an air-source heat pump, compression chiller and an accumulator tank. These components were removed from the model, while the ATES and SWTE technologies were added. Additionally, a distinction was made between poorly and well insulted buildings. This allows for a better alignment between the required heating supply temperatures and the technologies installed in the buildings.

The novel optimization approach was then applied to a real-world case. This had led to important insights on how the 5GDHC systems with ATES and SWTE should be designed and operated to achieve the lower annualized cost. Finally, the performance of the systems was evaluated with economic, technical and environmental performance indicators and compared to alternative heating and cooling concepts. The 5GDHC system with ATES and SWTE shows a cost reduction of 0.6%, has a lower primary energy requirement (-80.2%) and causes less CO_2-emissions (-81.6%) compared to a reference system with stand-alone natural gas installations. Compared to a conventional district heating operating at 70 °C, the system leads to substantially less total annualized costs (-15.4%). Also, savings are achieved with regard to primary energy requirement (-32.4%) and annual CO_2-emissions (-31.6%).

Contents

List of Figures **3**

List of Tables **4**

Nomenclature **5**

1 Introduction **7**
1.1 Problem definition 8
1.2 Research aim & Research questions 9

2 Theoretical background **11**
2.1 District heating and cooling 11
2.2 Aquifer thermal energy storage technology 16
2.3 Surface water thermal energy 20
2.4 Optimization of district heating and cooling systems 22
2.5 Evaluation of the existing design optimization approach 23

3 Research strategy and methodology **31**
3.1 Phase I: Development of optimization model for 5GDHC systems with ATES and SWTE 31
3.2 Phase II: Identification of the optimal design and operation of 5GDHC system with ATES and SWTE 33
3.3 Phase III: Assessment of techno-economic feasibility 35

4 Results **38**
4.1 Novel optimization model 38
4.2 Application of novel optimization model to a real-world case 48
4.3 Assessment of techno-economic feasibility 55

5 Discussion **60**
5.1 Theoretical implications 60
5.2 Societal implications 61
5.3 Limitations and future research 61

6 Conclusion **65**

Appendices **74**

A Expert interviews **74**

B Decision variables **77**

C Input parameters **79**

D Assessment of techno-economic feasibility **84**

List of Figures

1 Evolution of DHC systems . . . 11
2 Heating, cooling and aggregated demand curves for an individual customer . . 14
3 Impression of the Mijnwater system . . . 16
4 Operating principles of BTES systems during cold demand and heating demand 17
5 Operating principles of ATES systems during cooling demand and heating demand . . . 17
6 Temperature ranges for heat extraction and cold extraction in SWTE systems . 21
7 Operation of SWTE and ATES at different surface water temperatures . . . 22
8 Energy system structure with energy hub, accumulator tank and building energy system that is being optimized in the existing design optimization approach . . 24
9 Schematic overview of research strategy steps and corresponding methods. . . . 31
10 Flow diagram of model development process. . . . 32
11 Methods for developing space heating, domestic hot water and cooling profiles. 34
12 Energy system structure with energy hub and building energy systems that is being optimized in the novel design optimization approach. . . . 38
13 Cumulated space heating, DHW and cooling demands of the 15 buildings considered in the case study . . . 48
14 Geographical arrangement of the 15 buildings and their annual space heating, DHW and cooling demands. . . . 49
15 Surface water temperature profile . . . 49
16 Costs structure of the 5GDHC system with ATES and SWTE . . . 50
17 Balancing of the thermal demands in 5GDHC system . . . 52
18 Operation of ATES and SWTE systems . . . 53
19 Operation of BESs in poorly insulated buildings during the day of the peak heating demand. . . . 55
20 Performance indicators of the three heating and cooling concepts . . . 56
21 Influence of interest rate on TAC. . . . 58
22 Influence of electricity price on TAC. . . . 58
23 Influence of natural gas price on TAC. . . . 59
C.1 Plots with corresponding trendlines used to determine specific and fixed investment costs for ATES, SWTE and HP . . . 80

List of Tables

1 Simultaneity factors space heating 35
2 Values for sensitivity analysis 37
3 Cumulated capacities and operation of technologies installed in BESs 50
4 Total annualized costs and investment costs of the heating and cooling concepts 56
B.1 Decision variables existing optimization model 77
B.2 Decision variables included in the constructed optimization model. 78
C.1 Technical parameters for calculation of COPs of HPs, BHPs and CCs 79
C.2 Economic parameters for the generation and storage devices considered in the energy hub and building energy systems. 79
C.3 Economic parameters for IDPs, IHPs and HIUs 80
C.4 Prinspipe type 1 characteristics 81
C.5 Economic parameters for the pipes and hydraulic pumps 82
C.6 Pipe geometries and costs 5GDHC network. 83
C.7 Characteristics of buildings considered in the case study. 83
D.1 Decision variables included in the constructed optimization model for the conventional DH system operating at 70 °C. 85
D.2 Pipe geometries and costs conventional DH network. 90
D.3 Economic parameters for GBs and ACs 90

Nomenclature

Abbreviations

5GDHC	Fifth Generation District Heating and Cooling
AC	Air Conditioner
ACC	Accumulator tank
ASHP	Air-Source Heat Pump
ATES	Aquifer Thermal Energy Storage
BES	Borehole Thermal Energy Storage
BES	Building Energy System
BHP	Booster Heat Pump
CC	Compression Chiller
CHP	Combined Heat and Power
COP	Coefficient Of Performance
DH	District Heating
DHC	District Heating and Cooling
DHW	Domestic Hot Water
DRC	Direct Cooling
EH	Energy Hub
GB	Gas Boiler
HIU	Heat Interface Unit
HP	Heat Pump
IDP	Internal Distribution Pipe
IHP	Internal Hydraulic Pump
LP	Linear Programming
MILP	Mixed-Integer Linear Programming
O&M	Operation and maintenance
PER	Primary Energy Requirement
PV	Photovoltaic
SoC	State of Charge
SWTE	Surface Water Thermal Energy
TA	Technical Area
TAC	Total Annualized Costs
TES	Thermal Energy Storage
UTES	Underground Thermal Energy Storage

Indices and Sets

b $\in B$	Buildings
i $\in I$	Set of temperature intervals
k $\in K$	Technologies
s $\in s$	Network segments
t $\in T$	Time steps

Parameters

η	Efficiency
λ	Specific thermal conductivity
ΔT_{CE}	Temperature change during cold extraction
$\Delta T_{HE,max}$	Maximum allowable temperature change during heat extraction
ϕ_v	Volumetric flow
ϕ_{loss}	Loss factor
ρ	Density
a_{inv}	Capital recovery factor
c_p	Specific heat capacity
D_i	Inner diameter insulation layer
d_i	Inner pipe diameter
D_o	Outer diameter insulation layer
e	Specific electricity use
f	Friction factor
f_{om}	Cost share for operation and maintenance
i	Specific investment
p	Specific price
R_{th}	Thermal radius
v	Velocity
A	Surface of water body
EF	Emission Factor
h	Distance between surface and centre of distribution pipe
kA	Thermal transmittance
L	Length
M	Big-M coefficient
PEF	Primary Energy Factor
R	Thermal resistance
r	Interest rate

s	Distance warm and cold distribution pipe
V	Volume
z	Thermal energy exchange

Sub- and Superscripts

aq	aquifer
c	cooling
cap	capacity
CE	cold extraction
ch	charge
ch	cold well to hot well
cp	cold pipe
cw	cold well
dch	discharge
dec	decrease
dem	demand
el	electric
h	heating
hc	hot well to cold well
HE	heat extraction
HEX	Heat exchanger
hw	hot well
i	insulation
inc	increase
int	interval
max	maximum
min	minimum
netw	network
nom	nominal
op	operational
ps	pipe and soil
res	residual
rp	return pipe
s	soil
sh	space heating
sp	supply pipe
sup	supply
SW	Surface Water
th	thermal
var	variable
w	water
wp	warm pipe

Variables

$\bar{T}$	Mean temperature
$\dot{Q}$	Thermal power
θ	Binary variable (temperature interval)
C	Annualized costs
cap	Capacity
E	Electric energy
G	Gas energy
I	Investment costs
P	Power
Q	Thermal energy
SoC	State of Charge
T	Temperature
x	Binary variable (SWTE operation)
y	Binary variable (ATES operation)

1 Introduction

The decision of the Dutch government to stop the natural gas extraction in the province of Groningen and the published national Climate Agreement will have far-reaching consequences for urban energy systems in the Netherlands (Boesten et al., 2019; Ministry of Economic Affairs and Climate Policy, 2019). More than seven million residences and over one million utility buildings are currently still dependent on natural gas for their space heating and domestic hot water (DHW) supply (Ministry of Economic Affairs and Climate Policy, 2019). To make the transition towards sustainable heating systems more manageable, the Dutch government opted for a neighbourhood-oriented approach. Optimal energy systems that are low in greenhouse gas emissions and natural gas free need to be developed for each individual neighbourhood based on specific characteristics like building types, heating and cooling demands and the availability of potential heat sources (Ministry of Economic Affairs and Climate, 2018).

Many of the possible alternative systems to provide space heating and DHW are all-electric solutions that operate using solar panels, infrared heating and heat pumps. These concepts require a significant amount of space and are therefore difficult to implement in densely built urban areas (LenteAkkoord Zeer Energiezuinige Nieuwbouw, 2018; RVO, 2018b). For these regions, district heating (DH) is identified as the most viable solution (Lake et al., 2017; Ministry of Economic Affairs and Climate Policy, 2019; Stratelligence, 2020). Traditional DH systems supply heat to a group of buildings, neighbourhoods or entire cities by distributing hot water or steam to consumers through a pipe network. About 4% of the heat demand of the built environment in the Netherlands is currently covered in this way (Boesten et al., 2019). Nevertheless, existing DH networks are generally fed by fossil based high-temperature sources like combined heat and power (CHP) plants, waste incinerators and industrial waste heat. These energy sources are scarce in the Netherlands and often not available in the immediate vicinity of urban areas (CE Delft, 2019b). Besides, operating at high temperatures results in significant heat losses and high installation costs, which comprise the economic viability (van Vliet et al., 2016). Traditional DH systems are also unable to provide cooling, for which demand is growing as a result of climate change, higher insulation standards and urban heat island effects (Larsen et al., 2020; Roossien et al., 2020). Thus, there is a need for DH systems that can provide both heating and cooling without the use of high-temperature heat sources.

As a result of this need, current research on DH systems is focused on so-called fifth generation district heating and cooling (5GDHC) systems (Buffa et al., 2019). In 5GDHC systems, buildings are connected to a network consisting of a warm and a cold pipe. The temperature difference between the two pipes is typically 5-10 K, while the temperatures of both pipes are at near-ground temperatures (5-35 °C) (Wirtz et al., 2020a). This limits distribution heat losses, makes the integration of low temperature heat sources possible and allows for bi-directional exchange of heat and cold between buildings (Boesten et al., 2019; Buffa et al., 2020). Heat pumps in buildings use water from the warm pipe as heat source and raise the temperature to the level required for space heating and DHW. The cooled water is then discharged into the cold pipe. In case of cooling demand, chillers use the 5GDHC system as heat sink. Water from the cold pipe is heated during the cooling process and injected into the warm pipe (Buffa et al., 2019). A cooling demand therefore results in heat being supplied to the network and vice-versa (Boesten et al., 2019).

The use of thermal energy storage is crucial for the effective operation of 5GDHC systems (Boesten et al., 2019; Revesz et al., 2020). Although the bi-directional exchange of heat and cold between buildings can balance out a substantial amount of the thermal energy demand, there will still be a temporal mismatch between demand and supply of heat and cold (Revesz et al., 2020). On warm days, the cooling demand of a group of buildings will exceed the heating demand. This will lead to a surplus of heat that can not be used directly. In case the heating demand is dominant, a surplus of cold will be generated (Boesten et al., 2019). Seasonal thermal energy storage allows for these surpluses of heat and cold to be used to cover demands in opposing seasons. Aquifer thermal energy storage (ATES) is considered the most effective solution for this purpose due to its advantages of easy implementation, large storage capacity and good economy (Gao et al., 2017). The Netherlands is recognized as the global technological leader on this technology (Fleuchaus et al., 2018).

Furthermore, short-term energy storage in buffer vessels in buildings can be used to supply part of the peak demand. When buffers are properly sized, required heat pump and network pipe capacities can be reduced significantly. This has a major impact on the investment costs of a 5GDHC system (Boesten et al., 2019). In case there is a difference in heating and cooling demand in the long term, an additional thermal energy source is required to supply heat or cold to the system (Buffa et al., 2019). A technology with high potential to supply heat and cold, especially in the Netherlands, is surface water thermal energy (SWTE). CE Delft (2018) concluded that about 43% of the total heating demand of the Dutch built environment can by provided when SWTE and ATES systems are integrated in DH systems. However, as far as we know, no 5GDHC systems with ATES and SWTE are currently installed.

1.1 Problem definition

Despite the recognized potential of 5GDHC systems with ATES and SWTE, only a few publications on this subject are available. Besides, the knowledge about the 5GDHC technology is primarily clustered in a few companies (Bünning et al., 2018; Revesz et al., 2020). Several pilot projects have proven that 5GDHC principles can be applied to provide heating and cooling in large scale districts (Bünning et al., 2018). However, more research on optimization approaches at the design and operation level is necessary to ensure the widespread implementation of the technology in Dutch urban energy systems (Ruesch & Evins, 2014). It is currently unclear how heat pumps, buffer vessels, network pipes, SWTE installations and ATES systems can be sized and operated optimally to achieve the lowest costs.

To our knowledge, only two optimization models for 5GDHC systems have been described in literature. Wirtz et al. (2020a) presented an optimization model based on Linear Programming (LP) to determine the optimal selection and sizing of the different components of 5GDHC systems with respect to annualized costs. However, the proposed model is based on the integration of non-renewable thermal energy generation units and does not consider the use of seasonal thermal energy storage. The non-renewable generation units comprise a gas-fired CHP unit, a gas boiler, an electrical boiler and a cooling tower that can be switched on and off depending on the demand. When SWTE is used as energy source, the water temperature determines how much heat or cold can be extracted (Stowa, 2017). This requires a different optimization approach. Moreover, constant network temperatures are assumed in the model. In reality, the temperatures of the hot and cold pipe in a 5GDHC system may fluctuate over time (Roossien et al., 2020).

Wirtz et al. (2021) presented a mixed-integer linear program (MILP) to optimize the operation of 5GDHC systems. The model was adopted from Wirtz et al. (2020a) and allows for optimizing network temperatures and the operation of thermal energy generation and storage units. An air-source heat pump (ASHP) and compression chiller (CC) that can respectively extract heat and cold from the ambient air are considered, as well as a short-term thermal storage unit. Although this model can be considered an improvement compared to the model presented by Wirtz et al. (2020a), it cannot be used for the optimization of 5GDHC system with ATES and SWTE. This is because the working principles of ATES and SWTE are different from those of the technologies considered in the model. Furthermore, the model can only be used to optimize the operation of a 5GDHC system and not to determine the optimal capacities of the system's components (Wirtz et al., 2021). The existing optimization approaches should therefore be modified to enable the design and operation optimization of 5GDHC systems with ATES and SWTE.

1.2 Research aim & Research questions

1.2.1 Research aim

The main aim of this research is to develop an optimization model for designing and operating 5GDHC systems which include ATES and SWTE in their configuration.

1.2.2 Research question

The main research question is therefore as follows:
How to develop an optimization model for designing and operating 5GDHC systems which include ATES and SWTE in their configuration?

1.2.3 Sub-questions

Three sub-research questions are introduced to help answering the main research question:

SQ. 1) What supplementary constraints are required to integrate ATES and SWTE into the current optimization approach?

The MILP model developed by Wirtz et al. (2021) aims to minimize operational costs, while satisfying a set on constraints. To be able to integrate ATES and SWTE in the optimization approach, understanding of what supplementary constraints are needed is required. After answering this sub-question, the novel optimization approach can be developed.

SQ. 2) What is the most cost-effective design and operation of a 5GDHC system with ATES and SWTE for a real-world case?

The novel optimization model can then be applied to a real-world case. By answering this sub-research question, insights into the optimal design and operation of 5GDHC systems with respect to minimizing costs will be obtained. This includes the sizing and operation of the different components in the system, as well as the optimal network temperatures. As no 5GDHC systems with ATES and SWTE are currently installed to our knowledge, these insights will be essential.

SQ. 3) How does the 5GDHC solution compare to alternative heating and cooling concepts in terms of annualised costs, primary energy requirements and annual CO_2-emissions?

After the novel optimization approach is applied to a real-world case, the 5GDHC solution can be compared to alternative concepts in terms of annualised costs, primary energy requirements and annual CO_2-emissions. The techno-economic feasibility of 5GDHC systems with ATES and SWTE can be assessed in this way.

2 Theoretical background

This chapter starts with an overview of district heating and cooling systems. This is followed by a description of the working principles, network design principles and state-of-the-art of 5GDHC systems. Next, the ATES and SWTE technologies are discussed. An overview of optimization approaches for conventional DH system is provided subsequently. Finally, an evaluation of the optimization approach presented by Wirtz et al. (2021) is performed.

2.1 District heating and cooling

The European Commission defines district heating and district cooling as the distribution of thermal energy in the form of steam, hot water or chilled liquid, from a central source of production through a network to multiple buildings or sites, for the use of space or process heating or cooling (European Commission, 2010). District heating and cooling (DHC) systems have evolved radically over the years, with the introduction of 5GDHC systems as the latest development (von Rhein et al., 2019). This evolution is illustrated in Figure 1. The first three generations operate at high supply temperatures using steam and pressurized water as heat carrier. In fourth generation DH systems, water is supplied to buildings at temperatures between 40 and 70 °C (Tereshchenko & Nord, 2018). This paves the way for excess heat recovery and the integration of renewables as large-scale solar thermal energy into the network (Lund et al., 2014). Furthermore, lower supply temperatures increase the energy efficiency of DH systems. Distribution heat losses are reduced due to the lower temperature difference with the surroundings (CE Delft, 2018; von Rhein et al., 2019).

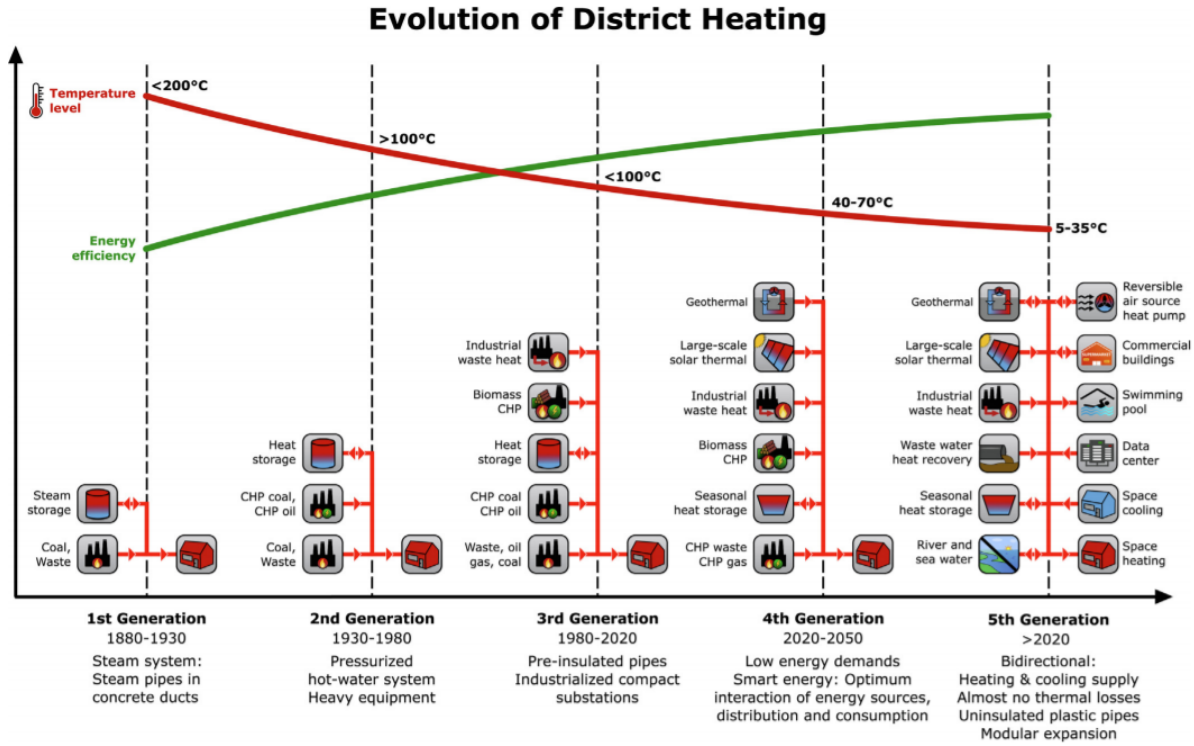

Figure 1: Illustration of the evolution of DHC systems. Retrieved from: (Wirtz et al., 2020b).

Fourth generation DH systems, however, are unable to supply both heating and cooling to buildings using the same pipes (Buffa et al., 2019). In 5GDHC systems, supply temperatures are further reduced to 5-35 °C. Operating at these temperature levels allows for the simultaneous supply of both heat and cold, while making the integration of low-temperature thermal energy sources possible (Wirtz et al., 2021). The working principles, design principles and state-of-the-art of 5GDHC systems are described in the next sections.

2.1.1 Working principles of 5GHDC

5GDHC systems operate using two pipes at near-ground temperatures (Wirtz et al., 2020a). These temperatures are not high enough to directly supply heat to buildings. A heat pump should therefore be installed in each building to raise the temperature to the required temperature for space heating and DHW supply (CE Delft, 2018). This required temperature for space heating and DHW supply is dependent on the insulation level and the heating system of the building. For example, a well insulated building with an underfloor heating system can be heated with lower temperatures compared to an outdated building with conventional radiators (CE Delft, 2019b). In case of cooling demand, water from the cold pipe is used as heat sink (Boesten et al., 2019). When the temperature required for cooling is higher than the temperature of the cold pipe, heat can directly be transferred from the building to the network by heat exchangers. However, in case the required cooling temperature is lower than the temperature of the cold pipe, a chiller must be used to reach this temperature (Roossien et al., 2020). In both concepts, water from the cold pipe is warmed up and injected into the warm pipe. As a consequence of this bidirectional principle, cooling consumers can supply buildings with heating demand and vice-versa (Buffa et al., 2019).

The cooling and heating demand of buildings are often not equal to each other and do not occur at the same time. To maintain the temperature levels of the warm and cold pipes, balancing of the network is required (Wirtz et al., 2021). This can be done by connecting thermal energy storage technologies such as ATES, phase change materials and thermochemical storage to the network (Ruesch & Haller, 2017). When cooling demand exceeds the heating demand, excess heat fed into the network can be stored and used at times when the heating demand is dominant. Thermal energy storage can thus be used to balance out the temporal mismatch between heating and cooling supply and demand (Revesz et al., 2020; Ruesch & Haller, 2017). In the event of structural mismatch between demands, the network needs to be heated or cooled by a thermal energy source. Heat can be supplied by geothermal energy and solar thermal collectors, while surface water and ambient air are examples of thermal energy sources that can supply both heat and cold to the network (Roossien et al., 2020).

Another important consideration for designing 5GDHC systems is the integration of short-term storage solutions in buildings (Boesten et al., 2019). 5GDHC systems must be designed to satisfy heating and cooling demands of buildings at all times. The thermal capacity of the network pipes is therefore based on the peak heat and cold extraction from the network (Roossien et al., 2020). However, these peaks can be reduced by using short-term storage solutions. For example, hot and cold water buffer vessels can be used to shift part of the thermal energy demand over time. At times of low demands, the thermal energy is stored in the buffers. The stored thermal energy can then be used during peak demands (Buffa et al., 2020). In this way, network pipe capacities can be reduced which have a major impact on the investment costs (Boesten et al., 2019).

Furthermore, the temperatures of the warm and cold distribution pipes have a large impact on the operation of 5GDHC systems and may fluctuate over time (Wirtz et al., 2021). Firstly, the temperatures of the cold and warm pipe affect the coefficient of performance (COP) of heat pumps and chillers (Elmegaard et al., 2016). Secondly, as mentioned above, the temperature of the cold pipe determines whether chillers are required to provide cooling (Roossien et al., 2020). Furthermore, the network temperatures affect the possibility of connecting thermal energy sources to the network. For example, when the temperature of the warm pipe exceeds the temperature of the thermal energy source, heat cannot be directly supplied to the network (Wirtz et al., 2021). Operating temperatures also influence the thermal energy flows from and to the warm and cold distribution pipes. The larger the temperature difference between the pipes and the soil, the higher the thermal energy flow (Roossien et al., 2020; Wirtz et al., 2021). This issue is discussed in more detail in section 2.1.2. Finally, the amount of thermal energy that can be distributed by the network is determined by the temperature difference between the two pipes. The larger the temperature difference, the higher the thermal capacity of the distribution network (Roossien et al., 2020). It should be noted that the listed effects are partly contradictory. This makes determining optimal network operating temperatures a difficult task (Wirtz et al., 2021). A case study conducted by Wirtz et al. (2021) indicated that optimizing network temperatures results in significant lower operational costs compared to when network temperatures are kept constant.

2.1.2 Network design principles

Designing distribution networks in traditional DH systems is a relatively simple task (Roossien et al., 2020). The required thermal capacity of a traditional distribution network is based on the highest aggregated demand of buildings (Guelpa et al., 2019). In 5GDHC systems, customers can locally exchange heat and cold. This makes it more difficult to calculate the aggregated demand. Using the traditional approach for designing DH systems may therefore lead to underestimation of the required thermal capacity of the network (Roossien et al., 2020; Wirtz et al., 2020b). An example is provided by Roossien et al. (2020). When there is a heating demand of 10 MW and a cooling demand of 8 MW, provision of 2 MW heating is required. Using the traditional approach, the network would be sized based on this 2 MW of thermal power. However, the required thermal energy flow in the network may be up to 10 MW due to the local exchange of heating and cooling.

To determine the required thermal power of a 5GDHC distribution network, modelling of thermal demand curves for individual customers is required. This can be done by aggregation of the heating demand curve subtracted by the cooling demand curve, as shown in Figure 2. The required thermal energy flow in the distribution network for each time interval can then be determined using the thermal demand curves for all customers. The required thermal power of the distribution network equals the highest thermal flow (Roossien et al., 2020).

The inner diameter of the warm and cold pipes (d_i), the velocity at which water flows through the pipes (v) and the temperature difference between the warm and cold pipe (ΔT_{netw}) are the three main parameters that influence the thermal power of a 5GDHC network (P_{th}):

$$P_{th} = \frac{\pi}{4} c_w \rho_w \Delta T_{netw} d_i^2 v \tag{1}$$

with c_w and ρ_w being the specific heat capacity and density of water (Roossien et al., 2020). Another important consideration in designing 5GDHC systems is the pressure drop (Δp) induced

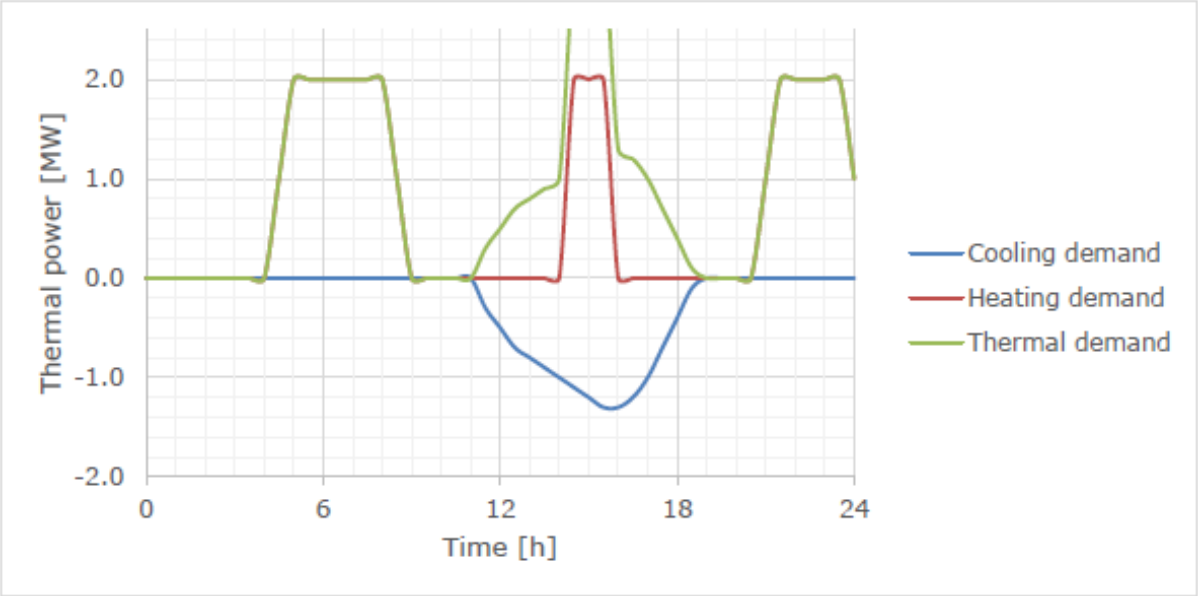

Figure 2: Heating, cooling and aggregated demand curves for an individual customer. Retrieved from: (Roossien et al., 2020).

by frictional losses. When water is flowing through the distribution pipes, frictional losses occur that reduce the pressure of the flow over distant (Nord et al., 2018). To ensure proper functioning of the network, a pump must be engaged to overcome the pressure drop. The Darcy-Weisbach equation can be used to calculate the pressure drop in the distribution pipes:

$$\Delta p = -\frac{8fL}{d_i^5 \pi^2 \rho_w} \left(\frac{P_{th}}{c_w \Delta \mathrm{T_{netw}}} \right)^2 \tag{2}$$

where L and f represent the length and the friction factor of the pipes respectively (Nord et al., 2018; Roossien et al., 2020). In DHC networks, the friction factor is typically in the range of 0.015 to 0.04 (Roossien et al., 2020). It should be noticed that the pressure drop increases exponentially when the diameter of the piper is decreased. This results in an important consideration. Using smaller distribution pipes reduces the investment costs as less digging work needs to be done. On the other hand, a larger pump needs to be installed to overcome the larger pressure drop (Roossien et al., 2020). The required pumping power (P_{pump}) can be calculated with:

$$P_{pump} = \eta_{el} \eta_{pump} \Delta p \phi_v \tag{3}$$

with η_{el} and η_{pump} being the efficiency of the electric motor and the pump efficiency of the pump respectively and ϕ_v the volumetric flow through the pipe (Nord et al., 2018; Roossien et al., 2020).

From Eq. (1), it can be concluded that the temperature difference between the warm and cold pipes influences the thermal capacity of the distribution network. The temperatures of the pipes also affect the thermal distribution losses (Dalla Rosa et al., 2011; Wirtz et al., 2021). As described in section 2.1, distribution heat losses are significantly lower in 5GDHC systems compared to conventional high-temperature DH systems (Wirtz et al., 2020a). However, heat may still flow from or to the warm and cold pipe due to temperature differences with the soil (Dalla Rosa et al., 2011). The heat flow between a single pipe and the soil (P_{ps}) can be calculated

with:

$$P_{ps} = \frac{\Delta T_{ps}}{R_i + R_s} \tag{4}$$

where ΔT_{ps} represents the temperature difference between the pipe and the soil. R_i and R_g represent the thermal resistance of the insulated pipe and the soil respectively (Dalla Rosa et al., 2011; Roossien et al., 2020). The thermal resistance of the insulated pipe is dependent on the inner and outer diameter of the insulation layer (D_i and D_o), the length op the pipe (L) and its specific thermal conductivity (λ_i):

$$R_i = \frac{1}{2\pi\lambda_i L} ln\left(\frac{D_o}{D_i}\right) \tag{5}$$

The thermal resistance of the soil can be calculated using:

$$R_s = \frac{1}{2\pi\lambda_s L} ln\left(\frac{4h}{D_o}\right) \tag{6}$$

with h being the distance between the surface and the centre of the distribution pipe and λ_s being the specific thermal conductivity of the soil (Roossien et al., 2020).

2.1.3 5GDHC state-of-the-art

5GDHC is widely regarded as one of the key technologies to realize the transition towards sustainable heating and cooling systems in the built environment (Bünning et al., 2018). This is primarily due to the key advantages of providing simultaneously both heating and cooling services and the possibility to use low-temperature renewable thermal energy sources (Buffa et al., 2019). However, the 5GDHC technology is currently still at the early stage of development (Revesz et al., 2020). Buffa et al. (2019) performed a statistical analysis on 40 existing 5GDHC systems that are currently in operation in Europe, most of which started as pilot projects. The results show a strong increase in typical scale of 5GDHC systems in the last years. Furthermore, a large variety in exploitation of thermal energy sources can be seen. Most systems operate using renewable sources as seawater, groundwater and rivers, while others use excess heat from data centers or industrial processes (Buffa et al., 2019).

One of the most technologically advanced 5GDHC systems is the Mijnwater system in the Netherlands (Boesten et al., 2019; Buffa et al., 2019). This system, which is located in Heerlen, was originally designed as a DHC system using flooded coal mines as thermal energy source. However, this system was unsustainable in the long term because of depletion of the mine water reservoir (Verhoeven et al., 2014). The system was therefore transformed into a 5GDHC system that operates using residual heat from a data center, supermarkets and small-scale industry. The mines are now used as enormous ATES systems (Boesten et al., 2019; CE Delft, 2018). A simplified visualisation of the Mijnwater system is provided in Figure 3. Clusters grids are connected to a two-pipe backbone via heat exchangers. The clusters are partly balanced internally, which reduces the required capacity of the backbone. Heat pumps and chillers in buildings use the cluster grids as thermal energy source (CE Delft, 2018; Verhoeven et al., 2014). Furthermore, building-level buffer vessels with capacities of 1000-3000 litres are used to provide space heating at peak demands. In the individual buildings, additional booster heat pumps and buffers of 120-200 litres are used to provide DHW (Boesten et al., 2019).

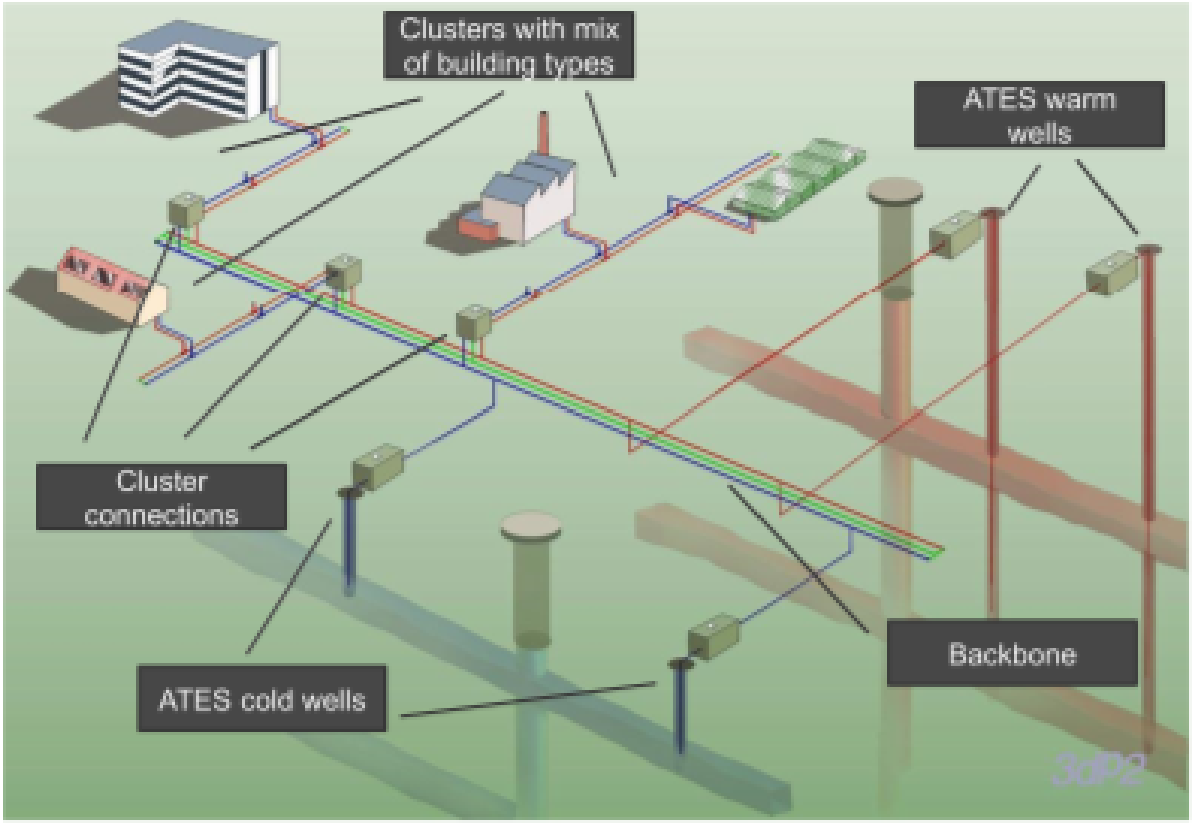

Figure 3: Impression of the Mijnwater system. Retrieved from: (Boesten et al., 2019).

2.2 Aquifer thermal energy storage technology

In this section, operating principles of ATES systems are discussed. Subsequently, advantages and disadvantages of including ATES in 5GDHC systems are described. Factors that affect the energetic performance and that should be considered when designing ATES systems are discussed next. This section ends with an overview of the challenges of designing ATES system in 5GDHC networks.

2.2.1 Operating principles of ATES systems

Buildings in moderate climates generally have a heating demand in winter and a cooling demand in summer (Wirtz et al., 2020b). Many renewable thermal energy sources, on the other hand, are only capable of providing heat in summer and cold in winter. Thermal energy storage (TES) can be used to tackle this seasonal mismatch between thermal energy availability and demand (L. Xu et al., 2018). Underground thermal energy storage (UTES) is a sensible TES technology considered the most effective solution for seasonal TES (Sarbu & Sebarchievici, 2018). This is due to its high storage capacities and storage efficiencies (Lee, 2010). Two main types of UTES systems can be distinguished: closed-loop and open-loop systems (Hendriks et al., 2008). Closed-loop systems, called Borehole thermal energy storage (BTES), consist of multiple vertical u-tubes in the subsurface (Welsch et al., 2018). The operating principles of BTES systems are presented in Figure 4. Excess heat can be stored in the subsurface by circulating hot water through the tubes. The operation is reversed in times of heating demand. By circulating cold water, heat is transferred from the subsurface to the water (Hendriks et al., 2008; Welsch et al., 2018).

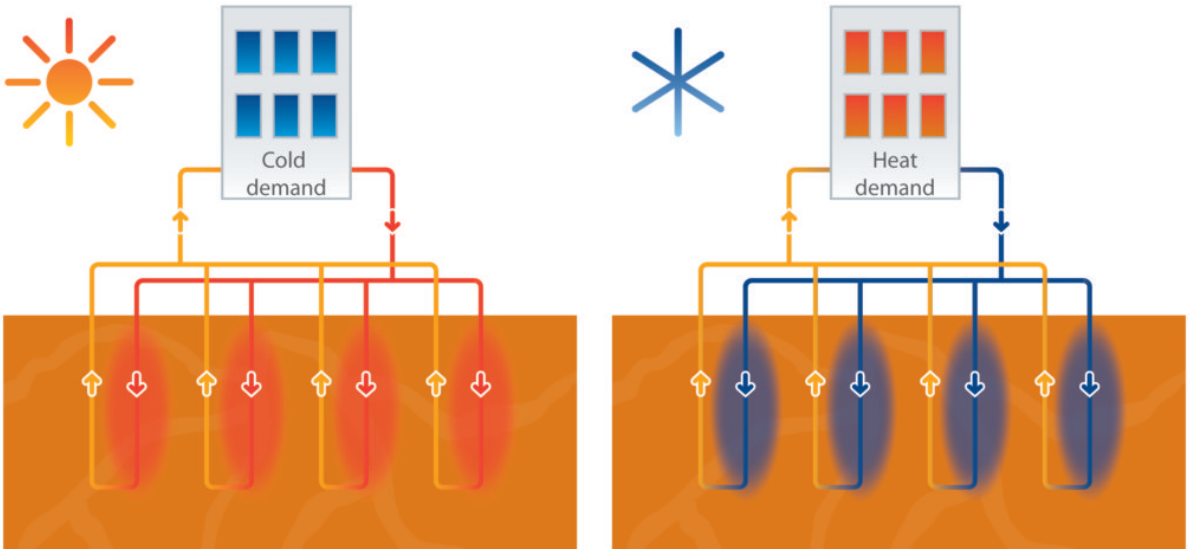

Figure 4: Operating principles of BTES systems during cooling demand (left) and heating demand (right). Retrieved from: (IF Technology, n.d.-b).

ATES systems are open-loop UTES systems characterized by higher storage capacities compared to BTES, making them more suitable for large-scale applications (Matos et al., 2019). The operating principles of ATES systems are presented in Figure 5. ATES systems operate by infiltrating and extracting groundwater from sandy layers in the subsurface (aquifers) through one or more pairs of hot and cold wells (Fleuchaus et al., 2018; Lee, 2010). In the event of heating demand, groundwater is pumped out the hot well. Low-temperature heat is then extracted from the groundwater flow by a heat exchanger and the cooled groundwater is injected into the cold well. The extracted low-temperature heat can be upgraded by central or individual heat pumps and then be used for the provision of space heating and DHW (Schmidt et al., 2018). The system operates the other way around in case of cooling demand. Groundwater is pumped from the cold well, thermal energy is exchanged with the network after which the warmed up water is injected into the hot well (IF Technology, n.d.-a; Lee, 2010; Pellegrini et al., 2019).

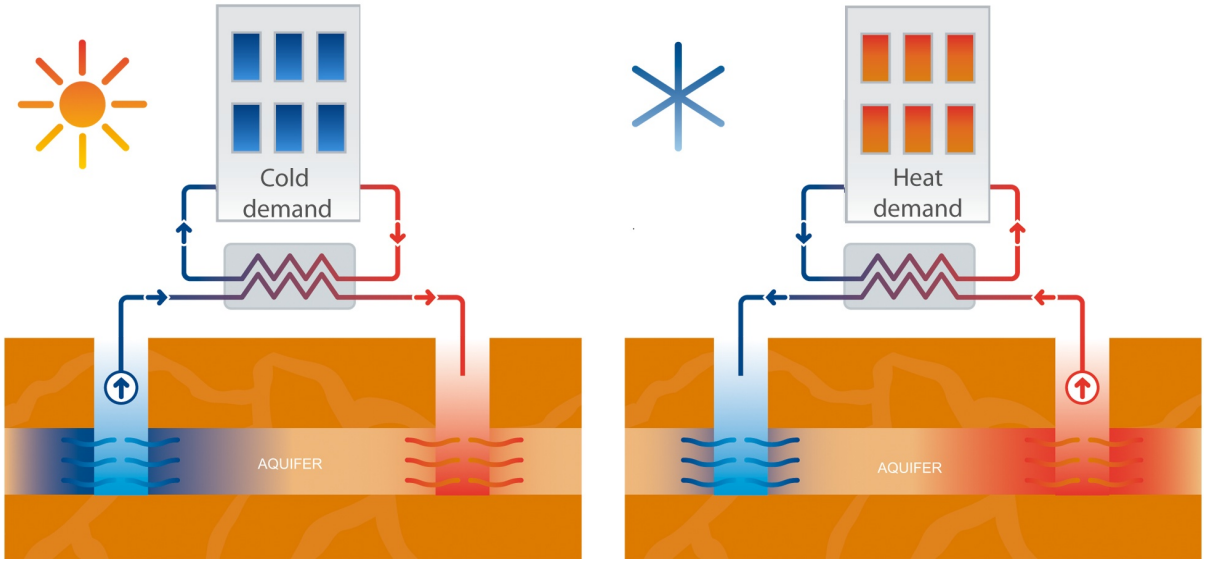

Figure 5: Operating principles of ATES systems during cooling demand (left) and heating demand (right). Retrieved from: (IF Technology, n.d.-a).

2.2.2 (Dis)advantages of pairing ATES with 5GHDC

In addition to tackling the seasonal mismatch between thermal energy supply and demand, there are more advantages of coupling 5GDHC systems with ATES. At first, the capacities of thermal energy generation units can be reduced. At times of low demands, heat or cold can be stored in the ATES system. This stored thermal energy can then be used later during peak demands. This reduces the required capacities of the generation units, while increasing their operating hours (Guelpa & Verda, 2019). Another advantage of using ATES in 5GDHC systems is that the specific installation costs reduce with increasing system size (Fleuchaus et al., 2018). Finally, ATES systems are characterized by relatively low investment costs and short payback periods compared to other seasonal TES technologies (Guelpa & Verda, 2019). According to Gao et al. (2017), payback times of ATES systems can be less than five years.

The listed advantages are accompanied by several drawbacks. At first, integration of ATES in a 5GDHC system may result in increased investment costs. Although the capacities of the thermal energy generation units can be reduced, the associated savings are generally not high enough to compensate for the additional investment costs for the ATES system (Fleuchaus et al., 2018; Guelpa & Verda, 2019). Secondly, the use of ATES requires some specific hydrogeological conditions. ATES requires the presence of an aquifer layer with sufficient thickness (>20 m) and hydraulic conductivity (>1.10 m/s) (Guelpa & Verda, 2019; J. Xu et al., 2014). Two confining rock layers, one on top and one below the aquifer, must be present to effectively store thermal energy (J. Xu et al., 2014). Furthermore, the flow of the groundwater in the aquifer layer should be at low as possible as this effects the energetic performance (Bloemendal & Hartog, 2018). These issues are addressed in more detail in the following section.

2.2.3 Energetic performance

The performance of ATES systems can be described by the recovery efficiency (η_{th}), which is defined as the fraction of thermal energy stored (E_{in}) that can be recovered (E_{out}) (Rostampour et al., 2019). The total amounts of thermal energy stored and recovered are dependent on the pumping rates (Q_{in} and Q_{out}) and the temperature difference between the cold and hot wells ($\Delta T = T_{well,hot} - T_{well,cold}$). According to Bloemendal and Hartog (2018), the recovery efficiency of an ATES well can be described by:

$$\eta_{th}(t_0 \rightarrow t) = \frac{E_{out}}{E_{in}} = \frac{\int_{t_0}^{t} \Delta T_{out} Q_{out} dt}{\int_{t_0}^{t} \Delta T_{in} Q_{in} dt} = \frac{\Delta T_{out} V_{out}}{\Delta T_{in} V_{in}} \tag{7}$$

The recovery efficiency of an ATES well is determined by several factors. At first, part of the stored energy cannot be recovered as a result of heat losses due to the displacement of ambient groundwater (Bloemendal & Hartog, 2018). Secondly, heat losses at the boundaries of stored bodies of thermal energy may occur because of mechanical dispersion and conduction. The thermal radiuses (R_{th}) of the wells therefore influence the recovery efficiency (Bloemendal & Hartog, 2018). According to Doughty et al. (1982), the thermal radius can be defined as:

$$R_{th} = \sqrt{\frac{c_w V_{in}}{c_{aq} \pi L}} \tag{8}$$

with, V_{in} being the yearly storage volume, L the screen length of the well and c_w and c_{aq} the

volumetric heat capacities of water and the aquifer respectively. The required yearly storage volume is dependent on the heating or cooling demand that must be met by the ATES system (Q_{dem}) and can be calculated by:

$$V = \frac{Q_{dem}}{c_w \Delta T \rho_w} \tag{9}$$

where ρ_w represents the density of water (Schüppler et al., 2019). The optimal screen length of a well is a function of V, c_w and c_{aq} and can be estimated with:

$$L = \sqrt[3]{\frac{2.25 c_w V}{c_{aq} \pi}} \tag{10}$$

(Schüppler et al., 2019). To prevent thermal interference between the warm and cold storages of an ATES system, warm and cold wells should be placed at a certain distance from each other (Bloemendal et al., 2014). According to Dutch regulations, a distance of at least three times the thermal radius must be held between wells (Sommer et al., 2015b).

Finally, disproportional large warm or cold zones must be avoided to sustainably exploit an ATES system. When seasonal thermal energy storage and recovery are imbalanced, large areas in the subsurface may become warm or cold which can result in thermal interference between wells (Bloemendal et al., 2014). Since the cooling and heating demands of buildings are generally not equal, supply of heat or cold is required to maintain the thermal balance of an ATES system (Sommer et al., 2015a). In the Netherlands, regulations are in place that require balancing of ATES systems over a period of five years (DWA & IF Technology, 2012).

2.2.4 Challenges of designing ATES in 5GDHC systems

Designing ATES systems is a complex task (Lee, 2010). At first, the presence of a suitable aquifer is a prerequisite for effective operation of an ATES system. Since hydrogeological conditions are highly variable at local scale, site investigations are an essential part in designing an ATES system (Courtois et al., 2007). Geological mapping, test drillings and pumping tests are procedures that can be used to assess hydrogeological conditions as groundwater flow and the porosity of the soil (Lee, 2010). These procedures may be costly and time consuming. In the early design phase, aquifer characterization is therefore often done by using expertise and existing data on hydrogeological conditions (Courtois et al., 2007).

Furthermore, exploitation conditions must be taken into consideration when designing ATES systems (Courtois et al., 2007). Extraction and injection rates and the temperatures in the cold and hot wells influence the energetic performance of an ATES system (Bloemendal & Hartog, 2018; Courtois et al., 2007). These factors should be considered when determining the optimal screen length of the wells and the distance between wells (Bloemendal & Hartog, 2018). Understanding of the working principles and factors that affect the energetic performance of ATES systems is therefore a prerequisite to effectively integrate the technology in the design optimization approach for 5GDHC systems.

2.3 Surface water thermal energy

This section starts with a description of the working principles of SWTE systems. Next, factors that determine the thermal capacity of surface water bodies are discussed. The section is concluded with the design principles of SWTE installations in 5GDHC systems. Since literature on this subject is limited, part of this section is derived from interviews with experts on SWTE systems.

2.3.1 Working principles of SWTE systems

SWTE technology involves the extraction of low-temperature thermal energy from water bodies as lakes, rivers and canals (Stowa, 2017). The temperature of surface water fluctuates significantly due to seasonal influences. Surface water in the Netherlands can reach temperatures of above 20 °C in summer, while it can be frozen in winter (Deltares, 2020). Due to these large fluctuations, both heat and cold can be extracted from surface water to compensate for the mismatch between heating and cooling demands in 5GDHC systems (de Boer et al., 2015).

In case the temperature of the surface water exceeds the network temperature, water can be pumped out of the water body. A heat exchanger can then be used to transport heat from the water to the warm pipe, after which the cooled surface water is reinjected into the water body. Contrariwise, cold can be transported from the surface water to the cold pipe in case of a surplus of cooling demand (de Boer et al., 2015). However, most SWTE systems must be coupled with seasonal storage (Stowa, 2017). Reason for this is that heating demand is dominant during winter, while heat can only be extracted from surface water in summer. And, inversely, cooling demand mainly occurs in summer when the surface water temperature is too high to extract cold (de Boer et al., 2015).

2.3.2 Thermal capacity of surface water bodies

The thermal capacity of a surface water body is mainly dependent on the volume, surface and width of the water body (de Boer et al., 2015; Stowa, 2018). Besides, the flow rate of the water and the distance between the inlet and outlet points of the SWTE installation need to be considered (Syntraal et al., n.d.). The latter is important since the temperature of the water at the injection side of a SWTE installation may not influence the temperature of the water at the extraction side. When this happens, thermal interference takes place between the extracted and injected water. This influences the performance of a SWTE system significantly (Stowa, 2018; Techniplan adviseurs bv, 2018). For flowing water bodies, this means that the injection point of the SWTE system must be located upstream the extraction point. In case of limited flowing and stagnant water, the extraction and injection points must be placed at a sufficient distance of each other to prevent thermal interference (Stowa, 2018).

In SWTE systems, heat can be extracted efficiently when the surface water temperature exceeds 15 °C. The maximum temperature decrease in the heat exchanger in 6 °C, while water cannot be cooled down further than 12 °C (de Boer et al., 2015). Cold can be extracted from a water body when the temperature of the surface water is between 0 and 7 °C. According to Dutch regulations, the temperature of the water may not rise by more than 3 °C (de Boer et al., 2015; Syntraal et al., n.d.). The temperature ranges for heat and cold extraction are presented in Figure 6.

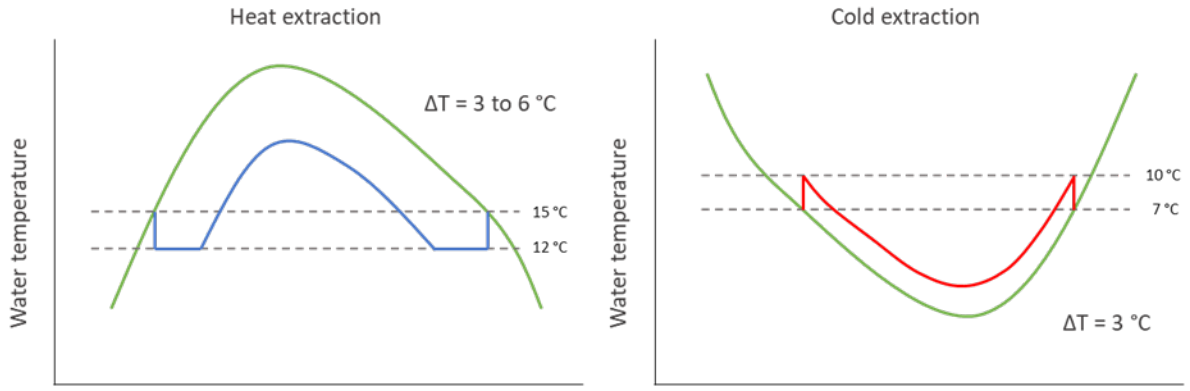

Figure 6: Temperature ranges for heat extraction (left) and cold extraction (right) in SWTE systems. The green lines represent the natural temperature of the surface water. The blue and red lines represent the temperature of the surface water after heat and cold extraction respectively. During heat extraction, the water is cooled down by 3-6 °C. During cold extraction, the temperature of the surface water rises by 3 °C. Adapted from: de Boer et al. (2015).

The allowable temperature change of surface water during heat extraction in a SWTE system (ΔT_{HE}) can be expressed as:

$$\Delta T_{HE} = max\left(min\left(T - T_{min}, \Delta T_{max}\right), 0\right) \tag{11}$$

where T_{min} represents the minimum required water temperature and ΔT_{max} the maximum allowable temperature change (Syntraal et al., n.d.). The amount of heat that can be extracted from a flowing water body ($Q_{th,flowing}$) is a function of the flow rate ($\dot{V}$) and the allowable temperature change:

$$Q_{th,flowing} = \dot{V} \Delta T_{HE} c_w \tag{12}$$

(Syntraal et al., n.d.; Waternet, 2021). For stagnant water bodies, the heat extraction capacity can be calculated by:

$$Q_{th,stagnant} = AZ\Delta T_{HE} \tag{13}$$

where A is the surface of the water body and Z represents the thermal energy exchange between the surface water and the ambient due to solar radiation and wind speed (Syntraal et al., n.d.; Waternet, 2021).

2.3.3 Designing SWTE installations in 5GDHC systems

According to Gertjan de Joode, who is considered an expert on SWTE systems, the first SWTE developed were designed based on the operation of the connected ATES systems (see Appendix A.1). Using the heating and cooling demands of buildings, it was determined how much thermal energy needed to be delivered by the hot and cold wells of the ATES system. Subsequently, the amount of thermal energy that had to be produced by the SWTE system to balance the ATES system was estimated. By taking the period of sufficiently high surface water temperatures into account, the required capacity of the SWTE system was determined (Appendix A.1). Nowadays, the aim is to employ thermal energy sources more efficiently. This means that ATES systems should no longer be seen as systems that supply thermal energy, but rather as storage systems to overcome the temporal mismatch between supply and demand. SWTE systems can supply thermal energy directly to the distribution network. In case the supply exceeds the demand for heat or cold, thermal energy can be stored in the ATES system.

However, this can only take place at times when the temperature of the surface water exceeds the temperature of the hot well of the ATES (Appendix A.1). This phenomenon is presented in Figure 7.

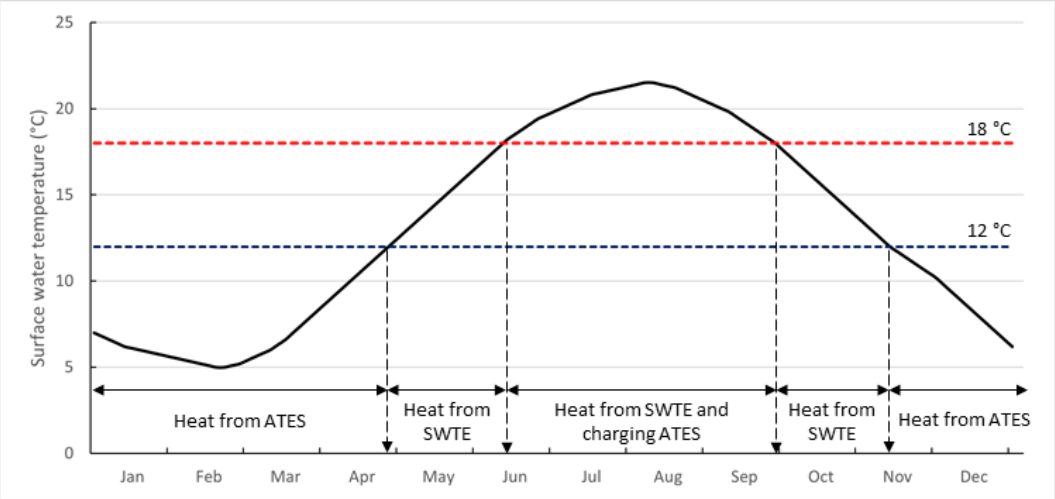

Figure 7: Operation of SWTE and ATES at different surface water temperatures. Adapted from: Eteck (2021).

When the surface water temperature is below to 15 °C, which is the minimum temperature required for heat extraction, all heat must be delivered by the ATES system. In case the temperature of the surface water is between 15 and 18 °C, the SWTE systems can deliver heat to the distribution network. However, these temperatures are not high enough to store heat in the ATES system. This can only happen when the surface water temperature exceeds the temperature of the hot well. Regarding dimensioning SWTE systems, the capacity must be sufficient to meet the thermal energy demand during spring and summer. At the same time, the installed capacity should be high enough the charge the ATES system during summer (Appendix A.1).

Moreover, Gertjan de Joode indicated that the filter type is an important aspect to consider when designing SWTE systems (Appendix A.1). The required type of filter is dependent on the water quality. For example, brackish, fresh and salt water need different types of filters. Since the costs vary significantly between filter types, this impacts the economic feasibility of SWTE systems. It should be noted that installing a more expensive filter increases the investment costs, but lowers the maintenance costs. As the maintenance costs are often the determining factor for the feasibility, the type of filter is an important consideration (Appendix A.1).

2.4 Optimization of district heating and cooling systems

As mentioned in section 1.1, optimization approaches for 5GDHC systems are rarely addressed in literature. Nevertheless, holistic optimization approaches for conventional DH systems have been widely discussed (Wirtz et al., 2021). Mathematic optimization, in the form of LP and mixed-integer linear programs (MILP), is considered the most suitable approach in this field (Wirtz et al., 2020a). Sameti and Haghighat (2017) presented a review on optimization approaches for conventional DH systems. They concluded that MILP is the most applied method, while objective functions are typically: minimizing CO_2-emissions, investment costs and operational costs and maximizing the exploitation of renewable thermal energy sources.

Mehleri et al. (2013) developed a MILP model to determine the optimal design of DH systems for the Greek residential sector. An optimal set of technologies, including micro-CHPs, boilers and thermal storages, is selected for each building. This is done by minimizing total energy costs while satisfying the electricity and heat demands. Several other authors presented similar optimization approaches (Omu et al., 2013; Wouters et al., 2014; Q. Wu et al., 2016). As far as known, only one scientific publication addresses the optimization a of DH system with seasonal thermal energy storage in an ATES system. Buoro et al. (2014) presented an algorithm based on a MILP model to optimize a DH system with solar heating and seasonal thermal energy storage. However, the model assumes specific heat storage costs of $€150/m^3$ (Buoro et al., 2014). In reality, the costs for ATES systems do not only depend on the storage size, but also on site-specific geological conditions as aquifer thickness and depth (Fleuchaus et al., 2018). Regarding SWTE systems, no studies were found that consider this technology in the optimization of conventional DH systems.

Furthermore, none of the aforementioned studies considers district cooling and the use heat pumps for waste heat recovery. Optimization approaches for conventional DHC systems have been proposed by Wouters et al. (2015) and Yang et al. (2015). However, in these approaches, DHC is supplied by two separate circuits without the use of heat pumps. As this fundamentally differs from the discussed bi-directional working principles of 5GDHC, these approaches are unsuitable for the optimization of 5GDHC networks (Wirtz et al., 2020a).

2.5 Evaluation of the existing design optimization approach

This section entails the evaluation of the design optimization approach presented by Wirtz et al. (2021). This is done by using a comprehensive approach for evaluating design optimization models developed by Herrmann (2007). With this approach, design optimization models can be evaluated along the attributes: scope, objective function, variable set and model structure. The deficiencies of the existing design optimization approached are discussed at the end of the section.

2.5.1 Model scope

The scope of a design optimization model describes the object or system that is being optimized. In the optimization model presented by Wirtz et al. (2021), the energy system structure that is being optimized consists of a central energy hub (EH), an accumulator tank (ACC) and a building energy system. The structure of the 5GDHC system is visualized in Figure 8. A compression chiller (CC) and an air source heat pump (ASHP) together form the EH and are used for balancing the residual demands in the 5GDHC system. In case of dominant heating demand, the ASHP can be used to fed heat into the network. When the cooling demand is dominant, the CC extracts cold from the ambient air and supplies it to the network. The ACC is a water tank in which thermal energy can be stored with the function of balancing the heating and cooling demands of buildings. The top of the ACC is hydraulically connected to the warm pipe of the 5GDHC distribution network, while the bottom is connected to the cold pipe. Furthermore, a connection with the power grid and photovoltaic (PV) modules are included in the energy system structure.

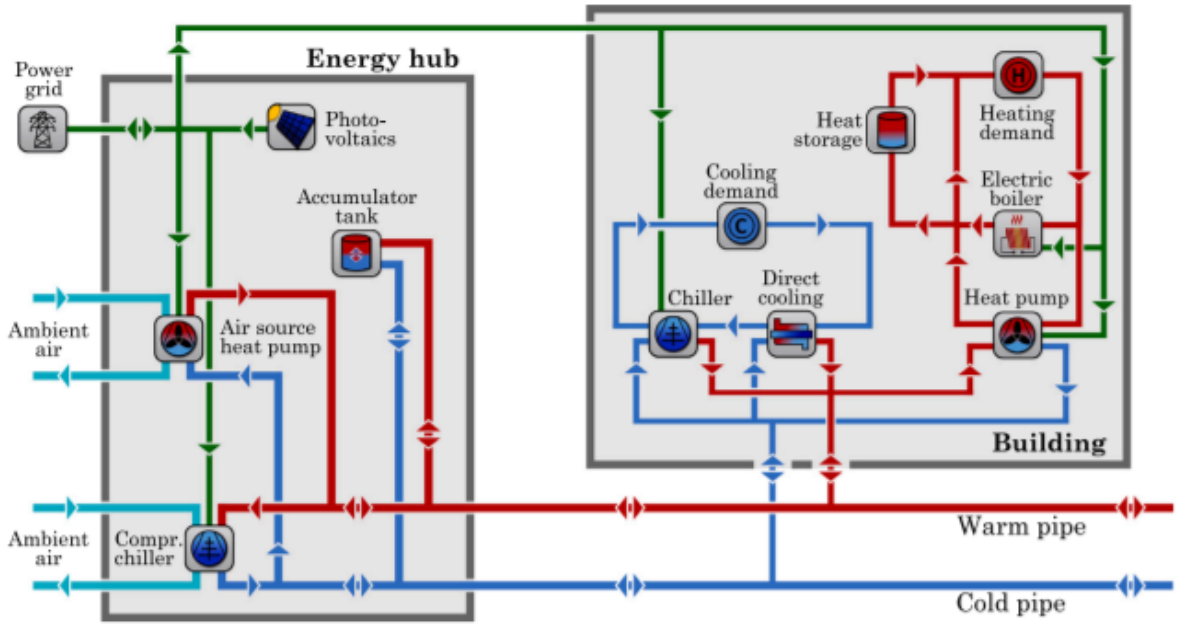

Figure 8: Energy system structure with energy hub, accumulator tank and building energy system that is being optimized in the existing design optimization approach. Green, red and blue arrows indicate the electricity, heat and cold flows through the system respectively. Retrieved from: Wirtz et al. (2021).

The buildings energy system (BES) that is installed in each building is shown in the right-hand side of Figure 8. A heat pump (HP) connected to the 5GDHC network pipes is used to cover the building's heating demand. Additionally, it is considered than an electric boiler can be used to store heat in a water buffer vessel. The stored heat can be used at times of peak heating demands. The cooling demand of buildings can be covered in two ways. At first, a CC is installed in each building to provide active cooling. The CC extracts cold from the cold pipe of the 5GDHC to cool the building. During this process, water is heated and it is discharged into the warm pipe of the 5GDHC network. Secondly, the cooling demand of buildings can be covered by a heat exchanger. When the required supply temperature of the cooling circuit of the building is higher than the temperature of the distribution network, the heat exchanger can be used to provide direct cooling to the building.

2.5.2 Objective function

An objective function defines the objective of the optimization and is a key element of an optimization model (Herrmann, 2007). In the optimization model of Wirtz et al. (2021), the objective function is minimizing the operational costs (C_{op}) of the 5GDHC system:

$$C_{\mathrm{op}} = \mathrm{p}_{\mathrm{el,sup}} \sum_{t \in T} P_{\mathrm{el,grid},t} \Delta \mathrm{t}_t - \mathrm{p}_{\mathrm{el,feed-in}} \sum_{t \in T} P_{\mathrm{el,feed-in},t} \Delta \mathrm{t}_t \tag{14}$$

with $P_{\mathrm{el,grid},t}$ and $P_{\mathrm{el,feed-in},t}$ being the power extracted from and the power fed in the electricity grid respectively. $\mathrm{p}_{\mathrm{el,sup}}$ represents the electricity supply price, while $\mathrm{p}_{\mathrm{el,feed-in}}$ denotes the electricity feed-in revenue. $\Delta \mathrm{t}_t$ is the length of a time step t.

2.5.3 Variable set

A decision variable is a variable for which the optimal value is determined during the optimization (Herrmann, 2007). A numerous amount of decision variables is included in the operation optimization model of Wirtz et al. (2021). An overview of all decision variables in the model is presented in Table B.1 in Appendix B.1.

2.5.4 Model structure

The structure attribute of the design optimization model describes the relationships between the objective function and the variables that must be satisfied (Herrmann, 2007). The optimization model presented by Wirtz et al. (2021) comprises a variety of constraints, which can be classified in six categories: energy balances, building energy systems, energy hub, network temperature intervals, coefficient of performance and storage and network temperature. The constraints are described below, with decision variables are written in italics.

Energy balances

The optimization model comprises four thermal energy balances and two electric energy balances. The first thermal energy balance describes the residual heating or cooling demand of a building b at timestep t:

$$\dot{Q}_{\mathrm{res,BES},b,t} = \left(\dot{Q}_{\mathrm{HP},b,t} - P_{\mathrm{HP},b,t}\right) - \left(\dot{Q}_{\mathrm{CC},b,t} + P_{\mathrm{CC},b,t}\right) - \dot{Q}_{\mathrm{DRC},b,t} \quad \forall\, b \in B, t \in T \tag{15}$$

The first term between brackets corresponds to the heat extracted from the warm pipe by the HP in times of heating demand. The amount of heat that is injected into the network, i.e. the waste heat of the CC, is represented by the second term. It should be noted that a negative residual demand indicates a residual cooling demand. The thermal energy flows to and from the distribution network are described by the second energy balance:

$$\dot{Q}_{\mathrm{res,netw},t} = \sum_{b \in B} \left(\dot{Q}_{\mathrm{res,BES},b,t}\right) + \dot{Q}_{\mathrm{loss,wp},t} - \dot{Q}_{\mathrm{loss,cp},t} + \dot{Q}_{\mathrm{netw},t} \quad \forall\, t \in T \tag{16}$$

Thus, the thermal energy flow to and from the network is determined by the residual demands of buildings, the heat losses from the warm and cold pipe and the thermal power for raising or lowering the network temperature. The third energy balance describes the relationship between the thermal power produced by the energy hub, the residual network demand and the charging/discharging power of the ACC:

$$\dot{Q}_{\mathrm{res,EH},t} = \dot{Q}_{\mathrm{res,netw},t} + \dot{Q}_{\mathrm{ACC},t} \quad \forall\, t \in T \tag{17}$$

When $\dot{Q}_{\mathrm{ACC},t} < 0$, heat is transferred from the ACC to the network. $\dot{Q}_{\mathrm{ACC},t} > 0$ indicates that the ACC is charged. Furthermore, the thermal power produced by the EH is negative ($\dot{Q}_{\mathrm{res,EH},t} < 0$) when cooling must be supplied by the EH. The thermal power produced by the ASHP and the CC must be equal to the power produced by the EH. This is described by the final thermal energy balance:

$$\dot{Q}_{\mathrm{res,EH},t} = \dot{Q}_{\mathrm{h,ASHP},t} - \dot{Q}_{\mathrm{c,CC},t} \quad \forall\, t \in T \tag{18}$$

The first electric energy balance ensures that the electricity demand of the building energy systems is equal to the electricity demands of the electric boiler, heat pump and CC installed in

the respective building:

$$P_{\mathrm{BES},b,t} = P_{\mathrm{EB},b,t} + P_{\mathrm{HP},b,t} + P_{\mathrm{CC},b,t} \quad \forall\, b \in B,\, t \in T \tag{19}$$

The sum of all building electricity demands and the EH electricity demand must be covered by the PV modules and the electricity grid. This is described by the second electric energy balance:

$$P_{\mathrm{el,grid},t} + P_{\mathrm{PV},t} = \sum_{b \in B} \left(P_{\mathrm{BES},b,t}\right) + P_{\mathrm{ASHP},t} + P_{\mathrm{CC},t} + P_{\mathrm{el,feed-in},t} \quad \forall\, t \in T \tag{20}$$

Building energy systems

The first constraint in this category ensures that the heating demand of a building ($\dot{\mathrm{Q}}_{\mathrm{h,dem},b,t}$) is met by the heat pump, electric boiler and the net thermal power of the water buffer vessel:

$$\dot{Q}_{\mathrm{h,HP},b,t} + \dot{Q}_{\mathrm{h,EB},b,t} + \dot{Q}^{\mathrm{dch}}_{\mathrm{h,TES},b,t} = \dot{\mathrm{Q}}_{\mathrm{h,dem},b,t} + \dot{Q}^{\mathrm{ch}}_{\mathrm{h,TES},b,t} \quad \forall\, b \in B,\, t \in T \tag{21}$$

Likewise, the cooling demand of a building ($\dot{\mathrm{Q}}_{\mathrm{c,dem},b,t}$) must be provided by the CC and DRC at each time step t:

$$\dot{Q}_{\mathrm{c,CC},b,t} + \dot{Q}_{\mathrm{c,DRC},b,t} = \dot{\mathrm{Q}}_{\mathrm{c,dem},b,t} \quad \forall\, b \in B,\, t \in T \tag{22}$$

Since the thermal output of the generation units installed in buildings is limited by their rated power, the authors introduced the following constraints:

$$\dot{Q}_{\mathrm{h},k,b,t} \leq \dot{\mathrm{Q}}^{\mathrm{nom}}_{\mathrm{h},k,b} \quad \forall\, k \in \{HP, EB\},\, b \in B,\, t \in T \tag{23}$$

$$\dot{Q}_{\mathrm{c},k,b,t} \leq \dot{\mathrm{Q}}^{\mathrm{nom}}_{\mathrm{c},k,b} \quad \forall\, k \in \{CC, DRC\},\, b \in B,\, t \in T \tag{24}$$

For the water buffer vessels installed in each building, the state of charge (SoC) at time step t is connected with the SoC at the previous time step $t-1$. This is described by:

$$SoC_{\mathrm{TES},b,t} = SoC_{\mathrm{TES},b,t-1}\left(1 - \phi_{\mathrm{TES,loss}}\right) + \eta^{\mathrm{ch}}_{\mathrm{TES}} \dot{Q}^{\mathrm{ch}}_{\mathrm{h,TES},b,t} - \frac{\dot{Q}^{\mathrm{dch}}_{\mathrm{h,TES},b,t}}{\eta^{\mathrm{dch}}_{\mathrm{TES}}} \quad \forall\, b \in B,\, t \in T : t \neq t_0 \tag{25}$$

Finally, the SoC of a water buffer vessel its limited by its nominal capacity:

$$SoC_{\mathrm{TES},b,t} \leq \mathrm{SoC}^{\mathrm{cap}}_{\mathrm{TES},b} \quad \forall\, b \in B,\, t \in T \tag{26}$$

Energy hub

The constraints in the Energy hub category are related to the thermal output of the generation units being limited by their rated power:

$$\dot{Q}_{\mathrm{h,ASHP},t} \leq \dot{\mathrm{Q}}^{\mathrm{nom}}_{\mathrm{h,ASHP}} \quad \forall\, t \in T \tag{27}$$

$$\dot{Q}_{\mathrm{c,CC},t} \leq \dot{\mathrm{Q}}^{\mathrm{nom}}_{\mathrm{c,CC}} \quad \forall\, t \in T \tag{28}$$

Furthermore, the SoC of the ACC is limited by its storage capacity:

$$S_{\mathrm{ACC},t} \leq \mathrm{S}^{\mathrm{cap}}_{\mathrm{ACC}} \quad \forall\, t \in T \tag{29}$$

Network temperature intervals

The authors introduced three variables to be able to describe the network temperatures: the mean network temperature ($\bar{T}_{\mathrm{netw},t}$) and the temperatures of the warm pipe ($T_{\mathrm{netw,wp},t}$) and cold pipe ($T_{\mathrm{netw,cp},t}$). The relationships between the variables are given by:

$$T_{\mathrm{netw,wp},t} = \bar{T}_{\mathrm{netw},t} + \frac{\Delta \mathrm{T}_{\mathrm{netw}}}{2} \quad \forall\, t \in T \tag{30}$$

$$T_{\mathrm{netw,cc},t} = \bar{T}_{\mathrm{netw},t} - \frac{\Delta \mathrm{T}_{\mathrm{netw}}}{2} \quad \forall\, t \in T \tag{31}$$

It is assumed that the temperature difference between the two network pipes ($\Delta \mathrm{T}_{\mathrm{netw}}$) is constant. Furthermore, the temperatures of the warm and cold pipe must be in a predefined range $[\mathrm{T}^{\mathrm{min}}_{\mathrm{netw,cp}}, \mathrm{T}^{\mathrm{max}}_{\mathrm{netw,wp}}]$. The temperature of the cold pipe ($\mathrm{T}^{\mathrm{min}}_{\mathrm{netw,cp}}$) cannot be lower than 6 °C, while the temperature of the warm pipe ($\mathrm{T}^{\mathrm{max}}_{\mathrm{netw,wp}}$) cannot exceed 40 °C. Next, the authors subdivided the range into $\mathrm{n}_{\mathrm{int}}$ discrete temperature intervals $[\mathrm{T}_{\mathrm{low},i}, \mathrm{T}_{\mathrm{up},i}]\ \forall\, i \in (0, ..., \mathrm{n}_{\mathrm{int}} - 1)$ with constant interval width $\Delta \mathrm{T}_{\mathrm{int}}$:

$$\mathrm{T}_{\mathrm{up},i} = \mathrm{T}^{\mathrm{min}}_{\mathrm{netw,c}} + \frac{\Delta \mathrm{T}_{\mathrm{netw}}}{2} + (i+1)\Delta \mathrm{T}_{\mathrm{int}} \tag{32}$$

$$\mathrm{T}_{\mathrm{low},i} = \mathrm{T}^{\mathrm{min}}_{\mathrm{netw,c}} + \frac{\Delta \mathrm{T}_{\mathrm{netw}}}{2} + i\Delta \mathrm{T}_{\mathrm{int}} \tag{33}$$

The binary variable $\theta_{i,t}$ was introduced, which equals 1 if the mean network temperature is in the interval $[T_{low,i}, T_{up_i}]$. To ensure that only 1 interval is active at time step t, the following constraints was included:

$$\sum_{i=0}^{\mathrm{n}_{\mathrm{int}}-1} \theta_{i,t} = 1 \quad \forall\, t \in T \tag{34}$$

Furthermore, the variable $T^{\theta}_{i,t}$ is implemented. The value of this variable is forced to be equal to the value of mean network temperature if the interval k is active:

$$T^{\theta}_{i,t} \geq \theta_{i,t} \mathrm{T}_{\mathrm{low},i} \quad \forall\, i \in (0, ..., \mathrm{n}_{\mathrm{int}} - 1),\ \forall\, t \in T \tag{35}$$

$$T^{\theta}_{i,t} \leq \theta_{i,t} \mathrm{T}_{\mathrm{up},i} \quad \forall\, i \in (0, ..., \mathrm{n}_{\mathrm{int}} - 1),\ \forall\, t \in T \tag{36}$$

The mean network temperature is equal to the sum of all variables $T^{\theta}_{i,t}$:

$$\bar{T}_{\mathrm{netw},t} = \sum_{i=0}^{\mathrm{n}_{\mathrm{int}}-1} T^{\theta}_{i,t} \quad \forall\, t \in T \tag{37}$$

Heat losses

In the model presented by Wirtz et al. (2021), heat losses from the warm and cold pipe depend linearly on the temperature difference between the distribution pipes and the soil. This is described by the constraints:

$$\dot{Q}_{\mathrm{loss,wp},t} = (\mathrm{kA})_{\mathrm{netw}} (T_{\mathrm{netw,wp},t} - \mathrm{T}_{\mathrm{soil},t}) \quad \forall\, t \in T \tag{38}$$

$$\dot{Q}_{\mathrm{loss,cp},t} = (\mathrm{kA})_{\mathrm{netw}} (\mathrm{T}_{\mathrm{soil},t} - T_{\mathrm{netw,cp},t}) \quad \forall\, t \in T \tag{39}$$

where $(\mathrm{kA})_{\mathrm{netw}}$ represents the heat loss coefficient of the distribution network and $\mathrm{T}_{\mathrm{soil},t}$ the

temperature of the soil at time step t.

Coefficient of performance and direct cooling

As described in section 2.1.1, the COP of heat pumps and chillers is dependent on the temperatures of the warm and cold distribution pipes and the required supply temperatures in a building. In the model presented by Wirtz et al. (2021), the COPs of the heat pumps and chillers are determined for each network temperature interval k prior to the optimization. The heating or cooling power for a heat pump or chiller is then described by:

$$\dot{Q}_{th} = \sum_{i=0}^{\mathrm{n_{int}}-1} [\mathrm{COP}_{i,t}\theta_{i,t}]P_t \tag{40}$$

Next, the authors introduced the auxiliary variable $P^{\theta}_{i,t}$. This variable equals the electric power consumed by the heat pump or CC is the interval i is active, otherwise it is 0:

$$P^{\theta}_{i,t} \leq \theta_{i,t}\mathrm{M_p}, \tag{41}$$

$$P^{\theta}_{i,t} \leq P_t, \tag{42}$$

$$P^{\theta}_{i,t} \geq P_t - (1-\theta_{i,t})\mathrm{M_p} \quad \forall\, i \in (0,...,\mathrm{n_{int}}-1),\ \forall\, t \in T \tag{43}$$

Subsequently, Eq. (40) is rewritten as:

$$\dot{Q}_{th} = \sum_{i=0}^{\mathrm{n_{int}}-1} [\mathrm{COP}_{i,t}P^{\theta}_{i,t}] \quad \forall\, t \in T \tag{44}$$

The possibility of using DRC is dependent on the temperatures of the warm and cold pipe in a 5GDHC system (Roossien et al., 2020). The authors included this in the model by introducing the binary variable $y_{\mathrm{DRC},b,t}$. If the temperature difference between the supply and return temperature of the cooling circuit in a building ($\mathrm{T_{c,return},}_{b,t} - \mathrm{T_{c,supply},}_{b,t}$) is greater than the temperature difference between the warm and cold pipe ($\Delta\mathrm{T_{netw}}$), the following constraint is used in the model:

$$T_{\mathrm{netw,c},t} + \Delta\mathrm{T_{min}} - \mathrm{T_{c,supply},}_{b,t} \leq (1-y_{\mathrm{DRC},b,t})\mathrm{M_{DRC},}_{b} \quad \forall\, b \in B,\ t \in T \tag{45}$$

Otherwise the constraint

$$T_{\mathrm{netw,h},t} + \Delta\mathrm{T_{min}} - \mathrm{T_{c,return},}_{b,t} \leq (1-y_{\mathrm{DRC},b,t})\mathrm{M_{DRC},}_{b} \quad \forall\, b \in B,\ t \in T \tag{46}$$

is active. Here, $\mathrm{M_{DRC},}_{b}$ is a big-M coefficient and $\Delta\mathrm{T_{min}}$ represents the minimum temperature difference across the heat exchanger. Eqs. (45) and (46) ensure that the binary variable $y_{\mathrm{DRC},b,t}$ is only equal to 1 at times when DRC can be used in a building. Furthermore, the cooling power supplied by the heat exchanger for DRC must be 0 when $y_{\mathrm{DRC},b,t}$ is 0. Otherwise, the cooling power of the heat exchanger is limited by its rated power ($\mathrm{Q^{nom}_{c,DRC},}_{b}$). This is described by:

$$\dot{Q}_{\mathrm{c,DRC},b,t} \leq y_{\mathrm{DRC},b,t}\mathrm{Q^{nom}_{c,DRC},}_{b} \quad \forall\, t \in T \tag{47}$$

Storage and network temperature

The constraints in the last category of model relationships in the optimization approach presented by Wirtz et al. (2021) are related to the temperatures of the ACC and the network pipes. The first constraint describes the relationship between the mean network temperature of two consecutive time steps:

$$\bar{T}_{\mathrm{netw},t} = \bar{T}_{\mathrm{netw},t-1} + \Delta T_t \quad \forall\, t \in T \;:\; t \neq t_0 \tag{48}$$

in which ΔT_t represents the temperature increase at time step t. Increasing or lowering the temperature of the water mass in the distribution pipes and the ACC requires a certain amount of thermal power. This is described by the constraint:

$$\dot{Q}_{\mathrm{netw},t} = \rho_{\mathrm{w}}(\mathrm{V}_{\mathrm{netw}} + \mathrm{V}_{\mathrm{ACC}})\mathrm{c}_{\mathrm{w}}\Delta T_t \frac{1}{\Delta \mathrm{t}_t} \quad \forall\, t \in T \tag{49}$$

where $\mathrm{V}_{\mathrm{netw}}$ and $\mathrm{V}_{\mathrm{ACC}}$ denote the water volume in the distribution pipes and the ACC respectively. Next, the authors introduced the binary variables $y_{\mathrm{inc},t}$ and $y_{\mathrm{dec},t}$ for modelling the operation of the ACC. If the network temperature is increased, i.e. $\Delta T_t \geq 0$, $y_{\mathrm{inc},t}$ is equal to 1. When $\Delta T_t \leq 0$, $y_{\mathrm{dec},t}$ must become 1. This is ensured by the constraints:

$$\Delta T_t \leq y_{\mathrm{inc},t}\mathrm{M}_{\mathrm{T}} \quad \forall\, t \in T \tag{50}$$

$$\Delta T_t \geq -y_{\mathrm{dec},t}\mathrm{M}_{\mathrm{T}} \quad \forall\, t \in T \tag{51}$$

with M_{T} being a large big-M coefficient. The final constraints of the model presented by Wirtz et al. (2021) are related to the SoC of the ACC. The network temperature can only be altered when the ACC is fully charged or discharged at two consecutive time steps:

$$2\mathrm{SoC}^{\mathrm{cap}}_{\mathrm{ACC}} y_{\mathrm{inc},t} \leq SoC_{\mathrm{ACC},t} + SoC_{\mathrm{ACC},t-1} \quad \forall\, t \in T \;:\; t \neq t_0 \tag{52}$$

$$2\mathrm{SoC}^{\mathrm{cap}}_{\mathrm{ACC}} (1 - y_{\mathrm{dec},t}) \geq SoC_{\mathrm{ACC},t} + SoC_{\mathrm{ACC},t-1} \quad \forall\, t \in T \;:\; t \neq t_0 \tag{53}$$

2.5.5 Model deficiencies

As described in section 1.1, the optimization approach presented by Wirtz et al. (2021) can be considered an improvement compared to the model presented in Wirtz et al. (2020a). This is because the model allows for optimizing the operating temperatures of the warm and cold pipe in a 5GDHC system. However, the model suffers from several deficiencies which will be discussed in this section.

Firstly, the objective of the optimization is to minimize the operational costs of the 5GHDC system (see Eq. (14)). The model can thus not be used to determine the optimal selection and sizing of thermal energy generation and storage units. As can be seen in section 2.5.4, the installed capacities of the generation and storage units are model parameters that need to be determined a priori to the optimization (Wirtz et al., 2021). Wirtz et al. (2021) calculated these capacities using an approach that is based on the model presented by Wirtz et al. (2020a). Furthermore, the model is not capable of determining the optimal pipe diameters. Instead, the diameters of the warm and cold pipe used in the model were adopted from Wirtz et al. (2020a).

Furthermore, no distinction is made between space heating demand and DHW demand in the model. As described by Eq. (21), the net thermal power of the heat pump, electric boiler and the heat storage must be equal to the heating demand of the building at each time step. The authors do not elaborate on whether DHW demand is included in the heating demand of a building (Wirtz et al., 2021). This is an important aspect to consider when designing 5GDHC systems, especially in the Netherlands. Reason for this is that space heating may be provided with temperatures as low as 35 °C in well-insulated buildings (Greenvis & Ecofys, 2016). For the provision of DHW, on the other hand, certain regulations apply. To prevent legionella, it is legally mandated to heat DHW to at least 60 °C (CE Delft, 2018; Greenvis & Ecofys, 2016). In Dutch DH systems, heat pumps are used to supply space heating (CE Delft, 2018). Additionally, booster heat pumps, electric boilers and gas boilers can be installed in a building for reaching the temperature required for DHW (Greenvis & Ecofys, 2016).

The next deficiency of the existing optimization approach is related to the thermal energy generation units that are considered in the model. Heat and cold are delivered to the distribution network by an ASHP and a CC respectively. These appliances extract thermal energy from the ambient air and increase or decrease the temperature to the temperature of the warm or the cold pipe (Wirtz et al., 2021). As described by Eq. (40), the COP of the devices is dependent on the temperature of the ambient air. Nevertheless, the ASHP and CC can provide thermal energy at all times regardless of the outside air temperature (P. Wu et al., 2020). This does not apply when SWTE is used for balancing a 5GDHC system. As discussed in section 2.3.2, heat can only be extracted when the temperature of the surface water is higher than 15 °C. Cold can only be supplied to the cold pipe when the surface water temperature is between 0 and 7 °C. Furthermore, the amount of thermal energy that can be extracted from a surface water body is limited by its thermal capacity (Stowa, 2018). These issues need to be considered in the development of a design optimization approach for 5GDHC systems with SWTE.

Finally, ATES is not considered in the energy system structure in the model of Wirtz et al. (2021). Instead, an ACC is included that functions as an element to balance residual thermal energy demands of buildings (Wirtz et al., 2021). In case of a residual heating demand, a net mass flow from the warm to the cold distribution pipe is induced. To conserve mass, warm water from the top of the ACC tank enters the warm pipe and cold water flows from the cold pipe to the bottom of the tank. The volume of the warm water in the ACC tank decreases during this process, while the volume of the cold water increases. The system works in reverse in case of residual cooling demand (Franzen et al., 2019; Wirtz et al., 2021). Using these principles, the ACC is able to balance residual thermal energy demands as long as the water in the tank is not fully at the temperature of the warm or the cold pipe (Wirtz et al., 2021). Since this is different from the working principles of ATES systems discussed in section 2.2, the model of Wirtz et al. (2021) needs to be adapted to be able to optimize the design of 5GDHC systems with ATES.

3 Research strategy and methodology

The research strategy comprised three phases and is summarized in Figure 9. The first research phase entailed the development of a novel optimization model for 5GDHC systems with ATES and SWTE. During the second phase, the optimal design and operation of a 5GDHC system with ATES and SWTE was identified for a real-world case. This was done by applying the novel optimization approach obtained during the first research phase. The third phase comprised the assessment of the techno-economic feasibility, carried out by comparing the 5GDHC solution against alternative heating and cooling concepts. The three research phases with corresponding methods are described in greater detail in the following.

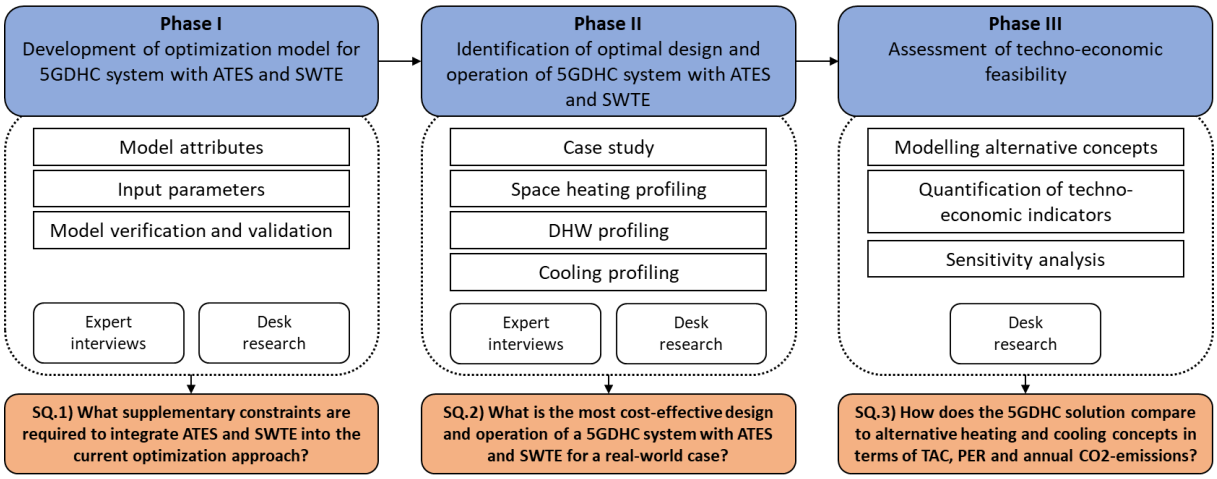

Figure 9: Schematic overview of research strategy steps and corresponding methods.

3.1 Phase I: Development of optimization model for 5GDHC systems with ATES and SWTE

As discussed in section 2.5.5, the optimization approach proposed by Wirtz et al. (2021) suffers from several deficiencies and is not suitable for the optimization of 5GDHC systems with ATES and SWTE. In this first research phase, a novel MILP model for the design and operation optimization of 5GDHC systems with ATES and SWTE was developed. This was done by constructing the model attributes: scope, objective function, variable set and structure. Moreover, technical and economic input parameters were collected and model verification and validation were carried out. A flow diagram of the model development process is presented in Figure 10. The methods with corresponding steps applied during this first research phase are discussed below.

Model attributes

The first step in the model development process comprised the definition of the model scope. This was partly derived from the model scope presented by Wirtz et al. (2021). In the novel MILP model, the air-source heat pump (ASHP), compression chiller (CC) and accumulator tank (ACC) were replaced by ATES and SWTE systems. Furthermore, a distinction was made between the space heating and DHW demand in buildings. As discussed in section 2.5.5, space heating may be provided with lower temperatures compared to DHW in well insulated buildings. Consequently, the technologies installed in building energy systems differ between well insulated

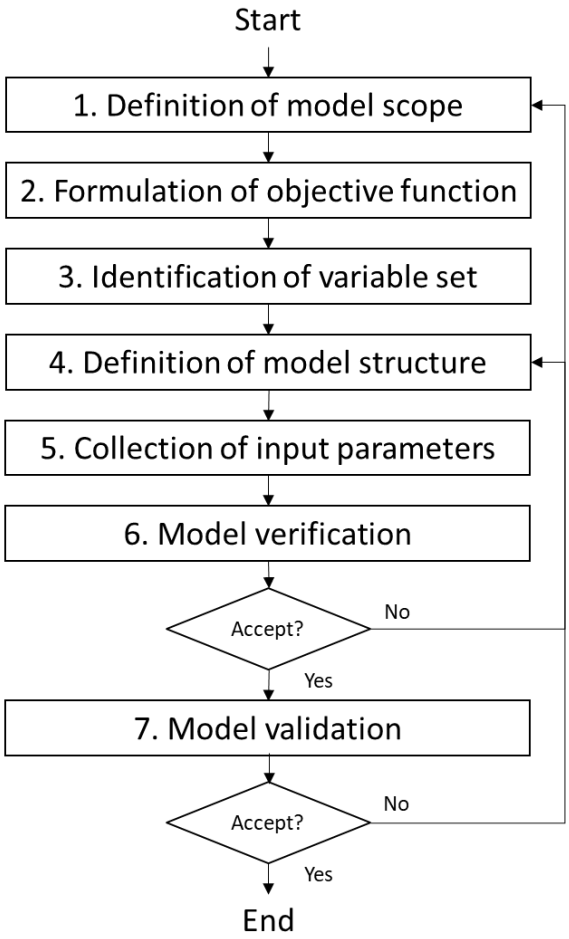

Figure 10: Flow diagram of model development process.

and poorly insulated buildings. The objective function was formulated next, based on the model scope. In the third step, the variable set considered in the novel MILP model was identified. This set includes all variables that change and affect the design and operation of the 5GDHC system. Subsequently, the model structure was defined. This includes the relationships between variables and the objective function. The constraints were partly derived from the model presented by Wirtz et al. (2021). The ASHP, CC and ACC were removed from the constraints, while the ATES and SWTE systems were added. The constraints were formulated using the working and design principles of ATES and SWTE systems discussed in sections 2.2 and 2.3. The novel MILP model was written in Python, using Gurobi software as optimization tool.

Input parameters

Technical and economic input parameters were retrieved during the fifth step of the model development process. This was done by conducting desk research and expert interviews. Academic and grey literature were collected via Google, Google Scholar and Scopus. The parameters that could not be retrieved by the desk research were collected by conducting interviews with experts on DH, ATES and SWTE systems. An overview of all input parameters is provided in Appendix C. The economic parameters required for the calculation of the investments costs of the HPs, SWTE and ATES were retrieved from a database of Waternet. This database, which is not publicly available, contains the capacities and corresponding investment costs for the tech-

nologies reported in numerous projects. The capacities were plotted against the investment costs. Subsequently, linear trend lines were fitted to the data. From the trend lines, the y-intercepts were used as fixed investment costs component for the respective technologies. The slopes were used as variable costs per capacity. The constructed graphs with corresponding trend lines are provided in Appendix C.2.

Model verification and validation

Model verification and validation are considered important steps in the overall model development process (Paez, 2008; Thacker et al., 2004). Verification of a model is concerned with determining that a model performs as intended, i.e. there are no programming errors (Kleijnen, 1995; Law et al., 2000). The model constructed in this research was verified by checking whether the solution for a real-world case is sound and logical. For each of the constraints, it was checked that it was not violated by the obtained solution. In case errors were detected, the model structure was redefined. The model verification procedure was carried out again after each improvement. This process was continued until the model performed as intended.

The final step comprised the validation of the constructed optimization model. According to Schwer (2009), validation can be defined as the process of determining the degree of which a model is an accurate representation of the real world. Model validation is ideally accomplished by comparing the outcomes of the model with real-world data (Kleijnen, 1995). Since no 5GDHC systems with ATES and SWTE are currently installed to our knowledge, this method of model validation could not be used in this research. Instead, the constructed model was validated by conducting an interview with an expert on modelling of 5GDHC systems. During the interview, the expert's opinion was used to judge whether the obtained solution reflects real-world conditions. If errors were detected, the model scope was redefined and all model development steps were carried out again. This process with reiterated until real-world conditions were reflected by the solution.

3.2 Phase II: Identification of the optimal design and operation of 5GDHC system with ATES and SWTE

Case study

The constructed optimization model was applied to a real-world case during the second research phase. To determine the most cost-effective design and operation of the 5GDHC system, technical and economic input parameters needed to be retrieved specifically for the test case. The parameters, of which a complete overview is given in Appendix C.4, were collected by conducting desk research. It was assumed that the system would not be installed before 2025. Considering the lifetime of the system, projections for the 2030 electricity and natural gas prices were used as input parameters (PBL, 2020). This is the last year for which the Dutch Climate and Energy Outlook provides projections. The hourly temperature profile of the surface water was retrieved from the open data source Waterinfo of Rijkswaterstaat (Rijkswaterstaat, 2021). The temperature profile of the measurement location closest to the test case was used. Furthermore, the hourly space heating, DHW and cooling demand profiles were required as input parameters for the optimization. Since these profiles were not available for the buildings in the test case, they were created during this research. The steps used for developing the profiles are summarized in Figure 11 and described in greater detail in the following.

Space heating	Domestic hot water	Cooling
• Buildings in test case were matched with the ECN model home types • Space heating demands of buildings were assessed from the total annual gas consumption and the annual gas consumption for DHW • ECN profiles were corrected for actual space heating demands • Simultaneity factors were applied for apartment buildings by shifting demand profiles of individual buildings in time	• Assumed natural gas consumption for DHW was multiplied by the efficiency of the gas boiler to obtain the annual DHW demands of buildings • Distribution that indicates the share of DHW demand for each hour of the day was used to convert the annual DHW demands of buildings to hourly DHW demand profiles.	• Cooling demand profile developed by Jansen et al. (2021) was used as reference • Annual cooling demands of buildings were calculated by multiplying the annual cooling demand per floor by the floor area of the respective building • The reference cooling demand profile was corrected for the annual cooling demands of the buildings

Figure 11: Methods for developing space heating, domestic hot water and cooling profiles.

Space heating demand profiling

The space heating demand profiles of the buildings were constructed using an adapted version of the ECN Wartevraagprofielenmodel (ECN, 2018; Menkveld et al., 2015). This adapted version, created by Ecofys and ECN, contains a dataset with hourly space heating demand profiles for 120 different model home types based on the meteorological year 2012. The model home types differ in dwelling type, insulation level and household type. Compared to the original version, the adapted version differentiates the thermostat setting between household types and between week and weekend days (Menkveld et al., 2015). For each building in the test case, it was determined which model home type most closely matched. The corresponding space heating demand profiles were then multiplied by a factor to account for the difference between the yearly space heating demands of the profiles and the actual space heating demands of the buildings. Accordingly, the space heating demand of a building b at time step t ($\dot{Q}_{\mathrm{h,dem,sh},b,t}$) was calculated by:

$$\dot{Q}_{\mathrm{h,dem,sh},b,t} = \dot{Q}_{\mathrm{ECN},b,t} \frac{(\mathrm{G}_{\mathrm{total},b} - \mathrm{G}_{\mathrm{DHW},b})\eta_{\mathrm{GB,sh}}}{\sum_{t \in T} \dot{Q}_{\mathrm{ECN},b,t}} \quad \forall\, b \in B, t \in T \tag{54}$$

Here, $\dot{Q}_{\mathrm{ECN},b,t}$ represents the space heating demand of building b at time step t selected from the ECN dataset. The annual gas consumptions of the buildings ($\mathrm{G}_{\mathrm{total},b}$) were provided by the environmental consultancy company Resourcefully. Furthermore, it is assumed that the annual gas consumption for DHW ($\mathrm{G}_{\mathrm{DHW},b}$) is equal to 2850 kWh. This value is retrieved from Tigchelaar (2013) and is based on the average household size in the Netherlands. For the efficiency of the gas boiler for space heating ($\eta_{\mathrm{GB,sh}}$), a value of 0.93 was used (ENERGYMATTERS, 2014).

The obtained space heating demand profiles were then used as input in the model. However, the majority of the buildings in the test case are apartment buildings that contain multiple dwellings. When aggregating demand profiles of individual dwellings to a demand profile of a group of dwellings, the simultaneity of the peak demand must be taken into account. This is because the peak demand of individual dwellings will not occur at the exact same time (Menkveld et al., 2015). To accurately construct the space heating demand profiles of the apartment buildings, the simultaneity factors presented in Table 1 were used. These simultaneity factors were retrieved from ISSO-publicatie 39 (2012) and are based on the number of individual dwellings in an apartment building. The space heating demand profiles individual dwellings were shifted in time (1-4 hours earlier or later). This process was continued until the aggregated peak demand was equal to the sum of the individual peak demands times the simultaneity factor. This approach ensured that the annual space heating demands were not affected.

Table 1: Simultaneity factors for space heating used in research. Retrieved from ISSO-publicatie 39 (2012).

Number of dwellings		**Simultaneity factor**
Lower bound	*Upper bound*	
1	5	1.00
6	13	0.95
14	25	0.90
26	40	0.85
41	60	0.80
61	85	0.75
86	115	0.70
116	155	0.65
156	205	0.60
206	-	0.55

DHW demand profiling

The hourly DHW demand profiles for the buildings in the test case were created using the model presented by Friedel et al. (2014). In this model, a distribution that indicates the share of DHW demand for each hour of the day is presented. The simultaneity of the DHW demand is already incorporated, as the distribution is based on the DHW demands of multiple buildings. There is no differentiation between days, seasons and building types. Firstly, the annual DHW demand was calculated for each building by multiplying the assumed natural gas consumption for DHW by the efficiency of the gas boiler. Here, it is assumed that the efficiency of the gas boiler for DHW ($\eta_{GB,DHW}$) is equal to 0.72 (CE Delft, 2019a). The distribution was then used to convert the annual DHW demand of buildings to hourly demand profiles.

Cooling demand profiling

The development of cooling demand profiles for buildings is considered a difficult task (RVO, 2018a). Heating demand can be created relatively easy based on heating degree days. When developing cooling demand profiles, factors as climate, urban heat island effects, thermal insulation of the building and solar radiation must be taken into account (RVO, 2018a). This requires complex modelling. Due to time limitations, this was beyond the scope of this research. Instead, the cooling demand profiles were created based on an existing profile developed by Jansen et al. (2021). This profile was created for a terraced house with a floor area of 123 m^2 and an annual cooling demand of 4 kWh/m^2. The cooling demand profiles of the buildings were obtained by correcting the existing profile for the annual cooling demand of the respective building. The annual cooling demands of the buildings were determined using the annual cooling demand per floor area for each building type presented by Jansen et al. (2021). The floor areas of the buildings in the test case were retrieved from Kadaster (n.d.).

3.3 Phase III: Assessment of techno-economic feasibility

The final phase of this research involved the assessment of the techno-economic feasibility of 5GDHC systems with ATES and SWTE. This was done by comparing the 5GDHC solution to a conventional DH system operating a 70 °C and a reference system with stand-alone natural gas installations. The first method of this research phase comprised the modelling of the alternative heating and cooling concepts. Subsequently, economic, technical and environmental performance indicators were calculated for the three concepts.

Modelling of alternative heating and cooling systems

The conventional DH system considered in this research consists of an ATES system, a SWTE system, a central HP and a central TES. The central HP is located in a technical building and is used to upgrade heat from the ATES and SWTE systems to 70 °C. Heat interface units in buildings are used to transfer from the distribution network to the heat supply system of the buildings. Since the heat is supplied to buildings at 70 °C, both space heating and DHW of buildings can be met. The return temperature of the distribution network is 40 °C. The central TES can be used to lower the required capacities for the central HP and the ATES and SWTE systems. Furthermore, air conditioners (ACs) are installed in individual dwellings to supply cooling. To determine the optimal capacities and operation of the ATES, SWTE, central HP and central TES, a LP optimization model was written. The model attributes scope, objective function, variable set and model structure are presented in Appendix D.1. The LP optimization model is considered significantly less complex compared to the optimization model developed for the 5GDHC system. This is because the supply and return temperatures of the network are constant and no HPs are installed in the individual buildings.

In the reference systems with stand-alone natural gas installations, space heating and DHW is supplied by natural gas boilers installed in individual dwellings. No TES is considered. This is how the buildings in the test-case are currently heated. Cooling is supplied in the same way as in the conventional DH concept. The annual gas consumption for space heating and DHW of the buildings was provided by consultancy company Resourcefully. The annual electricity use of the ACs in individual dwellings were taken from the solution of the optimization model for the conventional DH system. The technical and economic input parameters required for modelling of the alternative heating and cooling concepts were retrieved by conducting desk research. An overview of the input parameters is provided in Appendix D.2.

Quantification of technical, economic and environmental indicators

The economic, technical and environmental performances of the three concepts were evaluated by calculating the total annualised costs (TAC), primary energy requirement (PER) and annual CO_2-emissions. These performance indicators are frequently used in the assessment of DHC systems in literature (Dominković et al., 2020; Joelsson & Gustavsson, 2009; Morvaj et al., 2016; Wirtz et al., 2020a). The technical, economic and environmental input parameters used for calculating the performance indicators are reported in Appendix D.2.

The TAC consist of the annual expenditure needed for interest and depreciation, as well as the annual costs for fuel and operation and maintenance (O&M). In this study, the TAC represent the societal costs for installing, operating and maintaining an energy system. Taxes, subsidies and cash flows between actors were therefore excluded. The TAC of the 5GDHC system and conventional DH system were obtained from the design and operation optimization models developed for the systems. For the reference systems with stand-alone natural gas installations, the TAC were calculated by:

$$TAC_{\text{reference}} = C_{\text{GB,reference}} + C_{\text{AC,reference}} + C_{\text{gas,reference}} + C_{\text{el,reference}} \tag{55}$$

The annual costs for natural gas and electricity ($C_{\text{gas,reference}}$ and $C_{\text{el,reference}}$) were calculated by multiplying the annual gas and electricity use by the projected 2030 gas and electricity prices.

The annualized costs for natural gas boilers and ACs were determined using:

$$C_{\text{GB,reference}} = I_{\text{GB,reference}}(a_{\text{inv,GB}} + f_{\text{om,GB}}) \tag{56}$$

$$C_{\text{AC,reference}} = I_{\text{AC,reference}}(a_{\text{inv,AC}} + f_{\text{om,AC}}) \tag{57}$$

An elaboration on the calculation of the investment costs for the natural gas boiler and ACs ($I_{\text{GB,reference}}$ and $I_{\text{AC,reference}}$) is provided in Appendix D.2.

The PER refers to the total primary energy input required to provide a certain amount of final energy. The PER of the three heating and cooling concepts were calculated by multiplying the annual gas and electricity use by the primary energy factor (PEF) of the respective energy carrier:

$$\text{PER} = \text{G}_{\text{total}}\text{PEF}_{\text{gas}} + \text{E}_{\text{total}}\text{PEF}_{\text{electricity}} \tag{58}$$

Here, G_{total} and E_{total} represent the annual gas and electricity consumption. The PEFs of natural gas and electricity were adopted from the Dutch Climate and Energy Outlook 2020 (PBL, 2020). The PEF for electricity is based on the projected 2030 Dutch electricity mix. PER occurring during installation and end-of-life of the systems lie outside the scope of this analysis.

The annual CO_2-emissions for the three heating and cooling concepts were calculated using:

$$\text{Annual } CO_2 - \text{emissions} = \text{G}_{\text{total}}\text{EF}_{\text{gas}} + \text{E}_{\text{total}}\text{EF}_{\text{electricity}} \tag{59}$$

where EF_{gas} and $\text{EF}_{\text{electricity}}$ represent the emission factors (EFs) for natural gas and electricity. The EF for the projected 2030 Dutch electricity mix was obtained from Dutch Climate and Energy Outlook 2020 (PBL, 2020). Emissions resulting from installation and end-of-life operations were not included.

Sensitivity analysis

Finally, a sensitivity analysis was carried out. The aim of this analysis was twofold. Firstly, to show the uncertainty of the model outcomes. Secondly, to examine the influence of input parameters on the TAC of the three heating and cooling concepts. The input parameters and corresponding parameter values considered in the sensitivity analysis are presented in Table 2. The interest rate and future energy prices were selected because their values are uncertain and expected to have a significant impact on the TAC. Future energy prices are dependent on many factors, such as fuel prices and policy measures (PBL, 2020). A margin of uncertainty of $\pm 25\%$ was therefore used for the projected 2030 electricity- and natural gas prices. The interest rates considered were based on Steinbach and Staniaszek (2015).

Table 2: Values for sensitivity analysis (PBL, 2020, 2021a; Steinbach & Staniaszek, 2015).

Input parameter	Symbol	Lower	Base	Upper	Unit
Interest rate	r	1	3	5	%
Electricity price	p_{el}	0.109	0.145	0.181	€/kWh
Natural gas price	p_{gas}	0.581	0.774	0.968	€/m^3

4 Results

This chapter presents the findings of this study. Section 4.1 describes the constructed optimization model. The optimal design and operation of a 5GDHC system with ATES and SWTE for a real-world case are presented in section 4.2. Finally, section 4.3 presents the techno-economic performance indicators of the three heating and cooling concepts and the outcomes of the sensitivity analysis.

4.1 Novel optimization model

The constructed novel optimization model is presented in this section. Firstly, the scope of the model is discussed in section 4.1.1. The objective function and variable set of the model are presented next in sections 4.1.2 and 4.1.3. Finally, the model structure is discussed in section 4.1.4.

4.1.1 Model scope

The constructed MILP aims to determine the optimal 5GDHC system for covering the time-varying space heating, DHW and cooling demands of buildings. The optimization model selects and sizes the devices installed in individual buildings and defines their optimal operation. Simultaneously, the ATES and SWTE systems are sized and their optimal operation is determined. The duration of the time steps in the optimization approach is 1 hour, as this resolution is considered to provide the best trade-off between computational times and accuracy (Harb et al., 2015). Furthermore, the model is based on time series for one year.

The structure of the 5GDHC system that is considered in the novel optimization approach is presented in Figure 12. The energy hub (EH) consists of a SWTE installation and an ATES system. The SWTE installation can be used to supply both heat and cold to the distribution network, depending on the temperature of the surface water. The ATES functions as a storage system to overcome the temporal mismatch between thermal energy supply and demand. Furthermore, a connection with the power grid is included that supplies electricity to the different devices.

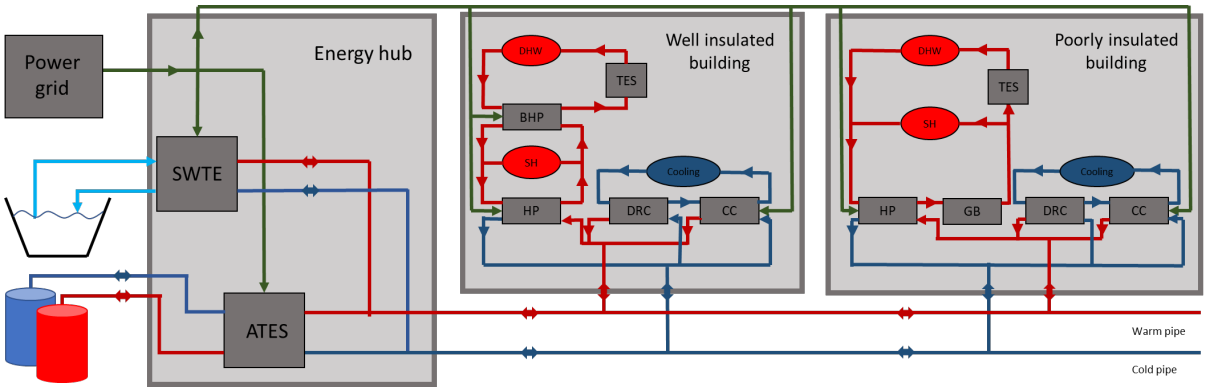

Figure 12: Energy system structure with energy hub and building energy systems that is being optimized in the novel design optimization approach. Green, red and blue arrows indicate the electricity, heat and cold flows through the system respectively.

For the buildings energy systems (BESs), a distinction has been made between well insulated and poorly insulated buildings. This is because space heating may be provided with temperatures as low as 35 °C in well insulated buildings, while higher temperature are required in poorly insulated buildings (Greenvis & Ecofys, 2016). The heat pump (HP) installed in well insulated buildings is used to provide space heating and to supply heat to the booster heat pump (BHP). The BHP is used to charge a thermal energy storage (TES) for the provision of DHW. In poorly insulated buildings, a gas boiler (GB) is installed instead of a BHP. The GB and the HP together provide space heating and DHW, and are used to charge the TES. The GB is installed to supply peak heating demands on cold days. Regarding cooling, the same installations are used in both building types. Just as in the model presented by Wirtz et al. (2021), the cooling demand can be covered in two ways. When the temperature of the cold pipe is lower than the required supply temperature of the cooling circuit in the building, direct cooling (DRC) can be provided by a heat exchanger. Otherwise, a compression chiller (CC) is used.

4.1.2 Objective function

The constructed model aims at determining the optimal design and operation of the 5GDHC system with respect to minimizing the total annualized costs (TAC). The TAC includes the annualized costs for the SWTE installation (C_{SWTE}), the ATES (C_{ATES}), the network infrastructure ($\mathrm{C}_{\mathrm{netw}}$) and the BESs ($C_{\mathrm{BES}}$), as well as the annual costs for gas and electricity (C_{gas} and C_{el}). The objective function of the novel optimization model is therefore:

$$\text{Minimize}: \quad TAC = C_{\mathrm{BES}} + C_{\mathrm{SWTE}} + C_{\mathrm{ATES}} + \mathrm{C}_{\mathrm{netw}} + C_{\mathrm{el}} + C_{\mathrm{gas}} \tag{60}$$

The costs for the network infrastructure consist of the costs for distribution pipes, hydraulic pumps and a technical area. To limit computational time, the costs were calculated prior to the optimization. As the network infrastructure costs do not affect the optimal solution, they are denoted by a constant in the objective function. An elaboration on the calculation of network infrastructure costs is provided in Appendix C.3.

4.1.3 Variable set

A multitude of binary, discrete and continuous variables are included in the optimization model. An overview of all decision variables considered is presented in Table B.2 in Appendix B.2.

4.1.4 Model structure

The constraints included in the model are presented in this section. The constraints are classified in seven categories: building energy systems, energy balances, SWTE, ATES, network temperature, coefficient of performance and costs. The constraints in each category are described below, with decision variables written in italics.

Building energy systems

In well insulated buildings (denoted by B_{high}), the heat pump is used to provide space heating and to deliver heat to the BHP. This is ensured by introducing the constraint:

$$\dot{Q}_{\mathrm{h,HP},b,t} = \dot{\mathrm{Q}}_{\mathrm{h,dem,sh},b,t} + (\dot{Q}_{\mathrm{h,BHP},b,t} - P_{\mathrm{BHP},b,t}) \quad \forall\, b \in B_{\mathrm{high}},\, t \in T \tag{61}$$

with the thermal output of the BHP being expressed by:

$$\dot{Q}_{\mathrm{h,BHP},b,t} = P_{\mathrm{BHP},b,t}\mathrm{COP}_{\mathrm{BHP}} \quad \forall\, b \in B_{\mathrm{high}},\, t \in T \tag{62}$$

Furthermore, the BHP in well insulated buildings is used to charge the TES:

$$\dot{Q}_{\mathrm{h,BHP},b,t} = \dot{Q}^{\mathrm{ch}}_{\mathrm{h,TES},b,t} \quad \forall\, b \in B_{\mathrm{high}},\, t \in T \tag{63}$$

In poorly insulated buildings (denoted by B_{low}), the heat outputs of the HP and GB must match the demand for space heating and the amount of heat charged in the TES:

$$\dot{Q}_{\mathrm{h,HP},b,t} + \dot{Q}_{\mathrm{h,GB},b,t} = \dot{\mathrm{Q}}_{\mathrm{h,dem,sh},b,t} + \dot{Q}^{\mathrm{ch}}_{\mathrm{h,TES},b,t} \quad \forall\, b \in B_{\mathrm{low}},\, t \in T \tag{64}$$

Furthermore, a constraint is introduced that can be used to limit the share of the GB:

$$\sum_{t \in T} \dot{Q}_{\mathrm{h,GB},b,t} \leq f_{\mathrm{GB,max}} \sum_{t \in T} (\dot{\mathrm{Q}}_{\mathrm{h,dem,sh},b,t} + \dot{Q}^{\mathrm{ch}}_{\mathrm{h,TES},b,t}) \quad \forall\, b \in B_{\mathrm{low}} \tag{65}$$

where $f_{\mathrm{GB,max}}$ represents the maximum allowable share of the space heating demand and the amount of heat supplied to the TES that can be met by the GB. GBs are characterized by lower specific investment costs compared to heat pumps. On the other hand, the use of GBs is considered less sustainable. It may therefore be desirable to limit the share of the GBs in certain projects (Royal HaskoningDHV, 2019).

The demand for DHW must be met by the TES in both building types. This is ensured by the constraint:

$$\dot{Q}^{\mathrm{disch}}_{\mathrm{h,TES}} = \dot{\mathrm{Q}}_{\mathrm{h,dem,DHW},b,t} \quad \forall\, b \in B,\, t \in T \tag{66}$$

With regard to the provision of cooling in buildings, the same installations are used in well insulated and poorly insulated buildings. The cooling demand of a building must be met by the cold generated by the CC and DRC in the respective building:

$$\dot{Q}_{\mathrm{c,CC},b,t} + \dot{Q}_{\mathrm{c,DRC},b,t} = \dot{\mathrm{Q}}_{\mathrm{c,dem},b,t} \quad \forall\, b \in B,\, t \in T \tag{67}$$

To ensure that the state of charge (SoC) of the TES in buildings is connected with the SoC of the previous time step, the following constraint is introduced:

$$\begin{aligned} SoC_{\mathrm{TES},b,t}\, cap_{\mathrm{TES},b} = {} & SoC_{\mathrm{TES},b,t-1}\, cap_{\mathrm{TES},b}(1-\phi_{\mathrm{TES,loss}}) \\ & + \eta^{\mathrm{ch}}_{\mathrm{TES}} \dot{Q}^{\mathrm{ch}}_{\mathrm{h,TES},b,t} - \frac{\dot{Q}^{\mathrm{disch}}_{\mathrm{h,TES},b,t}}{\eta^{\mathrm{disch}}_{\mathrm{TES}}} \quad \forall\, b \in B,\, t \in T \;:\; t \neq t_0 \end{aligned} \tag{68}$$

The SoC must be between a lower and an upper limit. This is ensured by the constraint:

$$SoC^{\mathrm{min}}_{\mathrm{TES},b} \leq SoC_{\mathrm{TES},b,t} \leq SoC^{\mathrm{max}}_{\mathrm{TES},b} \quad \forall\, b \in B,\, t \in T \tag{69}$$

Next, the capacity of the TES in buildings may be limited by an upper bound due to limited installation space:

$$cap_{\mathrm{TES},b} \leq cap^{\mathrm{max}}_{\mathrm{TES},b} \quad \forall\, b \in B,\, t \in T \tag{70}$$

Furthermore, the thermal power out of the GBs is linked with the gas consumption by a constant efficiency:

$$\dot{Q}_{\mathrm{h,GB},b,t} = \dot{G}_{\mathrm{GB},b,t}\,\eta_{\mathrm{GB}} \quad \forall\, b \in B,\, t \in T \tag{71}$$

The heat and cold output of the devices in the BES are limited by the capacity of the respective device:

$$\dot{Q}_{\mathrm{h},k,b,t} \leq cap_{k,b} \quad \forall\, k \in \{HP, GB, BHP\},\, b \in B,\, t \in T \tag{72}$$

$$\dot{Q}_{\mathrm{c},k,b,t} \leq cap_{k,b} \quad \forall\, k \in \{CC, DRC\},\, b \in B,\, t \in T \tag{73}$$

Finally, the capacity of BHPs is equal to zero in poorly insulated buildings. In well insulated buildings, no GBs are installed. This is ensured by the constraints:

$$cap_{\mathrm{GB},b} = 0 \quad \forall\, b \in B_{high} \tag{74}$$

$$cap_{\mathrm{BHP},b} = 0 \quad \forall\, b \in B_{low} \tag{75}$$

Energy balances

Three sets of thermal energy balances are included in the novel optimization model. The first energy balance is derived from the model presented by Wirtz et al. (2021) and describes the energy balance for every building b at time step t:

$$\dot{Q}_{\mathrm{res,BES},b,t} = \left(\dot{Q}_{\mathrm{HP},b,t} - P_{\mathrm{HP},b,t}\right) - \left(\dot{Q}_{\mathrm{CC},b,t} + P_{\mathrm{CC},b,t}\right) - \dot{Q}_{\mathrm{DRC},b,t} \quad \forall\, b \in B, t \in T \tag{76}$$

Secondly, an energy balance is introduced to describe the heat flows to and from the network fluid:

$$\dot{Q}_{\mathrm{res,netw},t} = \sum_{b \in B} \left(\dot{Q}_{\mathrm{res,BES},b,t}\right) + \dot{Q}_{\mathrm{loss,wp},t} - \dot{Q}_{\mathrm{loss,cp},t} + \dot{Q}_{\mathrm{netw},t} \quad \forall\, t \in T \tag{77}$$

The third thermal energy balance ensures that the residual network demand is met by the SWTE and ATES systems:

$$\dot{Q}_{\mathrm{res,netw},t} = \dot{Q}_{\mathrm{h,SWTE},t} - \dot{Q}_{\mathrm{c,SWTE},t} + \dot{Q}_{\mathrm{h,ATES},t} - \dot{Q}_{\mathrm{c,ATES},t} \quad \forall\, t \in T \tag{78}$$

In addition, two constraints that describe the electric energy balances are included in the optimization model. The electricity demand of the BES in building b at time step t is equal to the sum of the electric power of the HP, BHP and CC installed in the respective building:

$$P_{\mathrm{BES},b,t} = P_{\mathrm{HP},b,t} + P_{\mathrm{BHP},b,t} + P_{\mathrm{CC},b,t} \quad \forall\, b \in B, t \in T \tag{79}$$

Next, the sum of all BESs, the electricity demand for the distribution grid and the electricity demands of the SWTE and ATES systems must be met by the power imported from the grid:

$$P_{\mathrm{el,grid},t} = \sum_{b \in B} \left(P_{\mathrm{BES},b,t}\right) + P_{\mathrm{SWTE},t} + P_{\mathrm{ATES},t} + \mathrm{P}_{\mathrm{netw},t} \quad \forall\, t \in T \tag{80}$$

It should be noted that the latter constraint is slightly different from the electric energy balance proposed by Wirtz et al. (2021) (see Eq. (20)). This is because no PV modules are considered in the energy system structure and no excess power can be delivered to the electricity grid. Furthermore, the electricity required by the distribution pumps ($\mathrm{P}_{\mathrm{netw},t}$) is not part of the optimization. This is to limit computational time. An elaboration on the calculation of the required pumping

power is provided in Appendix C.3. Finally, the amount of gas imported from the gas grid is equal to the sum of the gas consumption by GBs installed in the buildings. This is ensured by the constraint:

$$\dot{Q}_{\text{grid},t} = \sum_{b \in B} \dot{G}_{\text{GB},b,t} \quad \forall\, t \in T \tag{81}$$

SWTE

The amount of heat that can be extracted by a SWTE system is dependent on the pump flow rate and the maximum allowable temperature change of the surface water. This is reflected by the constraint:

$$\dot{Q}_{\text{h,SWTE},t} = \text{c}_\text{w} \dot{V}_{\text{SWTE},t} \Delta T_{\text{HE},t} \quad \forall\, t \in T \tag{82}$$

Likewise, the following constraint is introduced for cold extraction:

$$\dot{Q}_{\text{c,SWTE},t} = \text{c}_\text{w} \dot{V}_{\text{SWTE},t} \Delta \text{T}_{\text{CE,t}} \quad \forall\, t \in T \tag{83}$$

Since the temperature increase of the surface water during cold extraction is 3 °C regardless of the surface water temperature, $\Delta \text{T}_{\text{CE,t}}$ is a constant (de Boer et al., 2015). During heat extraction, the allowable temperature change of the surface water ($\Delta \text{T}_{\text{HE,t}}$) is 3-6 K (de Boer et al., 2015). This is expressed by the constraint:

$$\Delta T_{\text{HE},t} = max(min(\text{T}_{\text{SW},t} - \text{T}_{\text{SW,min}}, \Delta \text{T}_{\text{HE,max}}), 0) \quad \forall\, t \in T \tag{84}$$

Here, $\text{T}_{\text{SW,min}}$ represents the minimum allowable temperature at the outlet of the SWTE system during heat extraction. According to Dutch regulations, surface water may not be cooled down below 12 °C (de Boer et al., 2015).

Furthermore, a SWTE system can only deliver heat to the distribution network efficiently when the surface water temperature exceeds 15 °C (de Boer et al., 2015; Syntraal et al., n.d.). Additionally, the temperature of the surface must be higher than the temperature of the warm pipe of the network while taking the minimum temperature difference across the heat exchanger into account. To incorporate this in the optimization model, the binary variables $x_{1,\text{HE},t}$ and $x_{2,\text{HE},t}$ are introduced:

$$\text{T}_{\text{SW,HE,min}} - \text{T}_{\text{SW},t} \leq (1 - x_{1,\text{HE},t}) \text{M}_{1,\text{HE}} \quad \forall\, t \in T \tag{85}$$

$$T_{\text{netw,wp},t} + \Delta \text{T}_{\text{HEX,min}} - \text{T}_{\text{SW},t} \leq (1 - x_{2,\text{HE},t}) \text{M}_{2,\text{HE}} \quad \forall\, t \in T \tag{86}$$

where $M_{1,HE}$ and $M_{2,HE}$ are big-M coefficients. Eqs. (85) and (86) force the binary variables to 1 if heat can be extracted by the SWTE system. Moreover, the heat generation of the SWTE system is limited by its capacity and by the capacity of the surface water:

$$\dot{Q}_{\text{h,SWTE},t} \leq cap_{\text{SWTE}} x_{1,\text{HE},t} x_{2,\text{HE},t} \quad \forall\, t \in T \tag{87}$$

$$\sum_{t \in T} \dot{Q}_{\text{h,SWTE},t} \leq \text{E}_{\text{h,SW}} \tag{88}$$

The first constraint ensures that heat can only be produced at times when both $x_{1,\text{HE},t}$ and $x_{2,\text{HE},t}$ are equal to 1. In the second constraint, $\text{E}_{\text{h,SW}}$ represents the amount of heat that can be extracted from the surface water body annually.

According to de Boer et al. (2015), cold can only be extracted from a surface water body when the temperature is below 7 °C. Furthermore, the temperature of the cold pipe must be higher than the temperature of the surface water. Consequently, the binary variables $x_{1,\mathrm{CE},t}$ and $x_{2,\mathrm{CE},t}$ are introduced:

$$\mathrm{T}_{\mathrm{SW},t} - \mathrm{T}_{\mathrm{SW,CE,max}} \leq (1 - x_{1,\mathrm{CE},t})\mathrm{M}_{1,\mathrm{CE}} \quad \forall\, t \in T \tag{89}$$

$$\mathrm{T}_{\mathrm{SW},t} + \Delta\mathrm{T}_{\mathrm{HEX,min}} - T_{\mathrm{netw,cp},t} \leq (1 - x_{2,\mathrm{CE},t})\mathrm{M}_{2,\mathrm{CE}} \quad \forall\, t \in T \tag{90}$$

with $M_{1,CE}$ and $M_{2,CE}$ being big-M coefficients. $x_{1,\mathrm{CE},t}$ and $x_{2,\mathrm{CE},t}$ are forced to 1 at times that cold can be generated by the SWTE system. The cold generation is limited by the capacity of the SWTE system:

$$\dot{Q}_{\mathrm{c,SWTE},t} \leq cap_{\mathrm{SWTE}} x_{1,\mathrm{CE},t} x_{2,\mathrm{CE},t} \quad \forall\, t \in T \tag{91}$$

Finally, the electricity demand of the SWTE system is dependent on the thermal energy production. This is expressed by the constraint:

$$P_{\mathrm{SWTE},t} = e_{\mathrm{SWTE}}(\dot{Q}_{\mathrm{h,SWTE},t} + \dot{Q}_{\mathrm{c,SWTE},t}) \quad \forall\, t \in T \tag{92}$$

where e_{SWTE} represents the specific electricity use of the SWTE system.

ATES

The thermal heating and cooling power retrieved from the groundwater in the ATES system are dependent on the pumping flow rates of the ATES wells along with the temperature difference between the hot and cold wells ($\Delta\mathrm{T}_{\mathrm{hc}}$):

$$\dot{Q}_{\mathrm{h,ATES},t} = c_w \dot{V}_{\mathrm{hc},t} \Delta\mathrm{T}_{\mathrm{hc}} \quad \forall\, t \in T \tag{93}$$

$$\dot{Q}_{\mathrm{c,ATES},t} = c_w \dot{V}_{\mathrm{ch},t} \Delta\mathrm{T}_{\mathrm{hc}} \quad \forall\, t \in T \tag{94}$$

It is assumed that $\Delta\mathrm{T}_{\mathrm{hc}}$ is constant. However, the temperatures of hot and cold wells ($T_{\mathrm{ATES,hw}}$ and $T_{\mathrm{ATES,cw}}$) are discrete decision variables. The relationship between the well temperatures is described by:

$$T_{\mathrm{ATES,hw}} = T_{\mathrm{ATES,cw}} + \Delta\mathrm{T}_{\mathrm{hc}} \tag{95}$$

The pumping flow rates of the hot and cold wells are limited by the maximum allowable flow rate per well:

$$\dot{V}_{\mathrm{hc},t} \leq n_{\mathrm{doublets}} \dot{\mathrm{V}}_{\mathrm{max,doublet}} \quad \forall\, t \in T \tag{96}$$

$$\dot{V}_{\mathrm{ch},t} \leq n_{\mathrm{doublets}} \dot{\mathrm{V}}_{\mathrm{max,doublet}} \quad \forall\, t \in T \tag{97}$$

where n_{doublets} is an integer variable that denotes the number of doublets installed.

The amount of heat and cold stored in the ATES wells is connected with the amount of thermal energy stored in the previous time step. This is ensured by the constraints:

$$E_{\mathrm{hw},t} = E_{\mathrm{hw},t-1} - \dot{Q}_{\mathrm{h,ATES},t} + \dot{Q}_{\mathrm{c,ATES},t} \quad \forall\, t \in T : t \neq t_0 \tag{98}$$

$$E_{\mathrm{cw},t} = E_{\mathrm{cw},t-1} - \dot{Q}_{\mathrm{c,ATES},t} + \dot{Q}_{\mathrm{h,ATES},t} \quad \forall\, t \in T : t \neq t_0 \tag{99}$$

Furthermore, Dutch regulations require balancing of ATES systems (DWA & IF Technology,

2012). This implies that the amount of heat extracted from the ATES system must be equal to the amount of cold extracted. This is ensured by the constraints:

$$\sum_{t \in T} \dot{Q}_{\mathrm{h,ATES},t} = \sum_{t \in T} \dot{Q}_{\mathrm{c,ATES},t} \tag{100}$$

The usable volumes of water stored in the hot and cold wells of the ATES system are linked to the amount of energy stored in the respective wells:

$$V_{\mathrm{hw},t} = \frac{E_{\mathrm{hw},t} * 3600}{\mathrm{c_w} \Delta \mathrm{T_{hc}}} \quad \forall\, t \in T \tag{101}$$

$$V_{\mathrm{cw},t} = \frac{E_{\mathrm{cw},t} * 3600}{\mathrm{c_w} \Delta \mathrm{T_{hc}}} \quad \forall\, t \in T \tag{102}$$

An ATES system can only deliver heat to the distribution network at times when the temperature of the warm pipe is lower than the temperature of the hot well. At the same time, the temperature of the cold well must be higher than the temperature of the cold pipe. This is to maintain the temperature in the cold well. To incorporate this in the optimization approach, the binary variables $y_{1,\mathrm{ATES,h},t}$ and $y_{2,\mathrm{ATES,h},t}$ are introduced. The binary variables are forced to 1 at times when heat can be provided by the ATES by the constraints:

$$T_{\mathrm{netw,wp},t} + \Delta \mathrm{T_{HEX,min}} - \mathrm{T_{ATES,hw}} \leq (1 - y_{1,\mathrm{ATES,h},t}) \mathrm{M_{1,ATES,h}} \quad \forall\, t \in T \tag{103}$$

$$T_{\mathrm{netw,cp},t} + \Delta \mathrm{T_{HEX,min}} - \mathrm{T_{ATES,cw}} \leq (1 - y_{2,\mathrm{ATES,h},t}) \mathrm{M_{2,ATES,h}} \quad \forall\, t \in T \tag{104}$$

with $\mathrm{M_{1,ATES,h}}$ and $\mathrm{M_{2,ATES,h}}$ being big-M coefficients. On the contrary, the temperature of the warm pipe must be higher than the temperature of the hot well during the provision of cold. Besides, the temperature of the cold well must be lower than the temperature of the cold pipe. This is insured by including the binary variables $y_{1,\mathrm{ATES,h},t}$ and $y_{2,\mathrm{ATES,h},t}$ into the constraints:

$$\mathrm{T_{ATES,hw}} + \Delta \mathrm{T_{HEX,min}} - T_{\mathrm{netw,wp},t} \leq (1 - y_{1,\mathrm{ATES,c},t}) \mathrm{M_{1,ATES,c}} \quad \forall\, t \in T \tag{105}$$

$$\mathrm{T_{ATES,cw}} + \Delta \mathrm{T_{HEX,min}} - T_{\mathrm{netw,cp},t} \leq (1 - y_{2,\mathrm{ATES,c},t}) \mathrm{M_{2,ATES,c}} \quad \forall\, t \in T \tag{106}$$

where $\mathrm{M_{1,ATES,c}}$ and $\mathrm{M_{2,ATES,c}}$ are big-M coefficients.

The thermal heating and cooling power delivered by the ATES is limited by the capacity of the system. At times when one of the binary variables equals 0, the thermal power is equal to zero. This is ensured by introducing the following constraints:

$$\dot{Q}_{\mathrm{h,ATES},t} \leq \mathrm{cap_{ATES}} y_{1,\mathrm{ATES,h},t} y_{2,\mathrm{ATES,h},t} \quad \forall\, t \in T \tag{107}$$

$$\dot{Q}_{\mathrm{c,ATES},t} \leq \mathrm{cap_{ATES}} y_{1,\mathrm{ATES,c},t} y_{2,\mathrm{ATES,c},t} \quad \forall\, t \in T \tag{108}$$

Finally, the electricity demand of the ATES system is determined by the heating and cooling power of the system:

$$P_{\mathrm{ATES},t} = e_{\mathrm{ATES}} (\dot{Q}_{\mathrm{h,ATES},t} + \dot{Q}_{\mathrm{c,ATES},t}) \quad \forall\, t \in T \tag{109}$$

where e_{ATES} denotes the specific electricity use of the ATES system.

Network temperature

Just like in the model presented by Wirtz et al. (2021), the temperatures of the warm and cold pipes are related to the mean network temperature:

$$T_{\mathrm{netw,wp},t} = \bar{T}_{\mathrm{netw},t} + \frac{\Delta \mathrm{T}_{\mathrm{netw}}}{2} \quad \forall\, t \in T \tag{110}$$

$$T_{\mathrm{netw,cp},t} = \bar{T}_{\mathrm{netw},t} - \frac{\Delta \mathrm{T}_{\mathrm{netw}}}{2} \quad \forall\, t \in T \tag{111}$$

Moreover, the temperatures of the pipes must be in a predefined range $[\mathrm{T}^{\mathrm{min}}_{\mathrm{netw,cp}}, \mathrm{T}^{\mathrm{max}}_{\mathrm{netw,wp}}]$. The range is subdivided into $\mathrm{n}_{\mathrm{int}}$ discrete temperature intervals $[\mathrm{T}_{\mathrm{low},i}, \mathrm{T}_{\mathrm{up},i}]\ \forall\, i \in (0, ..., \mathrm{n}_{\mathrm{int}} - 1)$ with constant interval width $\Delta \mathrm{T}_{\mathrm{int}}$:

$$\mathrm{T}_{\mathrm{up},i} = \mathrm{T}^{\mathrm{min}}_{\mathrm{netw,cp}} + \frac{\Delta \mathrm{T}_{\mathrm{netw}}}{2} + (i+1)\Delta \mathrm{T}_{\mathrm{int}} \tag{112}$$

$$\mathrm{T}_{\mathrm{low},i} = \mathrm{T}^{\mathrm{min}}_{\mathrm{netw,cp}} + \frac{\Delta \mathrm{T}_{\mathrm{netw}}}{2} + k\Delta \mathrm{T}_{\mathrm{int}} \tag{113}$$

Subsequently, the binary variable $\theta_{i,t}$ is introduced. This variable equals 1 when the mean network temperature is in the corresponding interval. To ensure that only 1 interval is active at one time step t, the following constraint is included:

$$\sum_{k=0}^{\mathrm{n}_{\mathrm{int}}-1} \theta_{i,t} = 1 \quad \forall\, t \in T \tag{114}$$

Next, the variable $T^{\theta}_{i,t}$ is introduced. The value of this variable is forced to be equal to the value of mean network temperature if the interval i is active by the constraints:

$$T^{\theta}_{i,t} \geq \theta_{i,t} \mathrm{T}_{\mathrm{low},i} \quad \forall\, i \in (0, ..., \mathrm{n}_{\mathrm{int}} - 1),\ \forall\, t \in T \tag{115}$$

$$T^{\theta}_{i,t} \leq \theta_{i,t} \mathrm{T}_{\mathrm{up},i} \quad \forall\, i \in (0, ..., \mathrm{n}_{\mathrm{int}} - 1),\ \forall\, t \in T \tag{116}$$

The mean network temperature is equal to the sum of all variables $T^{\theta}_{i,t}$:

$$\bar{T}_{\mathrm{netw},t} = \sum_{i=0}^{\mathrm{n}_{\mathrm{int}}-1} T^{\theta}_{i,t} \quad \forall\, t \in T \tag{117}$$

Subsequently, a constraint that describes the relationship between the mean network temperature of two consecutive time steps is introduced:

$$\bar{T}_{\mathrm{netw},t} = \bar{T}_{\mathrm{netw},t-1} + \Delta T_t \quad \forall\, t \in T\ :\ t \neq t_0 \tag{118}$$

Alternating the temperature of the water in the distribution pipes requires a certain amount of thermal power. This is described by the constraint:

$$\dot{Q}_{\mathrm{netw},t} = \rho_{\mathrm{w}} \mathrm{V}_{\mathrm{netw}} \mathrm{c}_{\mathrm{w}} \Delta T_t \quad \forall\, t \in T \tag{119}$$

where $\mathrm{V}_{\mathrm{netw}}$ represents the volume of the water in the distribution network.

Heat losses

According to Roossien et al. (2020), the heat flow between a distribution pipe and the soil can be calculated using Eq. 4. As the network infrastructure consists multiple segments s, the heat losses from the warm and cold pipes can be calculated using:

$$\dot{Q}_{\text{loss,wp},t} = \sum_{s \in S} \frac{(T_{\text{netw,wp}} - \text{T}_{\text{soil},t})}{\text{R}_{\text{i},s} + \text{R}_{\text{s},s}} \quad \forall\, t \in T \tag{120}$$

$$\dot{Q}_{\text{loss,cp},t} = \sum_{s \in S} \frac{(T_{\text{netw,cp}} - \text{T}_{\text{soil},t})}{\text{R}_{\text{i},s} + \text{R}_{\text{s},s}} \quad \forall\, t \in T \tag{121}$$

As the network topology is defined prior to the optimization, the thermal resistances of the distribution pipes and the soil of network segments are denoted by constants. An elaboration on the calculations is provided in Appendix C.3.

Coefficient of performance and direct cooling

The COPs of the heat pumps and chillers are determined for each interval i prior to the optimization. This is done using the method proposed by Jensen et al. (2018). The heating or cooling power of the heat pumps and chillers in each building is then described by:

$$\dot{Q}_t = \sum_{i=0}^{\text{n}_{\text{int}}-1} [\text{COP}_{i,t}\, \theta_{i,t}] P_t \quad \forall\, t \in T \tag{122}$$

As discussed in section 2.1.1, DRC can be provided to buildings at times when the required cooling supply temperature exceeds the temperature of the cold pipe. In case the temperature difference between the warm and cold pipe is greater than the difference between the supply and return temperatures of cooling circuit, the following constraint is used:

$$T_{\text{netw,wp},t} + \Delta\text{T}_{\text{HEX,min}} - \text{T}_{\text{c,return},b,t} \leq (1 - y_{\text{DRC},b,t})\text{M}_{\text{DRC},b} \quad \forall\, b \in B,\, t \in T \tag{123}$$

Otherwise the constraint:

$$T_{\text{netw,cp},t} + \Delta\text{T}_{\text{HEX,min}} - \text{T}_{\text{c,supply},b,t} \leq (1 - y_{\text{DRC},b,t})\text{M}_{\text{DRC},b} \quad \forall\, b \in B,\, t \in T \tag{124}$$

is active. Here, $\text{M}_{\text{DRC},b}$ is a big-M coefficient. The equations both ensure that no cooling is supplied by the heat exchanger when $y_{\text{DRC},b,t}$ is equal to zero. Moreover, the cooling power is the heat exchanger is limited by its capacity:

$$\dot{Q}_{\text{c,DRC},b,t} \leq y_{\text{DRC},b,t} cap_{\text{DRC},b} \quad \forall\, t \in T \tag{125}$$

Costs calculation

The annualized costs for the BESs in all buildings are dependent on the annualized investment costs and the annual O&M costs for the technologies installed in the buildings. Furthermore, internal distribution pipes (IDPs) and internal hydraulic pumps (IHPs) are required in apartment buildings to transfer heat from the heat pump to the individual dwellings. Moreover, heat interface units (HIUs) are needed to transfer heat from the IDPs to the heating systems of the

dwellings. The annualized costs for the BESs is therefore expressed by the constraint:

$$C_{\mathrm{BES}} = \sum_{b \in B} \sum_{k \in K_{\mathrm{BES}}} I_{k,b}(a_{\mathrm{inv},k} + f_{\mathrm{om},k}) + \sum_{b \in B} (I_{\mathrm{IDP},b}(a_{\mathrm{inv,IDP}} + f_{\mathrm{om,IDP}}) + I_{\mathrm{IHP},b}(a_{\mathrm{inv,IHP}} + f_{\mathrm{om,IHP}}) + I_{\mathrm{HIU},b}(a_{\mathrm{inv,HIU}} + f_{\mathrm{om,HIU}})) \tag{126}$$

Here, K_{BES} denotes the set of all technologies k in the BES. Furthermore, $a_{\mathrm{inv},k}$ represents the capital recovery factor for the respective technology. $f_{\mathrm{om},k}$ denotes the share for O&M. The investment costs $I_{k,b}$ are calculated using constant specific investment costs:

$$I_{k,b} = i_{k,\mathrm{BES}} cap_{k,b} \quad \forall\, k \in K_{\mathrm{BES}},\ b \in B \tag{127}$$

For the heating and cooling units in the BES, $cap_{k,b}$ denotes the rated heating and cooling power. For the TES installed in each building, $cap_{k,b}$ represents the storage capacity. An elaboration on the investment costs for the IDPs, IHPs and HIUs is provided in Appendix C.2. The annualized costs for the SWTE and ATES systems were determined using the constraints:

$$C_{\mathrm{SWTE}} = I_{\mathrm{SWTE}}(a_{\mathrm{inv,SWTE}} + f_{\mathrm{om,SWTE}}) \tag{128}$$

$$C_{\mathrm{ATES}} = I_{\mathrm{ATES}}(a_{\mathrm{inv,ATES}} + f_{\mathrm{om,ATES}}) \tag{129}$$

$$I_{\mathrm{SWTE}} = i_{\mathrm{SWTE}} cap_{\mathrm{SWTE}} \tag{130}$$

$$I_{\mathrm{ATES}} = i_{\mathrm{ATES}} cap_{\mathrm{ATES}} \tag{131}$$

Here, cap_{SWTE} and cap_{ATES} denote the rated thermal power of the SWTE and ATES systems respectively.

As described in section 4.1.2, the network topology is defined prior to the optimization. The annualized costs for the distribution network ($\mathrm{C_{netw}}$) is therefore a constant. The network infrastructure consists of distribution pipes, hydraulic pumps and a technical area. An elaboration on the calculation of the investment costs for the different components of the network infrastructure is provided in Appendix C.3.

Finally, the annual costs for gas (C_{gas}) are calculated by multiplying the total amount of gas imported from the grid by the gas price:

$$\mathrm{C_{gas}} = \sum_{t \in T} \dot{Q}_{\mathrm{grid},t}\, p_{\mathrm{gas}} \tag{132}$$

Accordingly, the annual costs for electricity are determined using:

$$\mathrm{C_{el}} = \sum_{t \in T} P_{\mathrm{el,grid},t}\, p_{\mathrm{el}} \tag{133}$$

4.2 Application of novel optimization model to a real-world case

This section starts with a description of the use case considered. Next, the costs structure of the 5GDHC solution is described. Finally, the optimal design and operation of the 5GDHC system for the real-world case are presented.

4.2.1 Use case description

The novel MILP optimization model was applied to the KNSM Island in Amsterdam. This is a man-made peninsula located in the IJ that mainly contains residential buildings built in the 1990s. Part of the buildings is already connected to a high-temperature DH network. The other 15 buildings were taken into consideration in this case study. The cumulated space heating, DHW and cooling demands of the buildings are shown in Figure 13. The annual space heating demand amounts to 9.3 GWh and shows a peak demand of 8.6 MW. The annual DHW demand is 2.8 GWh with a peak of 0.7 MW. Since no differentiation was made between days, the DHW profile follows the same pattern every 24 hours. The annual demand for cooling is significantly lower (0.3 GWh). The peak cooling demand is 5.7 MW.

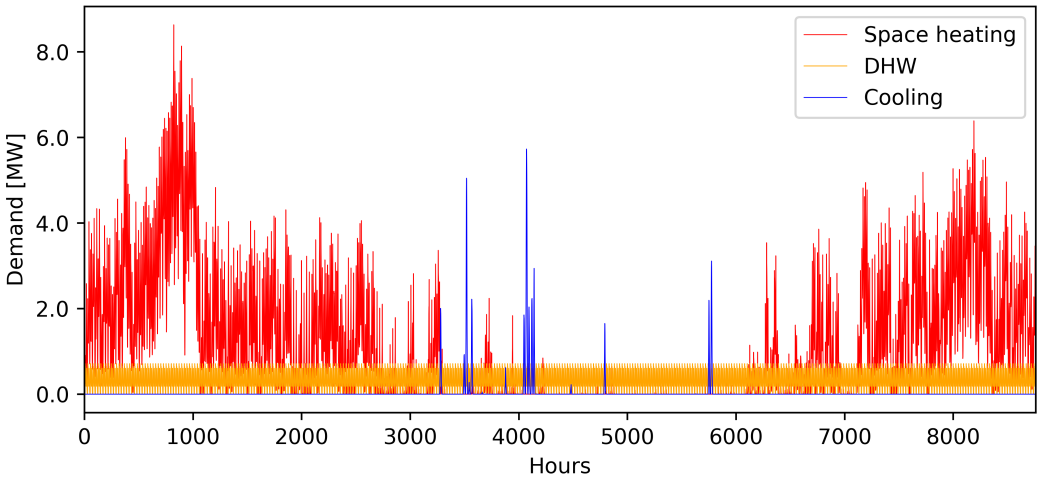

Figure 13: Cumulated space heating, DHW and cooling demands of the 15 buildings considered in the case study

The space heating, DHW and cooling demands and the geographical arrangement of the buildings is presented in Figure 14. The characteristics of the individual buildings are presented in Appendix C.4. The buildings stock consists of apartment buildings and a multi-tenant building for the creative industry (Building 1). Space heating represents the largest share of the total demand in all buildings, followed by DHW and cooling. Building 14 is the largest consumer, as it represents 27% (3.3 GWh) of the total thermal energy demand. Buildings 1, 11, 13 and 15 have energy label G, and are therefore considered poorly insulated buildings. The other buildings are considered to be well insulated, as they have energy label B.

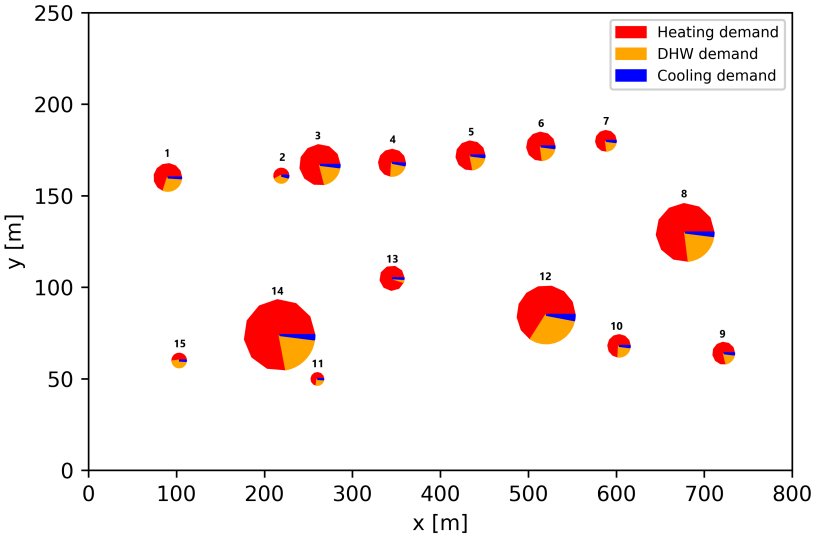

Figure 14: Geographical arrangement of the 15 buildings and their annual space heating (red), DHW (orange) and cooling (blue) demands.

The temperature profile of the surface water of the case study is presented in Figure 15. The temperature of the surface water exceeds 15 °C from the end of May to the end of September. This is the minimum temperature required for heat extraction. The maximum temperature of the surface water is 23 °C. Furthermore, the heat extraction capacity of the water body is 411 TJ/year.

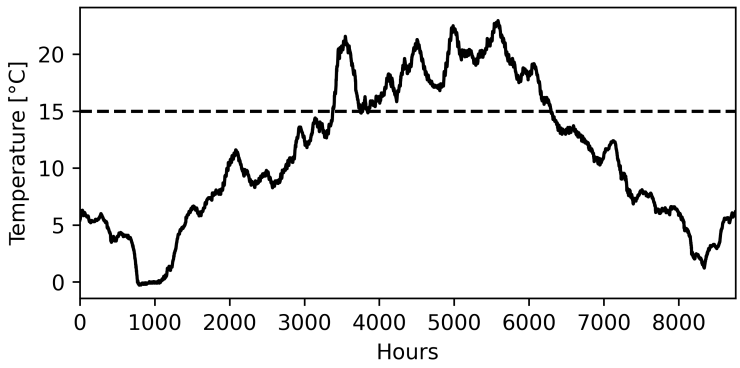

Figure 15: Surface water temperature profile

4.2.2 Costs structure

The TAC for the 5GDHC system with ATES and SWTE amount to 1.76 M€/a. The costs structure is depicted in Figure 16. The costs for the BES components represent the largest cost portion (0.90 M/€a, 51.1% of TAC). This is mainly caused by the HPs, IDPs and HIUs, as these components account for respectively 26.7%, 31.9% and 32.4% of the annualized costs for the BESs.

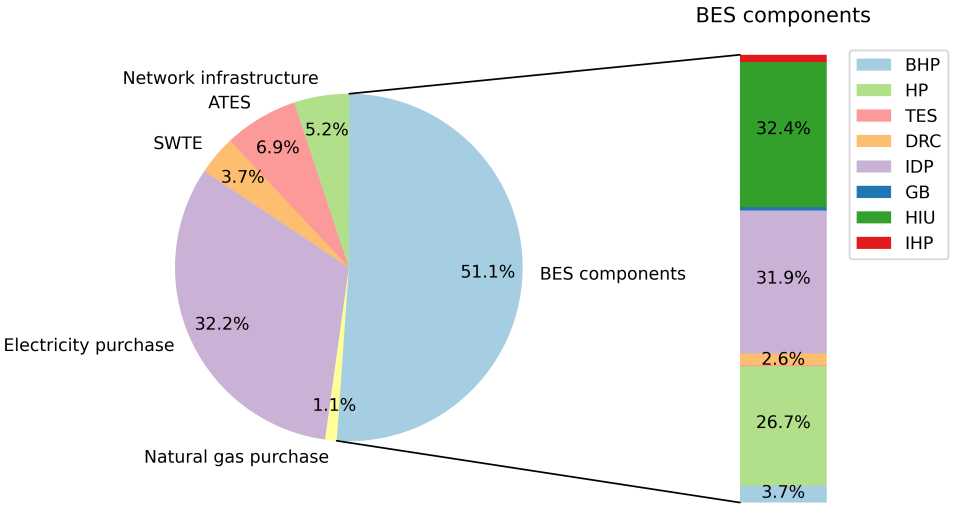

Figure 16: Costs structure of the 5GDHC system with ATES and SWTE, with the costs structure of the BESs presented in the bar chart. The TESs, GBs, and IHPs account for respectively 0.2%, 0.7% and 1.6% of the annualized costs for the BESs.

The second largest cost portion (0.57 M€/a, 32.2% of TAC) results from the electricity use of the various components in the 5GDHC system. The annual costs for natural gas purchase are significantly lower (0.02 M€/a, 1.1% of TAC). Furthermore, the results of the optimization show that the annualized costs for the ATES system exceed the costs for the SWTE installation (0.12 M€/a vs. 0.06 M€/a). Finally, the annualized costs for the network infrastructure amount to 0.09 M€/a. This includes the costs for the distribution pipes, the distribution pumps and the technical area. An elaboration on the calculation of the costs for the network infrastructure components is provided in Appendix C.4.

4.2.3 Installed capacities and generation

This section starts with a description of the optimal design and operation of the technologies installed in the BESs. Subsequently, the optimal operation of the energy hub and corresponding network temperatures are discussed.

Building energy systems

The cumulated capacities, annual thermal energy generation and full load hours of the technologies installed in the BESs are shown in Table 3. The installed capacity of the HPs is 8.2 MW. In total, the HPs produce 11.5 GWh of heat annually, which corresponds to 1406 full load hours. The average COPs of the HPs installed in poorly and well insulated buildings are respectively 3.8 and 4.3, resulting in an annual electricity use of 2.7 GWh.

Table 3: Cumulated capacities and operation of technologies installed in BESs

Technology	Capacity [MW]	Generation [GWh]	Full load hours [h/a]
HP	8.2	11.5	1406
BHP	0.3	2.9	8662
GB	1.0	0.2	214
CC	-	-	-
DRC	5.7	0.3	46

The BHPs installed in well insulated buildings are characterized by high full load hours (8662 h/a). This implies that the BHPs are almost always operated at full capacity to charge the TES for DHW. The total storage capacity of the TES installed in the buildings is 2.6 MWh. In poorly insulated buildings, GBs are used to cover the peak heating demand and provide 0.2 GWh of heat annually. This corresponds to exactly 20% of the space heating demand and the amount of heat supplied to the TES, which was set as the maximum allowable share that could be met by the GBs. Despite their limited operation (full load hours: 214 h/a), the GBs enable to reduce the required HP capacity in poorly insulated buildings. Furthermore, it stands out that no CCs are installed in any of the buildings. The cooling demands of the buildings are completely covered by DRCs. As the buildings in the case study only have a cooling demand during short periods of the year (see Figure 13), the DRCs are characterized by low full load hours (46 h/a).

The balancing of the thermal demands in the 5GDHC system is depicted in Figure 17. Figure 17.A shows the cumulated heating and cooling demands of the buildings. Here, the heating demand encompasses both the space heating demand and the demand for DHW. The heating and cooling demands that are not balanced within the BESs are depicted in Figure 17.B. It stands out that the heating demand is significantly lowered (from 12.1 to 8.4 GWh). Simultaneously, the peak heating demand is reduced from 9.1 MW to 5.9 MW. This is caused by several factors. Firstly, part of the heat supplied comes from the electricity consumption of the HPs and BHPs. Furthermore, part of the heating demand in poorly insulated buildings is provided by the GBs. This portion is excluded from the remaining BESs demand. The TESs also play a part, as they are used to shift part of the heating demand over time. Finally, the heating and cooling demands in individual buildings partially cancel each other out. The effect of this factor is limited, as the buildings only have a heating demand for DHW at times of cooling demand. As a result, the peak cooling demand is only slightly reduced from 5.7 MW to 5.5 MW.

The residual network demand that needs to be covered by the energy hub is presented in Figure 17.C. As discussed in section 4.1.4, the residual network demand is determined by the sum of the residual demands of the BESs, the heat losses of the warm and cold distribution pipes and the thermal power used to lower or raise the network temperature. The heating and cooling demands of different BESs will partially cancel each other out if they overlap. This is a result of BESs supplying others with waste heat or cold. As there is not much customers diversity in the case study, i.e. buildings generally have their heating and cooling demands at the same time, the heating and cooling profiles do not differ significantly from those in Figure 17.B. However, differences can be seen with regard to peak heating and cooling demands. The peak heating demand decreases to 5.7 MW. This is due to heat gains in the cold distribution pipe. The peak cooling demand increases to the exact same level due to of lowering the network temperature. The reasoning behind this is explained in the next section.

Energy hub and network temperatures

The optimal capacities of the ATES and SWTE systems are respectively 5.7 and 3.6 MW. Four ATES doublets are installed, each with a maximum pumping flow rate of 197 m^3/h. The optimal temperatures of the hot and cold wells are 13 °C and 7 °C. The operation of the ATES and SWTE systems is depicted in Figure 18. Figure 18.A shows the amount of heat and cold that is extracted from the groundwater by the ATES at each time step. The amount of thermal energy produced by the SWTE installation is shown in Figure 18.B. The residual network demand and mean network temperature profile are depicted in Figures 18.C and 18.D. When analysing the operation of the ATES and SWTE systems, four unique situations can be distinguished.

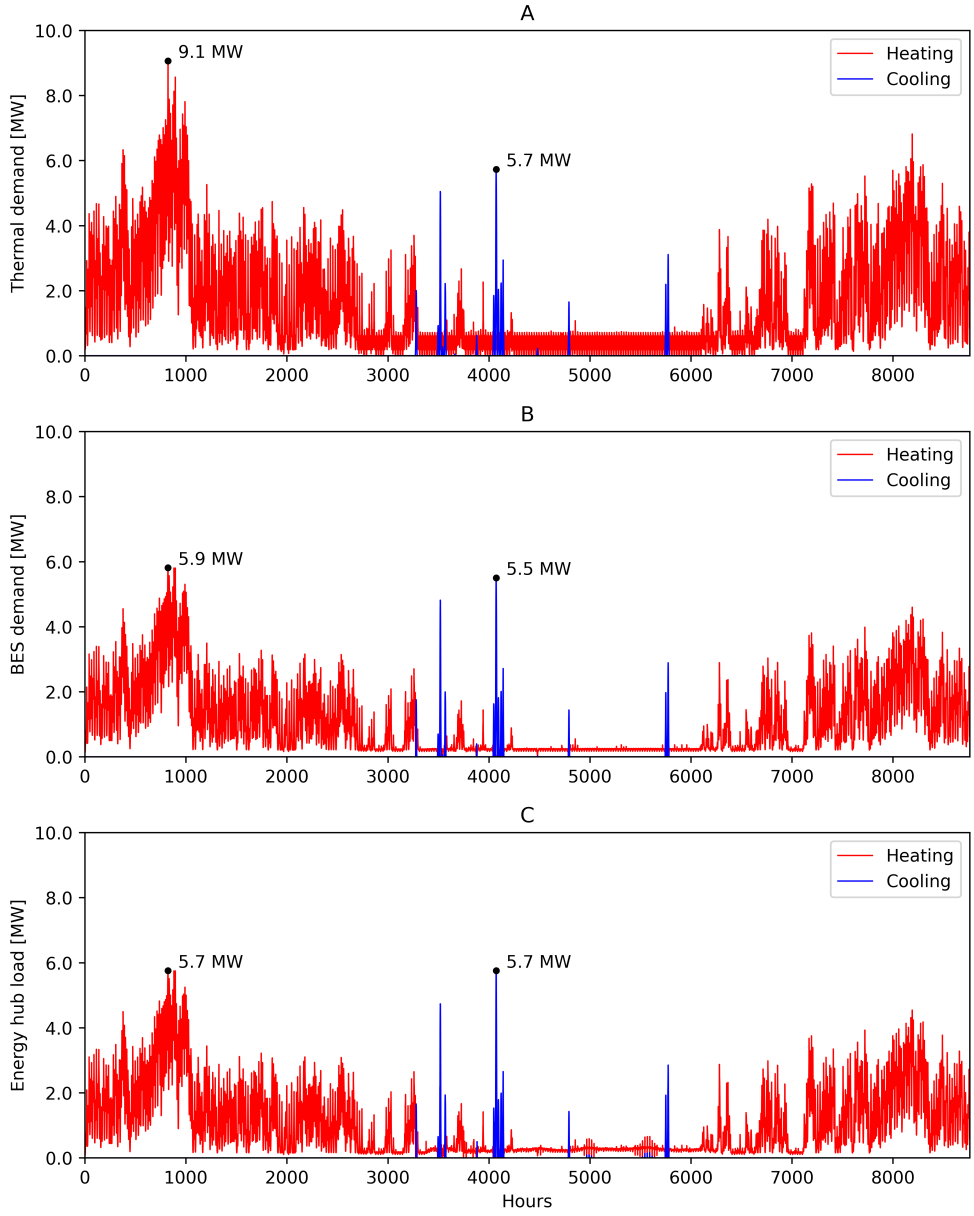

Figure 17: Balancing of the thermal demands in 5GDHC system. (A) shows the cumulated heating and cooling demands of the buildings. (B) depicts the heating and cooling demands that are not balanced with BESs. The thermal demands that must be met by the energy hub are presented in (C).

The first situation occurs when there is a residual network heating demand and the surface water temperature (depicted in Figures 18.E.) is below the threshold value of 15 °C. The SWTE installation is unable to produce heat at these times, so the heating demand must be met by the ATES system. Considering the temperature of the hot wells (13 °C) and the minimum temperature difference across the heat exchanger (1 K), this implies that the temperature of the warm distribution pipe must be equal to 12 °C. This value was defined as the minimum allowable temperature (see Appendix C.4). Consequently, the mean network temperature is 8 °C. Moreover, the peak heating demand occurs under the described circumstances. The capacity of the ATES system is determined by this peak.

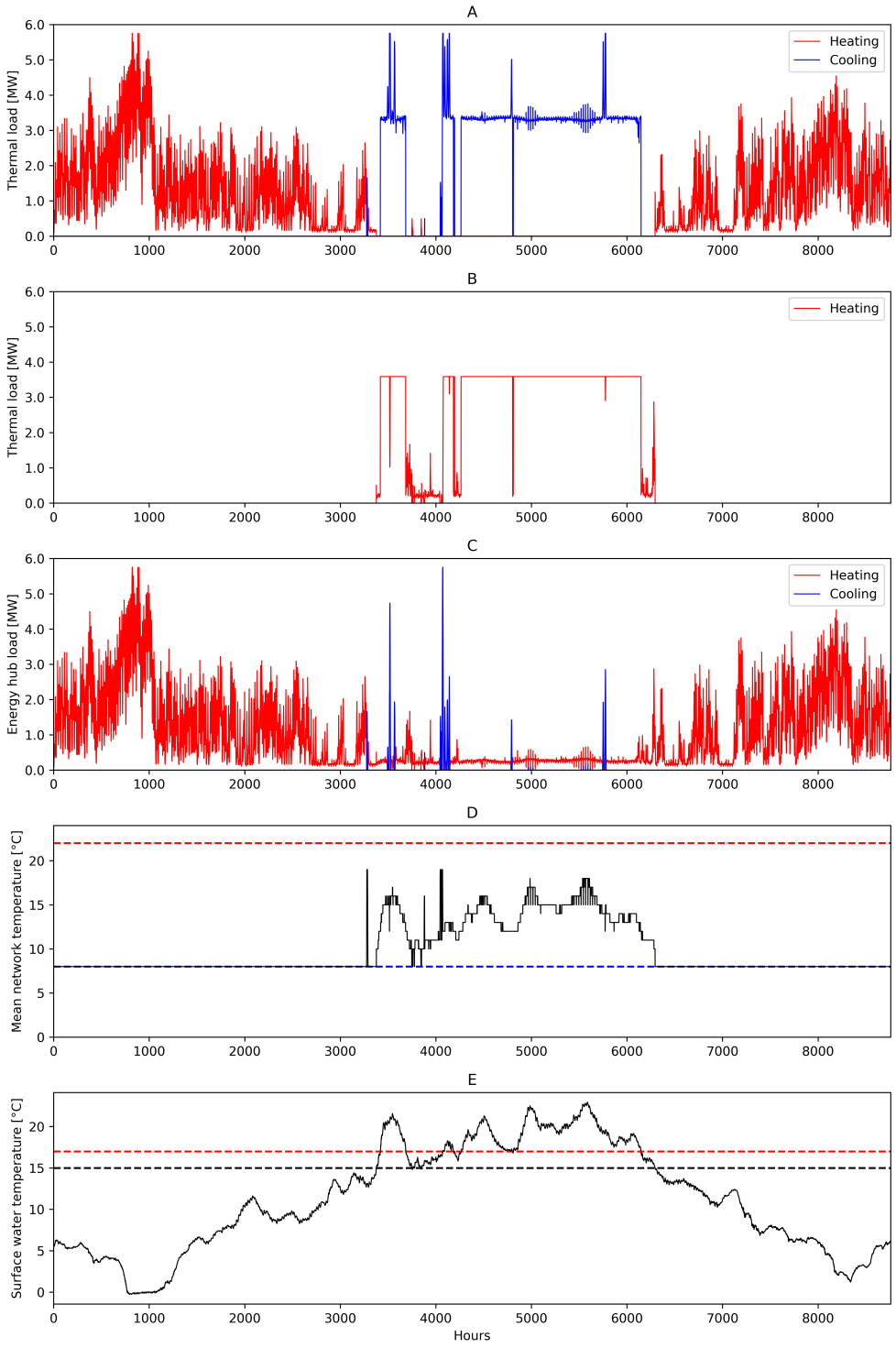

Figure 18: Operation of ATES and SWTE systems. (A) shows the thermal load extracted from the groundwater by the ATES. (B) depicts the thermal energy produced by the SWTE installation. The energy hub load is presented in (C). The mean network temperature profiles is presented in (D). The dashed red and blue lines indicate respectively the maximum and minimum allowable mean network temperature. (E) shows the surface water temperature profiles. Here, the dashed red line indicates the minimum required temperature for charging the extracted heat by the SWTE installation into the ATES (17 °C). The dashed black line represents the minimum required for heat extraction by the SWTE (15 °C).

The second situation happens at times of a residual heating demand and a surface water temperature between 15 °C and 17 °C. These surface water temperatures are high enough for heat extraction by the SWTE system. However, the system is unable to charge the extracted heat into the ATES system. To charge heat into the ATES, i.e. cooling is provided by the ATES, the temperature of the cold distribution pipe must be above the cold well temperature of 7 °C. Considering the temperatures difference between the warm and cold pipes of 8 K and the minimum temperature difference across the heat exchangers (2 K), this implies that a surface water temperature above 17 °C is required. So under the conditions of this situation, two things can happen. The residual network heating demand can be directly provided by the SWTE installation, or the required heat can be discharged from the ATES. The solution of the optimization shows that the first option is preferred. If the second option is used, the discharged heat must be recharged at a later time. This will ultimately lead to a larger required capacity of the SWTE installation. The network temperature follows the same pattern as the surface water temperature in this situation.

Subsequently, a situation is distinguished in which there is a residual cooling demand and a surface water temperature below 17 °C. Under these circumstances, the required cooling must be provided by the ATES system. This is because the SWTE installation is unable to extract cooling, as residual cooling demand only occurs at times of surface water temperatures higher than 7 °C. Moreover, it stands out that the network temperature is increased under the described conditions (for example, see peak around hour 3300 in Fig 18.D.). Since no heat needs to be extracted from the ATES, the mean network temperature is no longer bound to 8 °C. Instead, the mean network temperature is increased to 19 °C. This maximizes the COP of the HPs in buildings, while the temperature is still low enough to enable direct cooling.

The last situation occurs at times of surface water temperatures above 17 °C. When there is a residual heating demand, the SWTE installation extracts heat at full capacity. The surplus of heat produced is charged in the ATES system. At times of residual cooling demand, the amount of heat charged in the ATES equals the sum of the heat generated by the SWTE and the residual demand. This allows the SWTE to operate at full capacity most of the time. The heat extraction is only slightly reduced during a small number of moments (for example, see small dip at hour 5800 in Fig.B.). This is because the capacity of the ATES will be exceeded otherwise. Furthermore, it can be noticed that the network temperature follows the pattern of the surface water temperature in this situation.

As previously described, the residual network heating and cooling demands peak at the exact same level. The peak heating demand is decreased to a minimum in the optimal solution. This can be concluded from the fact that the network is operated at the minimum allowable temperature during the peak. Furthermore, maximum use is made of the GBs installed. The operation of the BESs in poorly insulated buildings during the day of the peak heating demand is shown in Fig. 19. Here, the demand includes the demand for space heating and the amount of heat charged in the TESs. The base load of the demand is covered by the HPs. The GBs cover the peak demands. During the hour of the peak heating demand (7 a.m.), the HPs are not operated. Instead, the capacities of the GBs are increased to cover the total demand. Moreover, the solution shows that the TESs are not charged during the peak in both building types. All in all, it can be concluded that all possible options are fully exploited to minimize the residual network peak heating demand.

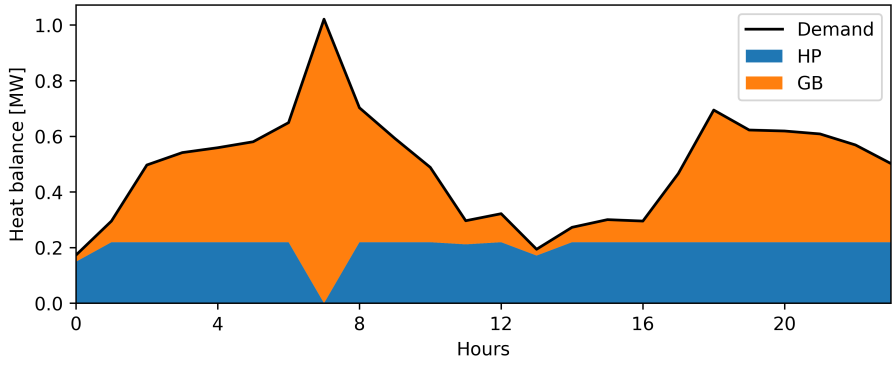

Figure 19: Operation of BESs in poorly insulated buildings during the day of the peak heating demand.

The peak of the residual cooling demand is significantly higher than the peak of the cumulated cooling demand of the BESs. This is because the peak occurs under the circumstances described in the third situation (residual cooling demand and a surface water temperature below 17 °C). Consequently, the network should be operated at the highest possible temperature to maximize the efficiency of the HPs. However, the surface water temperature reaches the threshold value of 17 °C shortly after the peak cooling demand. To extract heat with the SWTE installation, the network temperature should be lowered. The optimal solutions shows therefore that it is beneficial to extract additional cooling from the ATES. Since the ATES is sized to be able to meet the peak residual heating demand, sufficient capacity is available to lower the network temperature. During the peak residual cooling demand, part of the ATES capacity is used to supply the cooling demand of the BESs. The remaining capacity is used to lower the network temperature.

4.3 Assessment of techno-economic feasibility

The results of the techno-economic feasibility assessment are addressed in this section. Section 4.3.1 presents the technical, economic and ecological performance indicators for the three alternative heating and cooling concepts. Next, the performance indicators of the 5GDHC system are compared to the conventional DH system and the reference system with stand-alone natural gas installations in sections 4.3.2 and 4.3.3. Finally, the results of the sensitivity analysis are presented in section 4.3.4.

4.3.1 Technical, economic and ecological performance indicators

The technical, economic and ecological performance indicators, as introduced in section 3.1, of the three heating and cooling concepts are presented in Figure 20. Figure 20.A shows the calculated TACs. Here, the costs for the various components in the systems include both the annualized investment costs and the annual O&M costs for the respective component. Breakdowns of the TACs and investment costs are shown in Table 4. As discussed in section 4.2.2, the TAC of the 5GDHC system amount to 1.76 M€/a. The conventional DH system operating at 70 °C (from here denoted by 70DH) shows a higher TAC (2.08 M€/a). Although there is a slight decrease in annualized investment costs compared to the 5GDHC system, increased annual O&M and fuel costs lead to an overall increase in TAC. For the reference system with stand-alone natural gas installations, the TAC are slightly higher (1.77 M€/a). This is due to higher annual fuel costs.

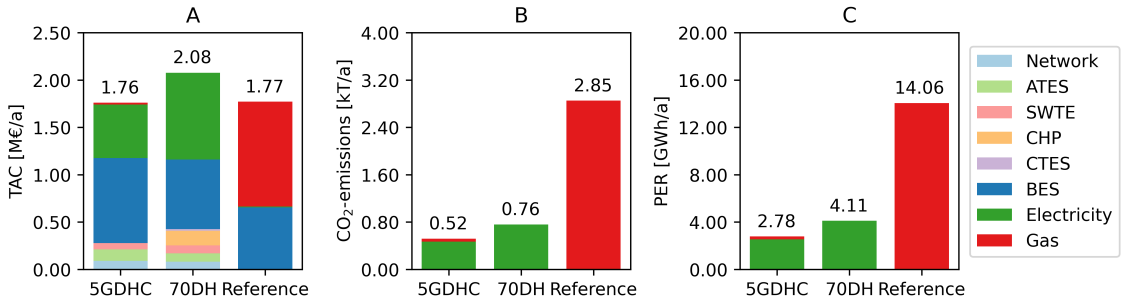

Figure 20: Performance indicators of the three heating and cooling concepts. (A) shows the total annualized costs. Annual CO_2-emissions and primary energy requirements are depicted in respectively (B) and (C).

Table 4: Total annualized costs and investment costs of the heating and cooling concepts

	5GDHC	**70DH**	**Reference**	**Unit**
Total annualized costs				
Annualized investment costs	0.91	0.82	0.40	M€/a
Annual operation and maintenance costs	0.27	0.34	0.26	M€/a
Annual fuel costs	0.59	0.92	1.12	M€/a
Total	1.76	2.08	1.77	M€/a
Investment costs				
Network infrastructure	2.05	1.82	-	M€
ATES	1.71	1.27	-	M€
SWTE	0.57	0.73	-	M€
CHP + CTES	-	1.83	-	M€
BES components	12.41	7.82	4.72	M€
Total	16.73	13.47	4.72	M€

The annual CO_2-emissions of the three heating and cooling concepts are depicted in Figure 20.B. In the 5GDHC system, the annual CO_2-emissions amount to 0.52 kT/a. The annual emissions are slightly higher for the 70DH system (0.76 kT/a), while the reference system causes substantially more emissions (2.85 kT/a). Similar proportions can be seen when analysing the PER of the three heating and cooling concepts, which are depicted in Figure 20.C. The PERs of the 5GDHC, 70DH and reference systems are respectively 2.78, 4.11 and 14.06 GWh/a.

4.3.2 5GDHC system compared to conventional DH system

The investment costs of the 70DH system are lower compared to the 5GDHC system. Firstly, savings are achieved in network infrastructure costs. Although the network in the 70DH system needs a higher transport capacity due to the central location of the heat pump, smaller pipe diameters are required. This is due to the higher temperature difference between the distribution pipes (30 K vs. 8 K). Furthermore, the ATES in the 70DH system can be sized significantly smaller (4.2 vs. 5.8 MW). In the 5GDHC system, the HPs are characterized by relatively high COPs compared to the central HP. Moreover, the TES installed in individual buildings can only be used to shift part of the demand for DHW in time. The central TES in the 70DH system, on the contrary, is also able reduce part of the peak space heating demand. These two factors reduce the amount of heat that needs to be extracted from the groundwater during the peak demand. The investment costs for the ATES system are lower in the 70DH system as a result.

In contrast, the investment costs for the SWTE installation are higher in the 70DH system. As no cooling is supplied by the network in the 70DH system, thermal demands are not balanced. This implies that all heat discharged from the ATES system in winter, needs to be recharged during the summer. In the 5GDHC system, heating and cooling demands partially cancel each other out. Given that the temperature of the surface water is only high enough during a short period of the year, a higher capacity for the SWTE installation is required in the 70DH system (4.8 vs. 3.6 MW). Furthermore, the investment costs for the BES components are significantly lower in the 70DH system. This is because no individual HPs, BHPs, DRCs, TESs and GBs are installed in the buildings. The associated savings exceed the additional investment costs for the ACs, central heat pump and central TES.

The lower investment costs of the 70DH system are also reflected by the lower annualized investment costs, as these represent the annual expenditure needed for depreciation and interest. The annual O&M costs for the technologies installed in the two systems were determined by a fixed proportion of the investment costs dependent on the respective technology. Therefore, one might not expect that the annual O&M are higher for the 70DH system. This is primarily caused by the high share for O&M (7%) for the ACs installed in the individual dwellings, resulting in annual O&M costs of 0.16 M€/a.

Also the annual fuel costs are higher for the 70DH system. This is due to the higher annual electricity consumption (6.32 vs. 3.91 GWh) caused by several factors. Firstly, the relatively low COP of the central heat pump. Secondly, the heat losses in the distribution pipes are significantly higher in the 70DH system (4.7 vs. -2.5 GWh). As the HP in the 70DH system is located near the ATES and SWTE systems, additional electricity is required to compensate for the heat losses. Lastly, the ACs installed in individual dwellings consume electricity to supply cooling. In total, the higher annual O&M and fuel costs results in higher TAC for the 70DH system. From Figure 20.B, it can be concluded that the 70DH system results in higher annual CO_2-emissions. Although no natural gas is consumed by the system, the CO_2-emissions still rise (46%) due to the higher electricity consumption. This is also reflected in the PERs of the systems presented in Figure 20.C. The PER of the 70DH system is 48% higher.

4.3.3 5GDHC system compared to reference system

Comparing the 5GDHC system to the reference system reveals that the investment costs for the reference system are substantially lower. As only GBs and ACs are installed in individual dwellings in the reference system, no investments are needed for a network infrastructure, ATES and SWTE. Furthermore, the investment costs for BESs are significantly lower. The annualized investment costs for the 5GDHC system are 128% higher as a result.

The annual O&M costs for the 5GDHC system are only slightly higher. This can be explained by the relatively high shares for O&M for the individual GBs and ACs installed in the reference system (respectively 4% and 7%). The biggest difference between the 5GDHC system and the reference system is observed in the annual fuel costs. Although less electricity is consumed in the reference system (0.24 vs. 3.91 GWh), the increased gas use by the individual GBs (14.01 vs. 0.07 GWh) leads to substantially higher annual fuel costs. Overall, this results in a slightly lower TAC for the 5GDHC system. Finally, it can be concluded that the 5GDHC system outperforms the reference system in terms of annual CO_2-emissions and PER. Once again, this is due to the higher natural gas consumption in the reference system.

4.3.4 Sensitivity analysis

The detailed results of the performed sensitivity analysis are shown in Figures 21 to 23. The main impacts of the changes in interest rate, electricity price and natural gas price are:

- The interest rate influences the annualized investment costs as a result of changes in interest payment. As the reference system requires less investments compared to the 5GDHC and 70DH systems, this system is less sensitive to a change in interest rate. A higher interest rate results in the reference system becoming the favourable heating and cooling concept in terms of TAC.
- The 5GDHC and 70DH systems are more sensitive to a change in electricity price as they consume more electricity annually. As the reference system only requires a small amount of electricity, the effect of a change in electricity price is limited. A lower price increases the cost difference between the 5GDHC system and the reference system. The reference system becomes more interesting when the electricity price increases.
- An opposite effect is caused by changes in the natural gas price. The reference system requires the largest amount of natural gas and is therefore most affected by the natural gas price. When natural gas decreases in price, the 5GDHC system becomes less attractive compared to the reference system.

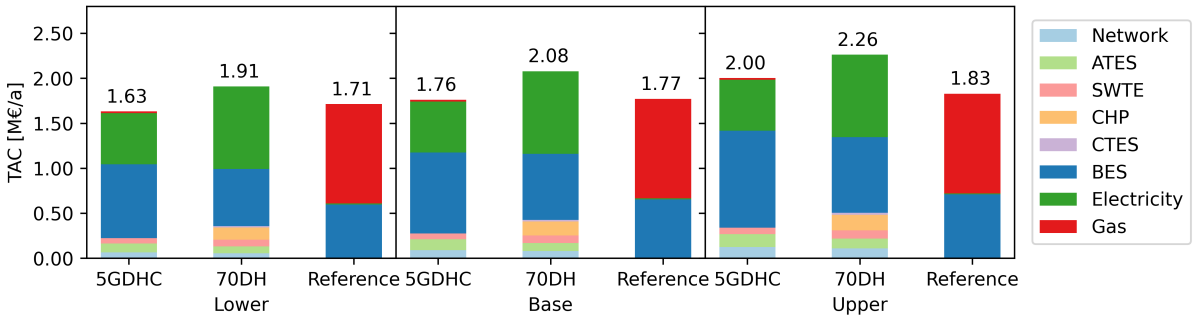

Figure 21: Influence of interest rate on TAC.

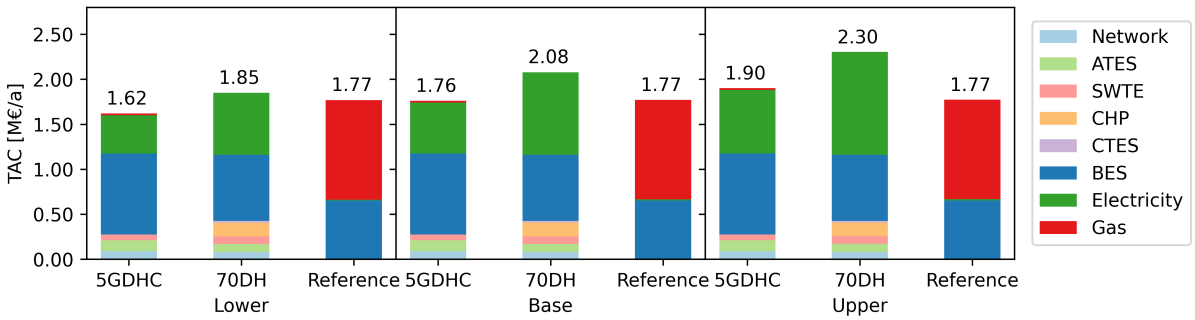

Figure 22: Influence of electricity price on TAC.

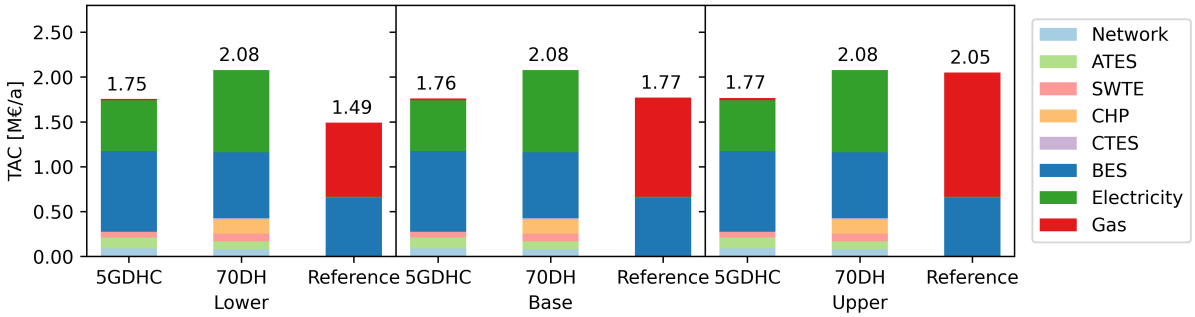

Figure 23: Influence of natural gas price on TAC.

5 Discussion

This chapter starts with a discussion of the theoretical implications of the constructed optimization model and the case study carried out. The societal implications are discussed next. Finally, the limitations of this research are discussed and avenues for further research are provided. Note that for a better understanding of the results, some points of discussion are already covered in Chapter 4.

5.1 Theoretical implications

Constructed optimization model

A novel design and operation optimization approach for 5GDHC systems is proposed in this study. Existing 5GDHC optimization approaches focus either on optimizing the design of non-renewable generation units, or on the optimal control of the network temperature (Wirtz et al., 2020a; Wirtz et al., 2021). The MILP model presented in this research enables the optimization of the design and operation of 5GDHC systems with ATES and SWTE in their configuration.

Moreover, the constructed model distinguishes between poorly and well insulated buildings. This allows for a better alignment between the technologies installed in the building energy systems and the required supply temperature of the heating circuit in the respective building. Such a distinction was not found in the 5GDHC optimization approaches present in literature (Wirtz et al., 2020a; Wirtz et al., 2021).

Case study

The application of the constructed MILP optimization model to a real-world case has led to several interesting insights on how the systems should be designed and operated to achieve the lowest annualized costs. Firstly, the case study demonstrates how the devices in building energy systems need to be sized and operated. The BHPs in well insulated buildings are operated almost constantly at full capacity. They are only turned off during peak heating demands. This maximizes the spreading of the DHW demand over time, while limiting the required HP capacity. In poorly insulated buildings, GBs reduce the required HP capacity by covering peak heating demands. Moreover, the optimization shows that direct cooling is preferred over the use of CCs. The relatively low investment costs of DRCs compared to CCs thus justify operating at lower network temperatures which leads to lower COPs of the HPs. The same conclusion was reached by Wirtz et al. (2021).

Secondly, the optimization tends to minimize the peak residual heating demand that needs to be covered by the energy hub as this peak determines the required ATES capacity. Interestingly, the capacities of the GBs are even increased to cover the total demand in poorly insulated buildings during the peak demand. This implies that the GBs are not only installed to reduce the required HP capacity, but also to lower the capacity of the ATES system.

Moreover, the results of the case study demonstrate that the temperatures of the hot and cold wells in the ATES should be as low as possible (respectively 13 °C and 7 °C). This compromises the efficiency of the HPs, as the distribution network must be operated at a relatively low temperature. However, this is justified by the extended period in which the heat produced by the SWTE installation can be charged into the ATES. A further finding is that the SWTE system is

operated as soon as the surface water temperature reaches the threshold value for heat extraction (15 °C). This is in line with the findings of Gertjan de Joode, who stated that ATES systems should solely be seen as a storage system to overcome the mismatch between supply and demand (Appendix A.1).

Finally, the results of this research indicate that the 5GDHC system outperforms the conventional DH system and the reference system with stand-alone installations in terms of TAC, annual CO_2-emissions and PER. This is particularly interesting considering the low customer diversity on the KNSM Island. Previous studies suggest that 5GDHC systems are deemed only feasible when heating and cooling demands are of the same magnitude and occur simultaneously (Abugabbara & Lindhe, 2021; Pass et al., 2018; Wirtz et al., 2020b). This research demonstrates that 5GDHC systems with ATES and SWTE can also be feasible in areas with a low customer diversity.

5.2 Societal implications

The MILP optimization model constructed in this research can be used to determine the optimal design and operation of 5GDHC systems with ATES and SWTE. This is particularly useful for Dutch municipalities, which are assigned with the task of identifying optimal energy systems for individual neighbourhoods (Ministry of Economic Affairs and Climate, 2018). However, municipalities often have insufficient expertise or lack the funds to perform a detailed neighbourhood-level analysis (PBL, 2021b). When data on thermal demand profiles, surface water and the subsurface are known for a neighbourhood, the model can be used to assess the techno-economic feasibility in a limited time.

Additionally, the outcomes of the case study can serve as input for the decision-making process of identifying optimal heating and cooling systems in the urban environment. Although the results are highly specific for the case of KNSM Island, they can still be used by local governments, energy suppliers and network operators as a reference point for the feasibility of 5GDHC systems in districts with similar heating and cooling profiles. In a broader perspective, this research can contribute to the transformation to natural gas free heating and cooling supply and to achieving the climate goals.

5.3 Limitations and future research

Limitations of constructed optimization model

The constructed optimization model is subject to certain limitations. Firstly, the network infrastructure needs to be determined prior to the optimization. A topology analysis tool for 5GDHC networks was presented by von Rhein et al. (2019). Incorporating such an approach into the constructed model would increase the complexity of the optimization problem. The choice of excluding the network infrastructure from the optimization was made to save computational time.

The second limitation of the optimization model is related to the simplified costs calculations. The investment costs for the different components in the 5GDHC system are determined using constant specific costs per capacity. In reality, it is likely that the specific costs for the technologies will decrease with increasing capacity. Furthermore, the investment costs for the components are not only dependent on the installed capacity. The costs for a SWTE installation, for example,

also depend on the distance between the inlet and outlet of the system and the type of filter required (Appendix A.1). The same applies for the ATES system, as hydrochemical conditions of the aquifer affect the economic viability (Schüppler et al., 2019). Moreover, no carbon price is included and the costs are not differentiated between parties.

Furthermore, the model does not include the recovery efficiency of the ATES system. As described in section 2.2.3, part of the thermal energy stored in ATES wells cannot be recovered as a result of the displacement of groundwater, mechanical dispersion and heat conduction. Martin Bloemendal stated that the differences between the temperatures of the hot and cold wells and the natural aquifer temperature are the dominant factors that determine the thermal losses in the ATES wells (Appendix A.3). In 5GDHC systems with SWTE, the optimal temperatures of the ATES wells are relatively low and comparable to the natural aquifer temperature. The temperature of the hot wells is slightly higher, while the temperature of the cold wells is slightly lower. This implies that the amount of heat lost in the hot wells will be largely cancelled out by the amount of heat gained in the cold wells. The amount of heat that must be produced by the SWTE installation to preserve the thermal balance in the ATES is not affected significantly. According to Martin Bloemendal, it is therefore acceptable to disregard the recovery efficiency of the ATES in the optimization approach (Appendix A.3). However, it is important to note that the heat flows from and to the hot and cold wells will decrease the temperature difference between the wells. When specific well temperatures are required, e.g. a supermarket requires low temperature cooling, thermal losses need to be determined in detail. This requires a complex numeric groundwater model, which was beyond the scope of this study (Appendix A.3).

The final limitation of the optimization approach is that the model does not address the impact of the 5GDHC system on the electricity grid. Electrification of the heating and cooling supply will require electricity grid reinforcements (CE Delft, 2020). However, the exact impact is difficult to assess as part of the electricity demand in 5GDHC systems is flexible. For example, TESs can be charged at times of low electricity prices and GBs can be operated at times of peak demands. To accurately determine the impact on the electricity grid that can be attributed to the 5GDHC system, factors as PV electricity generation and electric demands of electric vehicles and household appliances must be taken into account.

Limitations of case study

Also the performed case study is subject to limitations. Firstly, the input parameters used and assumptions made have an influence on the results. To provide insights into the uncertainties, the approach of being transparent on data and assumptions was adopted. Especially the energy prices have a significant impact on the feasibility of 5GDHC systems, as demonstrated by the sensitivity analysis. The projected 2030 electricity and natural gas prices are highly uncertain since they are heavily dependent on fuel prices and policy measures (PBL, 2020). Additionally, the energy prices, emission factors and primary energy factors will not remain constant during the lifetime of the system. As the optimization was based on time series for one year, this could not be incorporated in the model. Moreover, the maximum allowable flow rate of the ATES system used in this research was based on ATES systems already installed in Amsterdam. Here, the assumption was made that the KNSM Island possesses similar subsurface characteristics. Due to time limitations, an in-depth study required to accurately assess the hydrogeological conditions was beyond the scope of this study.

Secondly, the results of the case study are case highly case specific. The KNSM Island is a densely built area that mainly consist of apartment buildings. The costs for the network infrastructure are relatively small (5.2% of TAC) as a result. On the contrary, internal distribution pipes, hydraulic pumps and heat interface units need to be installed in the apartment buildings. These components account for 33.7% of the TAC for the 5GDHC system. Additionally, there is a low customer diversity in the case study. As described before, this is not beneficial for the economic feasibility.

Furthermore, the optimal design and operation of the system may differ for the real-life conditions on the KNSM Island. This is because the optimal solution was based on perfect foresight on the heating and cooling demands of the buildings and the surface water temperature at all time steps. In reality, it is difficult to accurately predict these variables both in the short and long term. To ensure reliable heating and cooling supply, it may therefore be desirable to increase the capacities of the system's components. Additionally, the thermal energy demand and surface water temperature profiles were based on the meteorological year 2012. This year is characterized by temperatures slightly above average. As the system must be designed to satisfy the thermal demands of buildings under all conditions, i.e. also in extremely warm and cold years, additional investments for reserve capacity may be required. Moreover, the spatial requirements of the components in the system were not considered in the case study. These can affect the optimal design of the system significantly. For example, the solution demonstrates that it is optimal to install four ATES doublets. If insufficient subsurface space is available on the KNSM Island, the system must be designed differently.

The final limitation of the case study is related to the methods used to create the hourly thermal demand profiles. Firstly, the simultaneity factor for space heating was incorporated by shifting the profiles of individual dwellings over time. However, the simultaneity factor only indicates how the peak demand of a group of dwellings relates to the sum of the peak demands of the individual dwellings. It does not specify how the space heating profiles of individual dwellings should be shifted over time. In this research, this was done based on logical reasoning. Most individual profiles were shifted one hour, fewer profiles two hours and so on. Nevertheless, the constructed space heating demand profiles will differ from reality.

The same applies for the hourly DHW demand profiles, as no differentiation was made between days, seasons and building types. Furthermore, the annual heating demand for DHW was determined based on the average household size in the Netherlands. Considering the characteristics of the case study, i.e. mainly apartment buildings and centrally located in Amsterdam, it is likely that the average household size on the KNSM Island is smaller. Unfortunately, no accurate data on household composition was available.

The constructed cooling demand profiles are especially uncertain. Ideally, hourly cooling demand profiles are created using complex models that take urban heat island effects, thermal insulation of the buildings, outside air temperature and solar radiation into account (Appendix A.2). Due to time limitations, this was beyond the scope of this research. Finally, the projected effects of climate change on the annual heating and cooling demands of the buildings were not incorporated.

Future research

Three avenues for future research are proposed in this section. Firstly, it is suggested that future work focuses on the enhancement of the presented optimization model by addressing the discussed limitations. Special attention should be paid to the integration of the impact of the 5GDHC system on the electricity grid, as 5GDHC systems are expected to become a central part of future smart energy systems.

Secondly, it is recommended that the constructed optimization model will be applied to neighbourhoods with different characteristics compared to the KNSM Island. As the results of the case study carried out are highly case specific, this will provide a more comprehensive overview of the techno-economic feasibility of 5GDHC systems which include ATES and SWTE in their configuration.

The final suggestion for future research is to integrate insulation measures in the optimization approach. The insulation level of buildings influences the annual thermal demands and the required supply temperature of the buildings. By introducing binary variables, it can be assessed if improving the insulation level of individual buildings results in lower annualized costs.

6 Conclusion

5GDHC systems with ATES and SWTE are expected to play an important role in the decarbonization of the Dutch urban heating and cooling supply. Existing optimization approaches are unsuitable for the optimization of these systems as they focus either on the optimal network temperature control or on the design of non-renewable generation units. The main aim of this research was therefore to develop an optimization model for designing and operating 5GDHC systems which include ATES and SWTE in their configuration.

The optimization model was partly derived from the model presented by Wirtz et al. (2021). This model comprises an air-source heat pump, compression chiller and accumulator tank. These components were removed from the model structure, while supplementary constraints required to integrate the ATES and SWTE technologies into the optimization approach were formulated. Additionally, a distinction was made between poorly and well insulated buildings. This allows for a better alignment between the required supply temperature of the heating circuit of a building and the technologies installed in the building's energy system. The novel optimization approach was then applied to a real-world case to determine the most cost-effective design and operation of the 5GDHC system. Finally, the techno-economic feasibility of the systems was assessed by comparing its performance to alternative heating and cooling concepts.

To integrate SWTE systems into the optimization approach, binary variables were introduced to ensure that heating and cooling can only be extracted by the system when the temperature of the surface water is sufficiently high or low enough. Furthermore, the SWTE system is only able to deliver heat to the network when the temperature of the surface water is higher than the temperature of the warm distribution pipe. Likewise, cooling can only be delivered to the network when the temperature of the surface water is lower than the temperature of the cold distribution pipe. This was ensured by introducing additional constraints with binary variables.

Regarding the ATES system, constraints were formulated that describe the thermal heating and cooling power retrieved from the groundwater. Furthermore, Dutch regulations require thermal balancing of the ATES system. This was incorporated in the model structure by adding a constraint that ensures that the annual amounts of heating and cooling extracted from the groundwater are equal to each other. Moreover, the ATES system can only deliver heat to the network when the temperatures of the hot and cold wells exceed the temperatures of the warm and cold distribution pipes respectively. Cooling can only be retrieved from the groundwater when the temperatures of the wells are lower compared to the temperatures of the distribution pipes. For this purpose, constraints with binary variables were included.

The application of the optimization model to the KNSM-Island has provided important insights on how the systems should be designed and operated to achieve the lowest annualized costs. Firstly, booster heat pumps and gas boilers are installed in respectively well and poorly insulated buildings to reduce the required heat pump capacity. The case study also shows that it is optimal to operate the network at temperatures that enable direct cooling in buildings. Although the cooling demands of the buildings are relatively small compared to the heating demands, the lower coefficients of performance of the heat pumps resulting from operating at lower network temperatures are justified by the low investment costs of direct cooling. In addition, it appears profitable to minimize the peak residual heating demand that must be covered by the energy hub as the ATES capacity is determined by this peak. The capacities of the gas boilers installed in poorly insulated buildings are even increased for this purpose. Finally, the temperatures of the

hot and cold wells of the ATES systems should be as low as possible. This reduces the required capacity for the SWTE installation, as the period in which heat from the SWTE system can be charged into the ATES is maximized.

This research also demonstrates that 5GDHC systems with ATES and SWTE are economically and technically feasible to be implemented in Dutch urban areas. Compared to the conventional DH system operating at 70 °C, the 5GDHC system leads to substantially less total annualized costs (-15.4%), has a lower primary energy requirement (-32.4%), and causes less CO_2-emissions (-31.6%). The total annualized costs of the 5GDHC system are only slightly lower in comparison to the reference system with stand-alone natural gas installations (-0.6%). The savings in primary energy requirement (-80.2%) and CO_2-emissions (-81.6%) are significantly higher.

All in all, the proposed optimization approach aims to facilitate future research on the identification of local sustainable heating and cooling supply solutions. It is suited for determining the most cost-effective design and operation of the ATES and SWTE systems and the energy conversion units installed in buildings, as well as the optimal control of the network temperature. The case study carried out showed the complex interaction of all components in the 5GDHC system, which emphasizes the importance of holistic design approaches. Finally, the insights into the techno-economic feasibility of the 5GDHC systems with ATES and SWTE may be beneficial to other studies focusing on areas with similar characteristics.

Acknowledgements

The completion of this thesis marks the end of my master's program Energy Science at Utrecht University. Despite of the Covid-19 regulations, the process of writing this thesis turned out to be a precious learning experience for me. Several people made invaluable contributions, to whom I wish to extend my deepest gratitude.

First of all, I would like to thank my supervisor at Utrecht University, dr. ir. Jesús Rosales Carreón, for giving me the freedom to work on a topic I was passionate about. Secondly, I would like to offer my special thanks to my supervisor at Waternet, ir. Stefan Mol. Our weekly meetings have provided me with new ideas, motivation and inspiration. The completion of this thesis would not have been possible without his support. Furthermore, I also wish to thank dr. Wen Liu for being my second reader. Finally, I would like to thank interviewees Gertjan de Joode, Bart Roossien and Martin Bloemendal for providing me with essential insights on the subject.

Bibliography

Abugabbara, M., & Lindhe, J. (2021). A Novel Method for Designing Fifth-Generation District Heating and Cooling Systems. *E3S Web of Conferences*, *246*, 9001.

Bloemendal, M., & Hartog, N. (2018). Analysis of the impact of storage conditions on the thermal recovery efficiency of low-temperature ATES systems. *Geothermics*, *71*, 306–319.

Bloemendal, M., Olsthoorn, T., & Boons, F. (2014). How to achieve optimal and sustainable use of the subsurface for Aquifer Thermal Energy Storage. *Energy Policy*, *66*, 104–114.

Blok, K., & Nieuwlaar, E. (2016). *Introduction to energy analysis*. Routledge.

Boesten, S., Ivens, W., Dekker, S. C., & Eijdems, H. (2019). 5th generation district heating and cooling systems as a solution for renewable urban thermal energy supply. *Advances in Geosciences*. https://doi.org/10.5194/adgeo-49-129-2019

Buffa, S., Cozzini, M., D'Antoni, M., Baratieri, M., & Fedrizzi, R. (2019). 5th generation district heating and cooling systems: A review of existing cases in Europe. https://doi.org/10.1016/j.rser.2018.12.059

Buffa, S., Soppelsa, A., Pipiciello, M., Henze, G., & Fedrizzi, R. (2020). Fifth-generation district heating and cooling substations: Demand response with artificial neural network-based model predictive control. *Energies*. https://doi.org/10.3390/en13174339

Bünning, F., Wetter, M., Fuchs, M., & Müller, D. (2018). Bidirectional low temperature district energy systems with agent-based control: Performance comparison and operation optimization. *Applied Energy*. https://doi.org/10.1016/j.apenergy.2017.10.072

Buoro, D., Pinamonti, P., & Reini, M. (2014). Optimization of a Distributed Cogeneration System with solar district heating. *Applied Energy*, *124*, 298–308.

CE Delft. (2018). Nationaal potentieel van aquathermie. https://www.ce.nl/publicaties/2171/nationaal-potentieel-van-aquathermie

CE Delft. (2019a). Factsheets warmtetechnieken.

CE Delft. (2019b). Functioneel ontwerp LTwarmtenetten gebouwde omgeving. https://www.rvo.nl/sites/default/files/2019/04/Functioneel%20ontwerp%20LT-warmtenetten.pdf

CE Delft. (2020). Elektrificatie en vraagprofiel 2030. https://www.tennet.eu/fileadmin/user_upload/Company/Publications/Technical_Publications/Dutch/CE_Delft_190446_Elektrificatie_en_Vraagprofiel_TenneT.pdf

Courtois, N., Grisey, A., Grasselly, D., Menjoz, A., Noël, Y., Petit, V., & Thiéry, D. (2007). Application of Aquifer Thermal Energy Storage for heating and cooling of greenhouses in France: a pre-feasibility study. *European Geothermal Congress*, *2007*.

Dalla Rosa, A., Li, H., & Svendsen, S. (2011). Method for optimal design of pipes for low-energy district heating, with focus on heat losses. *Energy*, *36*(5), 2407–2418.

de Boer, S., Scholten, B., Boderie, P., & Pothof, I. (2015). Kansenkaart voor energie uit oppervlaktewater. https://www.h2owaternetwerk.nl/images/2015/1506/1506-03_kansenkaart_energie_oppwater.pdf

Deltares. (2020). Monitoringsplan Ecologische Effecten Thermische Energie Oppervlaktewater. https://www.aquathermie.nl/bibliotheek/handlerdownloadfiles.ashx?idnv=1701100

Dominković, D. F., Stunjek, G., Blanco, I., Madsen, H., & Krajačić, G. (2020). Technical, economic and environmental optimization of district heating expansion in an urban agglomeration. *Energy*, *197*, 117243.

Doughty, C., Hellström, G., Tsang, C. F., & Claesson, J. (1982). A dimensionless parameter approach to the thermal behavior of an aquifer thermal energy storage system. *Water Resources Research*, *18*(3), 571–587.

DWA, & IF Technology. (2012). Onderzoek criteria energiebalans WKO.

ECN. (2018). Energietransitie rekenmodellen - Warmtevraagprofielen. https://www.netbeheernederland.nl/_upload/Files/Rekenmodellen_21_0db6cf249e.pdf

Elmegaard, B., Ommen, T. S., Markussen, M., & Iversen, J. (2016). Integration of space heating and hot water supply in low temperature district heating. *Energy and Buildings*, *124*, 255–264.

ENERGYMATTERS. (2014). Rendement HR-ketel.

ENERGYMATTERS. (2017). Roadmap warmtenetten. https://www.kasalsenergiebron.nl/content/docs/Restwarmte/Roadmap_warmtenetten.pdf

Eteck. (2021). Kennissessie over duurzame warmte.

European Commission. (2010). Energy Performance Building Directive. https://eur-lex.europa.eu/legal-content/EN/TXT/PDF/?uri=CELEX:32010L0031&from=EN

Fleuchaus, P., Godschalk, B., Stober, I., & Blum, P. (2018). Worldwide application of aquifer thermal energy storage – A review. https://doi.org/10.1016/j.rser.2018.06.057

Franzen, I., Nedar, L., & Andersson, M. (2019). Environmental comparison of energy solutions for heating and cooling. *Sustainability*, *11*(24), 7051.

Friedel, P., de Jong, A., & Horstink, M. (2014). Eindrapportage veldtesten: Energieprestaties van 5 warmtetechnieken bij woningen in de praktijk.

Gao, L., Zhao, J., An, Q., Wang, J., & Liu, X. (2017). A review on system performance studies of aquifer thermal energy storage. *Energy Procedia*. https://doi.org/10.1016/j.egypro.2017.12.242

Greenvis, & Ecofys. (2016). Collectieve warmte naar lage temperatuur. https://www.topsectorenergie.nl/sites/default/files/uploads/Urban%20energy/publicaties/Collectieve%20warmte%20naar%20lage%20temperatuur%20-%20definitief.pdf

Guelpa, E., Marincioni, L., Capone, M., Deputato, S., & Verda, V. (2019). Thermal load prediction in district heating systems. *Energy*, *176*, 693–703.

Guelpa, E., & Verda, V. (2019). Thermal energy storage in district heating and cooling systems: A review. *Applied Energy*, *252*, 113474.

Harb, H., Schwager, C., Streblow, R., & Müller, D. (2015). Optimal design of energy systems in residential districts with interconnected local heating and electrical networks. *Proceedings of the Building Simulation Conference, Hyderabad, India*, 7–9.

Hendriks, M., Snijders, A., & Boido, N. (2008). Underground thermal energy storage for efficient heating and cooling of buildings. *1st International Conference on Industrialised, Integrated, Intelligent Construction, Loughborough*, 315–324.

Herrmann, J. W. (2007). Evaluating design optimization models.

IF Technology. (n.d.-a). Aquifer Thermal Energy Storage. https://www.iftechnology.com/aquifer-thermal-energy-storage/

IF Technology. (n.d.-b). Borehole Thermal Energy Storage. https://www.iftechnology.com/borehole-thermal-energy-storage/

ISSO-publicatie 39. (2012). Energiecentrale met warmte- en koudeopslag. https://doi.org/ISBN: 978-90-5044-239-8

Jansen, S., Verhoeven, R., & Elswijk, M. (2021). Technisch handboek koele warmtenetten. https://energygo.blob.core.windows.net/kowanet/D1.4%20Technisch%20handboek/KoWaNet%20Technisch%20Handboek%20Koele%20Warmtenetten_V1.1_maart%202021.pdf

Jensen, J. K., Ommen, T., Reinholdt, L., Markussen, W. B., & Elmegaard, B. (2018). Heat pump COP, part 2: Generalized COP estimation of heat pump processes. *13th IIR Gustav Lorentzen Conference on Natural Refrigerants (GL2018)*, 1136–1145.

Joelsson, A., & Gustavsson, L. (2009). District heating and energy efficiency in detached houses of differing size and construction. *Applied Energy*, *86*(2), 126–134.

Kadaster. (n.d.). BAG Viewer. https://bagviewer.kadaster.nl/

Kleijnen, J. P. C. (1995). Verification and validation of simulation models. *European journal of operational research*, *82*(1), 145–162.

Lake, A., Rezaie, B., & Beyerlein, S. (2017). Review of district heating and cooling systems for a sustainable future. https://doi.org/10.1016/j.rser.2016.09.061

Larsen, M. A., Petrović, S., Radoszynski, A. M., McKenna, R., & Balyk, O. (2020). Climate change impacts on trends and extremes in future heating and cooling demands over Europe. *Energy and Buildings*. https://doi.org/10.1016/j.enbuild.2020.110397

Law, A. M., Kelton, W. D., & Kelton, W. D. (2000). *Simulation modeling and analysis* (Vol. 3). McGraw-Hill New York.

Lee, K. S. (2010). A review on concepts, applications, and models of aquifer thermal energy storage systems. *Energies*, *3*(6), 1320–1334.

LenteAkkoord Zeer Energiezuinige Nieuwbouw. (2018). Alternatieven voor aardgas.

Lund, H., Werner, S., Wiltshire, R., Svendsen, S., Thorsen, J. E., Hvelplund, F., & Mathiesen, B. V. (2014). 4th Generation District Heating (4GDH): Integrating smart thermal grids into future sustainable energy systems. *Energy*, *68*, 1–11.

Matos, C. R., Carneiro, J. F., & Silva, P. P. (2019). Overview of large-scale underground energy storage technologies for integration of renewable energies and criteria for reservoir identification. *Journal of Energy Storage*, *21*, 241–258.

Mehleri, E. D., Sarimveis, H., Markatos, N. C., & Papageorgiou, L. G. (2013). Optimal design and operation of distributed energy systems: Application to Greek residential sector. *Renewable Energy*, *51*, 331–342.

Menkveld, M., de Smidt, R. P., Oude Lohuis, J., van Melle, T., et al. (2015). De systeemkosten van warmte voor woningen.

Ministry of Economic Affairs and Climate. (2018). Gebouwde omgeving - Achtergrond notitie Wijkgerichte aanpak.

Ministry of Economic Affairs and Climate Policy. (2019). Climate Agreement. https://www.klimaatakkoord.nl/documenten/publicaties/2019/06/28/national-climate-agreement-the-netherlands

Mol, S., van Helvoort, P.-J., & Son, P. (2021). Rapport haalbaarheidsonderzoek duurzaam wijkwarmtenet in Hilversum Kerkelanden. https://www.hetcooperatie.nl/wp-content/uploads/2021/02/Def-Deelrapport-1-Haalbaarheid-warmtenet-Kerkelanden-technisch-en-financieel.pdf

Morvaj, B., Evins, R., & Carmeliet, J. (2016). Optimising urban energy systems: Simultaneous system sizing, operation and district heating network layout. *Energy*, *116*, 619–636.

Nord, N., Nielsen, E. K. L., Kauko, H., & Tereshchenko, T. (2018). Challenges and potentials for low-temperature district heating implementation in Norway. *Energy*, *151*, 889–902.

Omu, A., Choudhary, R., & Boies, A. (2013). Distributed energy resource system optimisation using mixed integer linear programming. *Energy Policy*, *61*, 249–266.

Paez, T. L. (2008). Introduction to Model Validation.

Pass, R. Z., Wetter, M., & Piette, M. A. (2018). A thermodynamic analysis of a novel bidirectional district heating and cooling network. *Energy*, *144*, 20–30.

PBL. (2020). Klimaat- en energieverkenning 2020. https://www.pbl.nl/sites/default/files/downloads/pbl-2020-klimaat-en-energieverkenning2020-3995.pdf

PBL. (2021a). Functioneel ontwerp Vesta Mais 5.0. https://www.pbl.nl/sites/default/files/downloads/pbl-2021-functioneel-ontwerp-vesta-mais-5.0-4583.pdf

PBL. (2021b). Warmtetransitie in de praktijk. Leren van ervaringen bij het aardgasvrij maken van wijken. https://www.pbl.nl/sites/default/files/downloads/pbl-2021-warmtetransitie-in-de-praktijk-4019.pdf

Pellegrini, M., Bloemendal, M., Hoekstra, N., Spaak, G., Gallego, A. A., Comins, J. R., Grotenhuis, T., Picone, S., Murrell, A. J., & Steeman, H. J. (2019). Low carbon heating and cooling by combining various technologies with Aquifer Thermal Energy Storage. *Science of the Total Environment*, *665*, 1–10.

Revesz, A., Jones, P., Dunham, C., Davies, G., Marques, C., Matabuena, R., Scott, J., & Maidment, G. (2020). Developing novel 5th generation district energy networks. *Energy*. https://doi.org/10.1016/j.energy.2020.117389

Rijkswaterstaat. (2021). Waterinfo. https://waterinfo.rws.nl/#!/nav/info/

Roossien, B., Barkmeijer, T., & Elswijk, M. (2020). A technical design framework for cold heating and cooling networks.

Rostampour, V., Jaxa-Rozen, M., Bloemendal, M., Kwakkel, J., & Keviczky, T. (2019). Aquifer Thermal Energy Storage (ATES) smart grids: Large-scale seasonal energy storage as a distributed energy management solution. *Applied Energy*, *242*, 624–639.

Royal HaskoningDHV. (2019). Basis ontwerp warmtenet.

Ruesch, F., & Evins, R. (2014). District heating and cooling with low temperature networks – sketch of an optimization problem. *Proceedings of COLEB workshop*, 39–40.

Ruesch, F., & Haller, M. (2017). Potential and limitations of using low-temperature district heating and cooling networks for direct cooling of buildings. *Energy Procedia*, *122*, 1099–1104.

RVO. (2018a). Ontwikkeling van koudevraag van woningen. https://www.rvo.nl/sites/default/files/2018/07/Rapport%20-%20Ontwikkeling%20koudevraag%20van%20woningen%20.pdf

RVO. (2018b). Verkenning tool aardgasvrije bestaande woningen.

Sameti, M., & Haghighat, F. (2017). Optimization approaches in district heating and cooling thermal network. *Energy and Buildings*, *140*, 121–130.

Sarbu, I., & Sebarchievici, C. (2018). A comprehensive review of thermal energy storage. *Sustainability*, *10*(1), 191.

Schmidt, T., Pauschinger, T., Sørensen, P. A., Snijders, A., Djebbar, R., Boulter, R., & Thornton, J. (2018). Design aspects for large-scale pit and aquifer thermal energy storage for district heating and cooling. *Energy Procedia*, *149*, 585–594.

Schüppler, S., Fleuchaus, P., & Blum, P. (2019). Techno-economic and environmental analysis of an Aquifer Thermal Energy Storage (ATES) in Germany. *Geothermal Energy*, *7*(1), 1–24.

Schwer, L. E. (2009). Guide for verification and validation in computational solid mechanics.

Sommer, W. et al. (2015a). Modelling and monitoring of aquifer thermal energy storage: impacts of heterogeneity, thermal interference and bioremediation. *Modelling and monitoring of aquifer thermal energy storage: impacts of heterogeneity, thermal interference and bioremediation.*

Sommer, W., Valstar, J., Leusbrock, I., Grotenhuis, T., & Rijnaarts, H. (2015b). Optimization and spatial pattern of large-scale aquifer thermal energy storage. *Applied energy*, *137*, 322–337.

Steinbach, J., & Staniaszek, D. (2015). Discount rates in energy system analysis. *Fraunhofer ISI, Building Performance Institute Europe (BPIE): Karlsruhe, Germany*.

Stowa. (2017). Thermische energie uit oppervlaktewater. https://www.uvw.nl/wp-content/uploads/2017/10/Handreiking-Thermische-energie-uit-oppervlaktewater-2017.pdf

Stowa. (2018). Handreiking aquathermie. https://www.uvw.nl/wp-content/uploads/2018/10/Handreiking-Aquathermie.pdf

Stratelligence. (2020). Een Laagdrempelige Energietransitie. https://www.energie-nederland.nl/app/uploads/2020/04/Laagdrempelige-energietransitie-stratelligence-3-april-1.2-min.pdf

Syntraal, Stowa, & Deltares. (n.d.). Rekenregels Warmte uit oppervlaktewater. https://stowa.omgevingswarmte.nl/upload/rekenregels_teo.pdf

Techniplan adviseurs bv. (2018). De potentie van TEO voor verduurzaming van de gebouwen van het Rijksvastgoedbedrijf en Rijkswaterstaat (kosten en baten).

Tereshchenko, T., & Nord, N. (2018). Future trends in district heating development. *Current Sustainable/Renewable Energy Reports*, *5*(2), 172–180.

Thacker, B. H., Doebling, S. W., Hemez, F. M., Anderson, M. C., Pepin, J. E., & Rodriguez, E. A. (2004). Concepts of model verification and validation.

Tigchelaar, C. (2013). Methodiek voor opsplitsing CBS statistiek huishoudelijk gas-en elektriciteitsverbruik.

van den Kieboom, W. (2009). Duurzame warmte- en koudevoorziening voor Overhoeks. http://www.nvoe.nl/Media/download/161240/Duurzame%20WKO.pdf

van Vliet, E., de Keijzer, J., Slingerland, E., van Tilburg, J., Hofsteenge, W., & Haaksma, V. (2016). Collectieve warmte naar lage temperatuur Een verkenning van mogelijkheden.

Verhoeven, R., Willems, E., Harcouët-Menou, V., De Boever, E., Hiddes, L., Veld, P. O. t., & Demollin, E. (2014). Minewater 2.0 project in Heerlen the Netherlands: Transformation of a geothermal mine water pilot project into a full scale hybrid sustainable energy infrastructure for heating and cooling. *Energy Procedia*. https://doi.org/10.1016/j.egypro.2014.01.158

von Rhein, J., Henze, G. P., Long, N., & Fu, Y. (2019). Development of a topology analysis tool for fifth-generation district heating and cooling networks. *Energy conversion and management*, *196*, 705–716.

Waternet. (2021). Omgevingswarmtekaart. https://waternet.omgevingswarmte.nl/waternet#c9eaed99-a69e-48eb-9642-61c0e0b77078

Weijers-Waalwijk. (n.d.). Warmte en koude distributieleidingen. http://www.weijers-waalwijk.nl / sites / default / files / bestanden / PRINSPIPE % 5C % 2C % 20CALPEX % 20en % 20EIGERFLEX%20Brochure%20voorgeisoleerde%20leidingen%20-%20Weijers%20Waalwijk_4.pdf

Welsch, B., Göllner-Völker, L., Schulte, D. O., Bär, K., Sass, I., & Schebek, L. (2018). Environmental and economic assessment of borehole thermal energy storage in district heating systems. *Applied energy*, *216*, 73–90.

Wirtz, M., Kivilip, L., Remmen, P., & Müller, D. (2020a). 5th Generation District Heating: A novel design approach based on mathematical optimization. *Applied Energy*. https://doi.org/10.1016/j.apenergy.2019.114158

Wirtz, M., Kivilip, L., Remmen, P., & Müller, D. (2020b). Quantifying Demand Balancing in Bidirectional Low Temperature Networks. *Energy and Buildings*, *224*, 110245.

Wirtz, M., Neumaier, L., Remmen, P., & Müller, D. (2021). Temperature control in 5th generation district heating and cooling networks: An MILP-based operation optimization. *Applied Energy*, *288*, 116608.

Wouters, C., Fraga, E. S., & James, A. M. (2015). An energy integrated, multi-microgrid, MILP (mixed-integer linear programming) approach for residential distributed energy system planning–a South Australian case-study. *Energy*, *85*, 30–44.

Wouters, C., Fraga, E. S., James, A. M., & Polykarpou, E. M. (2014). Mixed-integer optimisation based approach for design and operation of distributed energy systems. *2014 Australasian Universities Power Engineering Conference (AUPEC)*, 1–6.

Wu, P., Wang, Z., Li, X., Xu, Z., Yang, Y., & Yang, Q. (2020). Energy-saving analysis of air source heat pump integrated with a water storage tank for heating applications. *Building and Environment*, *180*, 107029.

Wu, Q., Ren, H., Gao, W., & Ren, J. (2016). Modeling and optimization of distributed energy supply network with power and hot water interchanges. *Applied Thermal Engineering*, *94*, 635–643.

Xu, J., Wang, R. Z., & Li, Y. (2014). A review of available technologies for seasonal thermal energy storage. *Solar energy*, *103*, 610–638.

Xu, L., Torrens, J. I., Guo, F., Yang, X., & Hensen, J. L. M. (2018). Application of large underground seasonal thermal energy storage in district heating system: A model-based energy performance assessment of a pilot system in Chifeng, China. *Applied Thermal Engineering*, *137*, 319–328.

Yang, Y., Zhang, S., & Xiao, Y. (2015). Optimal design of distributed energy resource systems coupled with energy distribution networks. *Energy*, *85*, 433–448.

Appendices

A Expert interviews

A.1 Gertjan de Joode (Eteck, 14 May 2021)

What are the steps in designing SWTE systems?

The first SWTE systems that we developed were designed based on the operation of ATES systems. The heating and cooling demands of buildings influence the amount of thermal energy that must be delivered by the hot and cold wells of the ATES. Subsequently, it was estimated how much heat or cold must be produced to balance the ATES. Nowadays, we aim at employing SWTE systems and other thermal energy sources more efficiently. ATES systems should no longer be seen as a system that supplies energy, but rather as a storage system to overcome the temporal mismatch between supply and demand. This means that thermal energy sources must supply directly to the distribution network. If the supply is larger than the demand, thermal energy can be saved in the ATES. In the past, the SWTE was only used to regenerate the ATES. This can only happen when the temperature of the surface water exceeds the temperature of the hot well (about 18 degrees). During spring, autumn and winter, all heat demand was provided by the ATES. This means that you are actually moving groundwater twice. At first, groundwater is pumped from the hot well to the cold well. Heat is extracted with the use of the heat exchanger, and the heat is supplied to the network. Secondly, groundwater is pumped from the cold well to the hot well during summer. Since you want to move as little groundwater as possible, it is beneficial to use the thermal energy produced by SWTE right away instead of storing it into the ground first. With regard to dimensioning the SWTE system, you want to be able to meet the demand during spring and autumn (when the temperature of the surface water is between 12 and 18 degrees). However, you also want enough capacity to charge the ATES during summer.

The temperatures of the water in the distribution pipes can vary in my model. This will influence the efficiency of the heat pumps and chillers, but also the operation of the SWTE and ATES systems. What is an optimal temperature range for an 5G network with SWTE and ATES?

Higher network temperatures will indeed increase the efficiency of the heat pumps. However, this would mean that the temperature of the hot well needs to be high enough. In winter, all other heat sources will be unavailable. So all heat required needs to be provided by the hot well of the ATES. We often use temperature difference between the wells of 6-8 K. When engineering DH systems, we keep 12 degrees Celsius as minimum supply temperature for the network in winter. The heat pumps can operate at this temperature. In spring and autumn, buildings can already have a cooling demand. During these periods, you want network temperatures that are suitable for passive cooling. Furthermore, you do not want the use heat from the ATES systems during these periods. So high temperatures are not beneficial, despite of the higher efficiencies for the heat pumps. At the moment that some buildings need cooling and some buildings need heating, the network will balance itself. During April, the ATES system can be turned off. When there is an imbalance in the network, the SWTE system can provide the required thermal energy.

What factors influence the investment and operational costs of SWTE systems?

The costs of a SWTE system depend on the distance between the inlet and outlet of the system, the capacity of the pumps and the capacity of the heat exchanger. Furthermore, the type of filter required is an important aspect to consider. A filter is required to protect the heat exchanger from contamination. The type of filter that is required is dependent on the water quality. For example, brackish, fresh and salt water need different types of filters. The costs for the filter can be significant. Furthermore, it should be noted that the maintenance costs are often determine the feasibility of a SWTE system. A good filter will increase the investment costs, but can be beneficial due to lower maintenance costs.

A.2 Bart Roossien (EnergyGO, 8 July 2021)

What is the best way to construct cooling demand profiles for the KNSM island in Amsterdam?

Ideally, hourly cooling demand profiles are constructed using complex models that take radiation into account. At the moment, no good reference profiles are available in the Netherlands. The most accurate is to use building software programs as TRNSYS or EnergyPlus. However, these programs have a steep learning curve.

Considering the length of my research, I don't think it's possible to use these kinds of programs. My idea now is to use an existing profile and then correct it for floor area and cooling demand per floor area. What do you think of this method?

I agree, I think it's too complex for your kind of research. Creating heating demand profiles is relatively easy, as this can be done based on heating degree days. I can't say for sure if it will work properly if you correct the existing profile for cooling demand. There will be a difference between the calculated cooling demand profiles and the actual cooling demand profiles. However, I think this is the best method for your research.

I also had a question about how I incorporated the ATES system in my model. During cold extraction, the temperatures of the warm and cold distribution pipes must me lower than the temperatures of the hot and cold wells. When you consider the minimum temperature difference across the heat exchanger, the temperature difference between the network pipes and a cold well temperature of 10 degrees, the temperature of the warm pipes must be higher than 19 degrees. This implies that you can only charge heat into the ATES system when the temperature of the surface water exceeds 20 degrees. This only happens in a short period of the year. Is it better to lower the temperatures of the ATES system?

This is an engineering issue. Using higher ATES temperature would result is higher COPs of the heat pumps in winter. At the same time, the SWTE system should be sized larger as the period to charge the hot well of the ATES system would become shorter. I would incorporate this in your optimization model. When you assume a constant temperature difference between the two wells, you should let the average temperature of the ATES wells vary.

A.3 Martin Bloemendal (KWR-TU Delft, 12 July 2021)

How should I integrate the thermal recovery efficiency in my optimization model?

You consider the temperature difference between hot and cold wells. In the hot wells, you loose heat. In the cold wells, you gain heat. The temperature difference between the water in the wells and the soil is the most important factor for the thermal losses. The amount of heat and cold that you lose in the hot and cold wells will largely cancel each other out, if the temperature differences between the wells and the soil are equal. So this has no influence on the amount of heat that must be delivered by the SWTE system. The temperature difference between the wells will decrease due to the heat losses. This will impact the COPs of the heat pumps. However, you will still be able to provide heating and cooling. Furthermore, the amount of heat and cold stored at a specific time step will influence the heat losses and heat gain at that time step.

When you need specific temperatures in the wells. For example, you need to cool with low temperatures. You should keep the temperature of the cold wells sufficiently low. In that case, you need to determine the conduction losses in detail. This will require a numeric groundwater model. If the temperature differences between the wells and the soil are approximately equal to each other, then it is acceptable to disregard the heat losses in your model.

B Decision variables

B.1 Decision variables model Wirtz et al. (2021)

Table B.1: Decision variables included in the model presented by Wirtz et al. (2021).

Decision variable	Description	Unit
Thermal power variables		
$\dot{Q}_{\text{res,BES},b,t}$	Residual heating or cooling demand of a building at time step t	kW_{th}
$\dot{Q}_{\text{HP},b,t}$	Heat produced by the heat pump in building b at time step t	kW_{th}
$\dot{Q}_{\text{CC},b,t}$	Cold produced by the compression chiller in building b at time step t	kW_{th}
$\dot{Q}_{\text{DRC},b,t}$	Direct cooling supplied to building b at time step t	kW_{th}
$\dot{Q}_{\text{res,netw},t}$	Residual network demand at time step t	kW_{th}
$\dot{Q}_{\text{loss,wp},t}$	Heat losses from the warm pipe at time step t	kW_{th}
$\dot{Q}_{\text{loss,cp},t}$	Heat losses from the cold pipe at time step t	kW_{th}
$\dot{Q}_{\text{netw},t}$	Thermal power to raise or lower the network temperature at time step t	kW_{th}
$\dot{Q}_{\text{res,EH},t}$	Thermal power provided by the energy hub to the network at time step t	kW_{th}
$\dot{Q}_{\text{ACC},t}$	Charging/discharging power of the accumulator tank at time step t	kW_{th}
$\dot{Q}_{\text{h,ASHP},t}$	Heat generated by air source heat pump at time step t	kW_{th}
$\dot{Q}_{\text{c,CC},t}$	Cold generated by compression chiller time step t	kW_{th}
$\dot{Q}_{\text{h,EB},b,t}$	Heat generated by electric boiler in building b at time step t	kW_{th}
$\dot{Q}^{\text{dch}}_{\text{h,TES},b,t}$	Heat discharged from water buffer vessel in building b at time step t	kW_{th}
$\dot{Q}^{\text{ch}}_{\text{h,TES},b,t}$	Heat charged in water buffer vessel in building b at time step t	kW_{th}
$\dot{Q}_{\text{h},u,b,t}$	Heat generated by unit u in building b at time step t	kW_{th}
$\dot{Q}_{\text{c},u,b,t}$	Cold generated by unit u in building b at time step t	kW_{th}
Electric power variables		
$P_{\text{el,grid},t}$	Power extracted from the electricity grid at time step t	kW_{e}
$P_{\text{el,feed}-\text{in},t}$	Power delivered to the electricity grid at time step t	kW_{e}
$P_{\text{HP},b,t}$	Electric power required by the heat pump in building b at time step t	kW_{e}
$P_{\text{CC},b,t}$	Electric power required by the compression chiller in building b at time step t	kW_{e}
$P_{\text{BES},b,t}$	Electricity demand of the building energy system in building b at time step t	kW_{e}
$P_{\text{EB},b,t}$	Electricity demand of the electric boiler in building b at time step t	kW_{e}
$P_{\text{HP},b,t}$	Electricity demand of the heat pump in building b at time step t	kW_{e}
$P_{\text{CC},b,t}$	Electricity demand of the compression chiller in building b at time step t	kW_{e}
$P_{\text{PV},t}$	Electricity generated by all PV modules at time step t	kW_{e}
$P_{\text{ASHP},t}$	Electricity demand of air source heat pump at time step t	kW_{e}
$P_{\text{CC},t}$	Electricity demand of compression chiller in energy hub at time step t	kW_{e}
$P^{\theta}_{k,t}$	Auxiliary variable that takes the value of the electric power consumed if interval k is active	kW_{e}
Storage level variables		
$S_{\text{TES},b,t}$	State of charge of water buffer vessel in building b at time step t	–
$S_{\text{ACC},t}$	State of charge of accumulator tank at time step t	–
Temperature variables		
$T_{\text{netw,w},t}$	Temperature of the warm pipe at time step t	°C
$T_{\text{netw,c},t}$	Temperature of the cold pipe at time step t	°C
$\bar{T}_{\text{netw},t}$	Mean network temperature at time step t	°C
$T^{\theta}_{k,t}$	Variable that is forced to take the value of the mean network temperature is interval k is active	°C
ΔT_t	Network temperature increase at time step t	°C
Binary variables		
$\theta_{k,t}$	Binary variable that equals 1 if temperature interval k is active	–
$y_{\text{DRC},b,t}$	Binary variable that takes the value of 1 if direct cooling can be used in building b	–
$y_{\text{inc},t}$	Binary variable that becomes 1 if the mean network temperature is increased	–
$y_{\text{dec},t}$	Binary variable that becomes 1 if the mean network temperature is decreased	–

B.2 Decision variables improved optimization model

Table B.2: Decision variables included in the constructed optimization model.

Decision variable	Description	Unit
Thermal power variables		
$\dot{Q}_{\mathrm{h,HP},b,t}$	Heat produced by heat pump in building b at time step t	kW_{th}
$\dot{Q}_{\mathrm{h,BHP},b,t}$	Heat produced by booster heat pump in building b at time step t	kW_{th}
$\dot{Q}_{\mathrm{h,GB},b,t}$	Heat produced by gas boiler in building b at time step t	kW_{th}
$\dot{Q}_{\mathrm{c,CC},b,t}$	Cold produced by CC in building b at time step t	kW_{th}
$\dot{Q}_{\mathrm{c,DRC},b,t}$	Direct cooling provided in building b at time step t	kW_{th}
$\dot{Q}^{\mathrm{dch}}_{\mathrm{h,TES},b,t}$	Heat discharged from water buffer vessel in building b at time step t	kW_{th}
$\dot{Q}^{\mathrm{ch}}_{\mathrm{h,TES},b,t}$	Heat charged in water buffer vessel in building b at time step t	kW_{th}
$\dot{Q}^{\mathrm{ch}}_{\mathrm{res,BES},b,t}$	Residual thermal demand of building b at time step t	kW_{th}
$\dot{Q}^{\mathrm{ch}}_{\mathrm{res,netw},t}$	Residual network demand at time step t	kW_{th}
$\dot{Q}_{\mathrm{loss,wp},t}$	Heat losses from the warm pipe at time step t	kW_{th}
$\dot{Q}_{\mathrm{loss,cp},t}$	Heat losses from the cold pipe at time step t	kW_{th}
$\dot{Q}_{\mathrm{netw},t}$	Thermal power to raise or lower the network temperature at time step t	kW_{th}
$\dot{Q}_{\mathrm{h,SWTE},t}$	Heat produced by SWTE at time step t	kW_{th}
$\dot{Q}_{\mathrm{c,SWTE},t}$	Cold produced by SWTE at time step t	kW_{th}
$\dot{Q}_{\mathrm{h,ATES},t}$	Heat produced by ATES at time step t	kW_{th}
$\dot{Q}_{\mathrm{c,ATES},t}$	Cold produced by ATES at time step t	kW_{th}
Electric power variables		
$P_{\mathrm{HP},b,t}$	Electric power required by the heat pump in building b at time step t	kW_{e}
$P_{\mathrm{BHP},b,t}$	Electric power required by the heat pump in building b at time step t	kW_{e}
$P_{\mathrm{CC},b,t}$	Electric power required by the compression chiller in building b at time step t	kW_{e}
$P_{\mathrm{BES},b,t}$	Electricity demand of building energy system in building b at time step t	kW_{e}
$P_{\mathrm{el,grid},t}$	Power extracted from the electricity grid at time step t	kW_{e}
$P_{\mathrm{netw},t}$	Electric power required by distribution network at time step t	kW_{e}
Temperature variables		
$T_{\mathrm{netw,w},t}$	Temperature of the warm pipe at time step t	°C
$T_{\mathrm{netw,c},t}$	Temperature of the cold pipe at time step t	°C
$\bar{T}_{\mathrm{netw},t}$	Mean network temperature at time step t	°C
$T^{\theta}_{k,t}$	Variable that is forced to take the value of the mean network temperature is interval k is active	°C
ΔT_t	Network temperature increase/decrease at time step t	°C
Binary variables		
$\theta_{k,t}$	Binary variable that equals 1 if temperature interval k is active	–
$y_{\mathrm{DRC},b,t}$	Binary variable that takes the value of 1 if direct cooling can be used in building b	–
$x_{\mathrm{HE},t}$	Binary variable for heat extraction by SWTE system	–
$x_{\mathrm{CE},t}$	Binary variable for cold extraction by SWTE system	–
$y_{\mathrm{ATES,h},t}$	Binary variable for heat extraction from groundwater in ATES	–
$y_{\mathrm{ATES,c},t}$	Binary variable for cold extraction from groundwater in ATES	–
Other variables		
C_k	Annualized costs for technology k	€
I_k	Investment costs for technology k	€
cap_k	Installed capacitiy of technology k	kW
$SoC_{\mathrm{TES},b,t}$	State of charge of water buffer vessel in building b at time step t	–
$\dot{V}_{\mathrm{hc},t}$	Pumping rate from hot to cold well in ATES system at time step t	m^3/s
$\dot{V}_{\mathrm{ch},t}$	Pumping rate from cold to hot well in ATES system at time step t	m^3/s
n_{doublets}	Integer variable that denotes the number of ATES doublets	–
$E_{\mathrm{hw},t}$	Heat stored in hot well ATES at times step t	kWh
$E_{\mathrm{cw},t}$	Cold stored in hot well ATES at times step t	kWh
$V_{\mathrm{hw},t}$	Usable volume of stored water in hot well ATES at times step t	m^3
$V_{\mathrm{cw},t}$	Usable volume of stored water in cold well ATES at times step t	m^3

C Input parameters

C.1 Technical parameters

The technical parameters considered in the improved optimization model are presented in this section. The COPs of the HPs, BHPs and CCs were determined using a model proposed by Jensen et al. (2018). The pinch point temperature differences (ΔT_{pp}), isotropic efficiencies of the compressors ($\eta_{is,c}$) and compressors heat losses (f_Q) for the devices were adopted from Wirtz et al. (2020a) and presented in Table C.1.

Table C.1: Technical parameters for calculation of COPs of HPs, BHPs and CCs. Data retrieved from Wirtz et al. (2020a).

	$\eta_{is,c}$ [-]	f_Q [-]	ΔT_{pp} [K]
HP	0.80	0.1	2
BHP	0.80	0.1	2
CC	0.75	0.1	2

Furthermore, a constant conversion efficiency (η_{GB}) of 0.91 is assumed for the gas boilers installed in poorly installed buildings (PBL, 2021a). The minimum temperature difference across the heat exchangers ($\Delta T_{HEX,min}$) is assumed to be 1 K. Regarding the water buffer vessels in the BESs, charging and discharging efficiencies (η_{TES}^{ch} and η_{TES}^{disch}) of 0.95 are considered. Moreover, a loss factor ($\phi_{TES,loss}$) of 0.005 is used (Wirtz et al., 2020a). For the specific energy use of the ATES and SWTE systems (e_{ATES} and e_{SWTE}) values of respectively 0.025 and 0.017 GJ_e/GJ_{th} are considered (PBL, 2021a).

C.2 Economic parameters

The economic parameters of the generation and storage devices considered in the EH and BESs are presented in Table C.2. The capital recovery factors (a_{inv}) for the devices k were calculated based on the service life (t_L) on the respective device and an interest rate (r) of 3% using:

$$a_{\text{inv},k} = \frac{r}{1-(1+r)^{-t_L}} \quad \forall\, k \in K \tag{134}$$

As described in section 3.3, the fixed and specific investment costs for ATES, SWTE and HP were retrieved from a Waternet database. The plots with corresponding trendlines are presented in Figure C.1.

Table C.2: Economic parameters for the generation and storage devices considered in the energy hub and building energy systems.

Parameter	**Symbol**	**HP**	**BHP**	**CC**	**DRC**	**GB**	**TES**	**ATES**	**SWTE**	**Unit**
Specific investment costs	i_{var}	236 [a]	1000 [a]	160 [b]	50 [b]	68 [b]	15.6 [a]	279 [a]	142 [a]	€/kW
Fixed investment costs	i_{fixed}	28 [a]	-	-	-	-	-	101 [a]	56 [a]	k€
Service life	T_L	20 [b]	20 [b]	15 [b]	30 [b]	20 [b]	30 [a]	30 [c]	15 [d]	years
Capital recovery factor	a_{inv}	6.72	6.72	8.38	5.10	6.72	5.10	5.10	8.38	%
Share for O&M	f_{om}	3.50 [e]	3.50 [e]	3.50 [b]	3.00 [b]	3.00 [b]	0.50 [a]	2.00 [e]	3.00 [e]	%

Note. Data are from Waternet database ([a]), Wirtz et al. (2020a) ([b]) , Sommer et al. (2015b) ([c]), Mol et al. (2021) ([d]), PBL (2021a) ([e]).

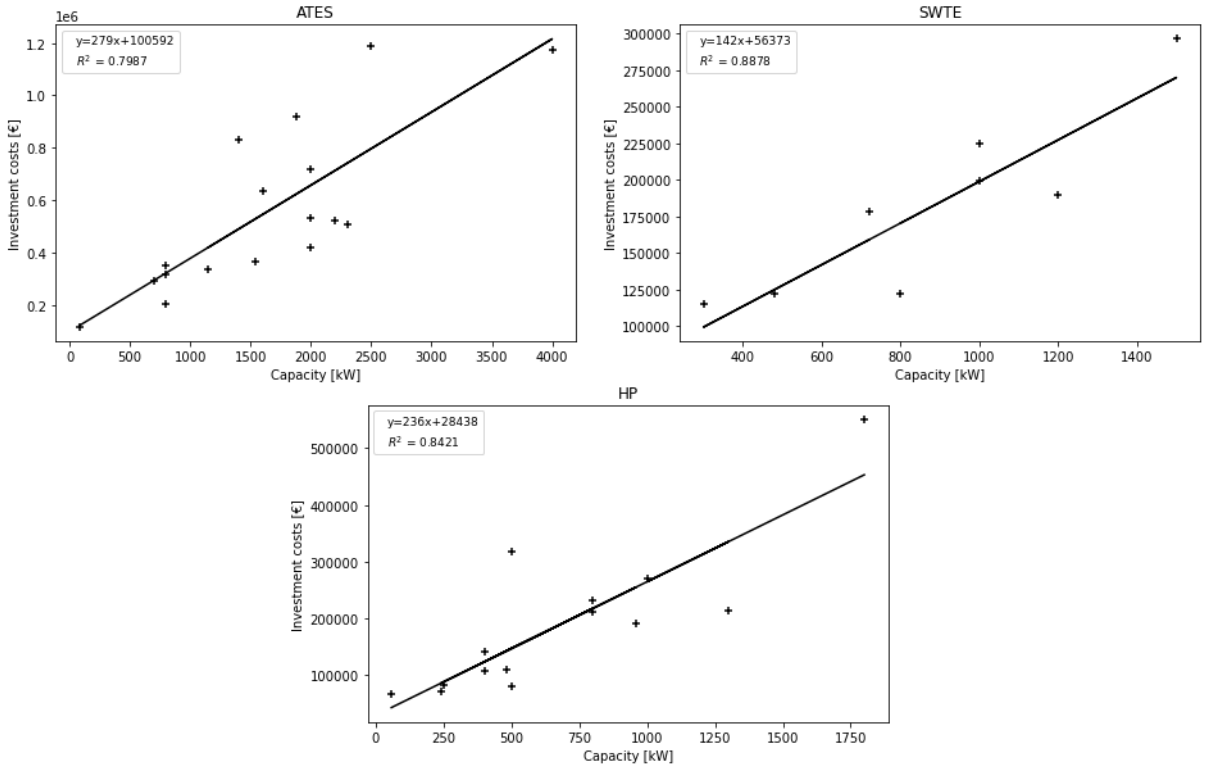

Figure C.1: Plots with corresponding trendlines used to determine specific and fixed investment costs for ATES, SWTE and HP. Retrieved from Waternet database.

For the internal distribution pipes (IDPs) in buildings, investment costs of €500 per meter are considered (Waternet Database). It is assumed that five meters of IDPs are required for each individual dwelling in poorly insulated buildings. In well insulated buildings, ten meters of IDPs are required per dwelling. This is because space heating and DHW are supplied at the same temperature in poorly insulated buildings, while the temperatures differ in well insulated buildings. For the same reason, two internal hydraulic pumps (IHPs) need to be installed in well insulated buildings. Investment costs of €5000 are used for the IHPs (Waternet Database). Furthermore, the heat interference units (HIUs) differ in poorly and well insulated buildings. Investment costs of €1500 and €2000 per individual dwelling are used for poorly and well insulated buildings respectively (Waternet Database). The service lives, capital recovery factors and shares for OM for the IDPs, IHPs and HIUs are presented in Table C.3.

Table C.3: Economic parameters for IDPs, IHPs and HIUs. Data retrieved from Waternet Database.

Parameter	**Symbol**	**IDP**	**IHP**	**HIU**	**Unit**
Service life	T_L	50	15	15	years
Capital recovery factor	a_{inv}	3.89	8.38	8.38	%
Share for O&M	f_{om}	0.50	3.00	2.50	%

C.3 Network infrastructure and heat losses

As described in section 2.1.2, the pressure drop in distribution pipes can be calculated using the Darcy-Weisbach equation (see Eq. 2). This equation can be used to determine the optimal inner pipe diameter. The recommended pressure drop is typically in the interval 50-200 Pa/m, while the friction factor lies between 0.015-0.04 (Roossien et al., 2020). Using these assumptions, it can be deduced that the optimal inner pipe diameter lies in the interval:

$$0.0361(\frac{P_{th}}{\Delta T_{netw}})^{0.4} \leq d_i \leq 0.0579(\frac{P_{th}}{\Delta T_{netw}})^{0.4} \tag{135}$$

In this research, it is assumed that the optimal diameter is equal to the mean of this interval. When the required thermal power and the temperature difference between the pipes are known, the pipe diameter can be determined for each segment in the distribution network. Subsequently, the optimal pipe type can be selected for each segment from Table C.4. This table contains the characteristic of the Prinspipe type 1 pipes made by manufacturer Weijers-Waalwijk (Weijers-Waalwijk, n.d.). After the network topology is defined, the thermal resistances of the insulated pipes and the soil can be determined for each network segment using Eqs. (5) and (6). Here, it is assumed that the distance between the surface and the centre of the distribution pipes is equal to one meter. Furthermore, a specific thermal conductivity of 1.5 $Wm^{-1}K^{-1}$ is assumed for the soil (Roossien et al., 2020). For the insulation pipes, a specific thermal conductivity of 0.426 $Wm^{-1}K^{-1}$ is used (Weijers-Waalwijk, n.d.). This value was provided by the manufacturer.

Table C.4: Prinspipe type 1 characteristics. Retrieved from: Weijers-Waalwijk (n.d.).

DN	d_i (mm)	D_i (mm)	D_o (mm)	Fluid volume (l/m)
20	21,70	27	90	0,37
25	28,50	34	90	0,67
32	37,20	42	110	1,09
40	43,10	48	110	1,46
50	54,50	60	125	2,33
65	70,30	76	140	3,88
80	82,50	89	160	5,35
100	107,10	114	200	9,01
125	132,50	140	225	13,79
150	160,30	168	250	20,18
200	210,10	219	315	34,67
250	263,00	273	400	54,33
300	312,70	324	450	76,80
350	344,40	356	500	93,16
400	393,80	406	560	121,80
450	444,60	457	630	155,25
500	495,40	508	710	192,75
600	595,80	610	800	278,80
700	695,00	711	900	379,37
800	795,40	813	1000	496,98
900	894,00	914	1100	627,22
1000	994,00	1016	1200	776,00

Next, the required pumping power can be calculated using Eq. (3). The pressure drop is calculated for each time-step using Eq. (2), while the volumetric flow through the pipes is determined using Eq. (1). Here, it is assumed that the efficiency of the electric motor and the pumping efficiency of the pump are 0.65 and 0.95 respectively (Roossien et al., 2020).

The investment costs for the network infrastructure comprise the costs for the distribution pipes, the costs for the hydraulic pumps and the costs for a technical area (TA). The investment costs for distribution pipes are determined by the costs for earth works and the costs for the pipes. For earth works, costs of €500 per meter are assumed (ENERGYMATTERS, 2017). The investment costs per pipe diameter are adopted from Wirtz et al. (2020a), yielding:

$$I_{\text{pipes}} = (500\,€/m + 2300\,€/m^3 * d_i^2) * L \tag{136}$$

Here, L represents the length of the pipe. Specific investment costs of 500 EUR/kW are used for the hydraulic pumps (Wirtz et al., 2020a). The investments costs for the pumps are therefore determined using:

$$I_{\text{pumps}} = 500\,€/kW cap_{\text{pumps}} \tag{137}$$

For the TA, fixed investment costs of €210.000 are used (Waternet database). Finally, the annualized costs for the distribution network are calculated using:

$$\mathrm{C_{netw}} = \mathrm{I_{pipes}}(a_{\text{inv,pipes}} + f_{\text{om,pipes}}) + \mathrm{I_{pumps}}(a_{\text{inv,pumps}} + f_{\text{om,pumps}}) + \mathrm{I_{TA}}(a_{\text{inv,TA}} + f_{\text{om,TA}}) \tag{138}$$

The economic parameters for the pipes and pumps are presented in Table C.5.

Table C.5: Economic parameters for the pipes and hydraulic pumps. Data retrieved from: Waternet database.

	Symbol	**Pipes**	**Pumps**	**TA**	**Unit**
Service life	t_L	50	15	50	years
Capital recovery factor	a_{inv}	3.89	8.38	3.89	%
Share for O&M	f_{om}	0.50	3.00	0.50	%

C.4 Case specific input parameters

The input parameters that are specific for the case study of the KNSM Island in Amsterdam are listed in this appendix. It was assumed that the temperature difference between the warm and cold pipe is 8 K (Roossien et al., 2020). Furthermore, a maximal network temperature ($\mathrm{T^{max}_{netw,wp}}$) of 22 °C and minimum network temperature ($\mathrm{T^{min}_{netw,cp}}$) of 4 °C were used. According to Gertjan de Joode, 12 °C is the minimum supply temperature at which heat pumps can operate efficiently (Appendix A.1). Considering a temperature difference of 8 K, the minimum network temperature was set at 4 °C. The maximum network temperature was based on the maximum temperature of the surface water of the case study and the temperature of the ATES system. Moreover, the temperature range was subdivided into 10 intervals k.

The distribution network topology was defined by identifying the minimum distance between two buildings. The ATES and SWTE systems were located between buildings 7 and 8 (see Figure 14). The pipe geometries and costs for the 5GDHC network are listed in Table C.6. The pipe diameters vary between 65 and 445 mm, while the total network length is 2.7 km. The heat loss coefficient is 7.5 kW/K.

Table C.6: Pipe geometries and costs 5GDHC network.

DN	d_i (mm)	L (m)	V [m^3]	kA [$\frac{kW}{k}$]	I_{pipes} [k€]	C_{pipes} [$\frac{k€}{a}$]
40	43	264	0,4	0,38	133	5,8
50	55	60	0,1	0,09	30	1,3
65	70	12	0,0	0,02	6	0,3
80	83	24	0,1	0,04	12	0,5
100	107	388	3,5	0,74	204	9,0
125	133	24	0,3	0,05	13	0,6
150	160	12	0,2	0,03	7	0,3
200	210	344	11,9	0,85	207	9,1
250	263	982	53,3	2,54	647	28,4
300	313	640	49,2	1,80	464	20,4
350	344	60	5,6	0,17	46	2,0
400	394	80	9,7	0,24	69	3,0
	SUM	2890	134,5	6,96	1839	80,7

Regarding the ATES system, a temperature difference between the hot and cold wells (ΔT_{hc}) of 6 K was assumed (Appendix A.1). The maximum temperature of the hot wells ($T_{ATES,hw}$) was set at 25 °C. Furthermore, a maximum allowable flow rate per well ($\dot{V}_{max,doublet}$) of 250 m^3/h was considered. This value is based on ATES systems already installed in Amsterdam (van den Kieboom, 2009).

The characteristics of the 15 buildings that were taken into consideration in the case study are presented in Table C.7. The energy labels of the buildings were provided by consultancy company Resourcefully. Buildings with energy label B were considered well insulated buildings, while buildings with energy label G were considered poorly insulated. In poorly insulated buildings, it was assumed that space heating and DHW are supplied at 65 °C. The return temperature is assumed to be 35 °C. Furthermore, it was assumed that the supply and return temperatures of the heating circuits in well insulated buildings are respectively 55 °C and 30 °C. DHW is supplied at 70 °C. Regarding cooling, supply and return temperatures of respectively 16 °C and 20 °C were considered.

Table C.7: Characteristics of buildings considered in the case study.

Building	Dwellings	Energy label	Space heating		DHW		Cooling	
			Demand [MWh/a]	Peak [kW]	Demand [MWh/a]	Peak [kW]	Demand [MWh/a]	Peak [kW]
1	68	G	342	368	139	36	3	66
2	25	B	78	104	51	13	5	133
3	100	B	828	873	204	52	21	455
4	52	B	340	405	106	27	11	254
5	52	B	416	496	106	27	11	254
6	52	B	392	468	106	27	11	254
7	27	B	203	253	55	14	6	135
8	225	B	1690	1393	459	118	46	949
9	27	B	233	290	55	14	6	137
10	36	B	230	291	74	19	7	180
11	12	G	69	94	25	6	1	15
12	331	B	1468	1250	676	173	68	1460
13	8	G	350	478	16	4	1	10
14	320	B	2582	2158	653	167	66	1399
15	29	G	66	82	59	15	1	31

Furthermore, the maximum allowable share of heat that can be supplied by the GBs ($f_{GB,max}$) in poorly insulated buildings was set at 20%. The electricity and gas prices considered in this research are respectively 0.145 €/kWh and 0.774 €/m^3 (PBL, 2020). Energy taxes were excluded.

D Assessment of techno-economic feasibility

D.1 Optimization model conventional DH system

The constructed optimization model for the conventional DH system operating at 70 °C is presented in this section. The model attributes scope, objective function, variable set and model structure are discussed in the following.

Model scope

The constructed LP model aims at determining the optimal design and operation of the ATES, SWTE, central HP and central TES considered in the conventional DH system. As in the optimization model constructed for the 5GDHC system, the duration of the time steps is 1 hour. The model is based on time series for one year.

The central HP is used to supply heat to the distribution network that operates at 70 °C. HIUs are used to transfer heat from the distribution network to the heat supply systems of the individual dwellings. The heat from the distribution network is used to provide both space heating and DHW. The return temperature is 40 °C. The heat required by the central HP is delivered by the ATES and SWTE systems. The SWTE system can supply heat at times of surface water temperature above 15 °C. The ATES system is used to overcome the temporal mismatch between supply and demand. Furthermore, the central TES can be used to lower the required capacities for the ATES and SWTE systems and the central HP. ACs in individual dwellings are used to supply cooling.

Objective function

The constructed LP model aims at minimizing the TAC for the conventional DH system. The TAC includes the annualized costs for the different components of the system as well as the annual costs for gas and electricity. The objective function is therefore:

$$TAC = C_{\text{SWTE}} + C_{\text{ATES}} + C_{\text{HP}} + C_{\text{TES}} + C_{\text{BES}} + C_{\text{gas}} + C_{\text{el}} \tag{139}$$

The costs for the network infrastructure are determined by the costs for the distribution, pipes, the hydraulic pumps and a technical area. The network infrastructure costs were calculated using the method presented in Appendix C.2.

Variable set

The variable set included in the LP optimization model are presented in Table D.1.

Model structure

The constraints included in the LP model are discussed in this section. The constraints are classified in five categories: energy balances, SWTE, ATES, heat losses and costs. The constraints in each category are described below, with decision variables written in italics.

Table D.1: Decision variables included in the constructed optimization model for the conventional DH system operating at 70 °C.

Decision variable	Description	Unit
Thermal power variables		
$\dot{Q}_{\text{h,HP},b,t}$	Heat produced by central heat pump at time step t	kW_{th}
$\dot{Q}_{\text{loss,rp},t}$	Heat losses from the return pipe at time step t	kW_{th}
$\dot{Q}_{\text{loss,sp},t}$	Heat losses from the supply pipe at time step t	kW_{th}
$\dot{Q}^{\text{dch}}_{\text{h,TES},b,t}$	Heat discharged from central TES at time step t	kW_{th}
$\dot{Q}^{\text{ch}}_{\text{h,TES},b,t}$	Heat charged in central TES at time step t	kW_{th}
$\dot{Q}_{\text{h,SWTE},t}$	Heat produced by SWTE at time step t	kW_{th}
$\dot{Q}_{\text{c,SWTE},t}$	Cold produced by SWTE at time step t	kW_{th}
$\dot{Q}_{\text{h,ATES},t}$	Heat produced by ATES at time step t	kW_{th}
$\dot{Q}_{\text{c,ATES},t}$	Cold produced by ATES at time step t	kW_{th}
$\dot{Q}_{\text{c,AC},b,t}$	Cold produced by air conditioner in building b at time step t	kW_{th}
Electric power variables		
$P_{\text{HP},t}$	Electric power required by the central heat pump at time step t	kW_{e}
$P_{\text{ATES},t}$	Electric power required by the ATES at time step t	kW_{e}
$P_{\text{SWTE},t}$	Electric power required by the SWTE system at time step t	kW_{e}
$P_{\text{AC},t}$	Electric power required by the air conditioners at time step t	kW_{e}
$P_{\text{el,grid},t}$	Power extracted from the electricity grid at time step t	kW_{e}
$P_{\text{netw},t}$	Electric power required by distribution network at time step t	kW_{e}
Binary variables		
$x_{\text{HE},t}$	Binary variable that equals 1 if surface water temperature exceeds 15 °C	–
$y_{\text{ATES,c},t}$	Binary variable that equals 1 if heat can be charged into ATES system	–
Other variables		
$SoC_{\text{TES},b,t}$	State of charge of central TES at time step t	–
cap_k	Installed capacity of technology k	kW
$\dot{V}_{\text{SWTE},t}$	Pump flow rate SWTE installation at time step t	m^3/s
$\dot{V}_{\text{hc},t}$	Pumping rate from hot to cold well in ATES system at time step t	m^3/s
$\dot{V}_{\text{ch},t}$	Pumping rate from cold to hot well in ATES system at time step t	m^3/s
n_{doublets}	Integer variable that denotes the number of ATES doublets	–
$E_{\text{hw},t}$	Heat stored in hot well ATES at times step t	kWh
$E_{\text{cw},t}$	Cold stored in hot well ATES at times step t	kWh
C_k	Annualized costs for technology k	€
I_k	Investment costs for technology k	€

Energy balances

Five thermal energy balances are introduced in the optimization model. The first thermal energy balance ensures that the heat output of the central HP is equal sum of the cummulated demands of the buildings for space heating and DHW and the net thermal output of the central TES:

$$\dot{Q}_{\text{h,HP},t} = \sum_{b\ inB} (\dot{\text{Q}}_{\text{h,dem,sh},b,t} + \dot{\text{Q}}_{\text{h,dem,DHW},b,t}) + \dot{Q}_{\text{loss,sp},t} + \dot{Q}_{\text{loss,rp},t} + \dot{Q}^{\text{ch}}_{\text{h,TES},t} - \dot{Q}^{\text{disch}}_{\text{h,TES},t} \quad \forall\, t \in T \tag{140}$$

The second thermal energy balances ensures that the heat required by the central HP is met by the ATES and SWTE systems:

$$\dot{Q}_{\mathrm{h,HP},t} - P_{\mathrm{HP},t} = \dot{Q}_{\mathrm{h,ATES},t} + \dot{Q}_{\mathrm{h,SWTE},t} \quad \forall\, t \in T \tag{141}$$

In order to ensure that the SoC of the central TES is connected with the SoC of the previous time step, a third thermal energy balance is introduced:

$$\begin{aligned} SoC_{\mathrm{TES},t} cap_{\mathrm{TES},b} = SoC_{\mathrm{TES},t-1} cap_{\mathrm{TES}} (1 - \phi_{\mathrm{TES,loss}}) \\ + \eta^{\mathrm{ch}}_{\mathrm{TES}} \dot{Q}^{\mathrm{ch}}_{\mathrm{h,TES},t} - \frac{\dot{Q}^{\mathrm{disch}}_{\mathrm{h,TES},t}}{\eta^{\mathrm{disch}}_{\mathrm{TES}}} \quad \forall\, t \in T \;:\; t \neq t_0 \end{aligned} \tag{142}$$

Furthermore, the SoC of the central TES must be between a lower and an upper limit. This is ensured by the constraint:

$$SoC^{\mathrm{min}}_{\mathrm{TES}} \leq SoC_{\mathrm{TES},t} \leq SoC^{\mathrm{max}}_{\mathrm{TES}} \quad \forall\, t \in T \tag{143}$$

The final thermal energy balance ensures that the cooling demand of the buildings is met by the ACs installed in individual dwellings:

$$\dot{Q}_{\mathrm{c,AC},b,t} = \dot{\mathrm{Q}}_{\mathrm{c,dem},b,t} \quad \forall\, b \in B,\, t \in T \tag{144}$$

In addition, a constraint is introduced that describes the electric energy balance. The electric power imported from the grid at time step t is equal to the sum of the power required by the central HP, the ACs, the ATES and SWTE system and the distribution grid:

$$P_{\mathrm{el,grid},t} = P_{\mathrm{HP},t} + P_{\mathrm{AC},t} + P_{\mathrm{SWTE},t} + P_{\mathrm{ATES},t} + \mathrm{P}_{\mathrm{netw},t} \quad \forall\, t \in T \tag{145}$$

The power required by the central HP is dependent on the thermal output of the device and the COP. This is described by the constraint:

$$P_{\mathrm{HP},t} = \frac{\dot{Q}_{\mathrm{h,HP},t}}{\mathrm{COP}_{\mathrm{HP}}} \quad \forall\, t \in T \tag{146}$$

The COP of the HP is determined using the model presented by Jensen et al. (2018). Consequently, the electric power required by the ACs installed in individual dwellings is dependent on the amount of cooling supplied by the ACs and the COP:

$$P_{\mathrm{AC},t} = \frac{\sum_{b \in B} \dot{Q}_{\mathrm{c,AC},b,t}}{\mathrm{COP}_{\mathrm{AC}}} \quad \forall\, t \in T \tag{147}$$

Here, it is assumed that the COP of the AC is constant throughout the year.

SWTE

The maximum allowable temperature change of the surface water and the pump flow rate determine the amount of heat that can be extracted by the SWTE system:

$$\dot{Q}_{\mathrm{h,SWTE},t} = \mathrm{c_w} \dot{V}_{\mathrm{SWTE},t} \Delta T_{\mathrm{HE},t} \quad \forall\, t \in T \tag{148}$$

with $\Delta T_{\mathrm{HE},t}$ being expressed by:

$$\Delta T_{\mathrm{HE},t} = max(min(\mathrm{T_{SW},}_t - \mathrm{T_{SW,min}}, \Delta \mathrm{T_{HE,max}}), 0) \quad \forall\, t \in T \tag{149}$$

Furthermore, heat can only be produced by the SWTE system when the temperature of the surface water exceeds 15 °C $\mathrm{T_{SW,HE,min}}$. To incorporate this into the optimization model, the binary variable $x_{\mathrm{HE},t}$ is introduced:

$$\mathrm{T_{SW,HE,min}} - \mathrm{T_{SW},}_t \leq (1 - x_{\mathrm{HE},t})\mathrm{M_{HE}} \quad \forall\, t \in T \tag{150}$$

where $\mathrm{M_{HE}}$ is a big-M coefficient. Moreover, the amount of heat that can be generated by the SWTE system is limited by its capacity and by the thermal capacity of the surface water:

$$\dot{Q}_{\mathrm{h,SWTE},t} \leq cap_{\mathrm{SWTE}} x_{\mathrm{HE},t} \quad \forall\, t \in T \tag{151}$$

$$\sum_{t \in T} \dot{Q}_{\mathrm{h,SWTE},t} \leq \mathrm{E_{h,SW}} \tag{152}$$

Finally, the electricity demand of the SWTE system is dependent on the thermal energy production. This is expressed by the constraint:

$$P_{\mathrm{SWTE},t} = e_{\mathrm{SWTE}}(\dot{Q}_{\mathrm{h,SWTE},t} + \dot{Q}_{\mathrm{c,SWTE},t}) \quad \forall\, t \in T \tag{153}$$

ATES

Just like in the model developed for the 5GDHC system, the thermal heating and cooling power retrieved from the groundwater in the ATES system are dependent on the pumping flow rates of the ATES wells and the temperature difference between the hot and cold wells ($\Delta \mathrm{T_{hc}}$):

$$\dot{Q}_{\mathrm{h,ATES},t} = c_w \dot{V}_{\mathrm{hc},t} \Delta \mathrm{T_{hc}} \quad \forall\, t \in T \tag{154}$$

$$\dot{Q}_{\mathrm{c,ATES},t} = c_w \dot{V}_{\mathrm{ch},t} \Delta \mathrm{T_{hc}} \quad \forall\, t \in T \tag{155}$$

It is assumed that $\Delta \mathrm{T_{hc}}$ is constant. The pumping flow rates of the hot and cold wells are limited by the maximum allowable flow rate per doublet:

$$\dot{V}_{\mathrm{hc},t} \leq n_{\mathrm{doublets}} \dot{\mathrm{V}}_{\mathrm{max,doublet}} \quad \forall\, t \in T \tag{156}$$

$$\dot{V}_{\mathrm{ch},t} \leq n_{\mathrm{doublets}} \dot{\mathrm{V}}_{\mathrm{max,doublet}} \quad \forall\, t \in T \tag{157}$$

where n_{doublets} is an integer variable that denotes the number of doublets installed.

The amount of heat and cold stored in the ATES wells is connected with the amount of thermal energy stored in the previous time step. This is ensured by the constraints:

$$E_{\mathrm{hw},t} = E_{\mathrm{hw},t-1} - \dot{Q}_{\mathrm{h,ATES},t} + \dot{Q}_{\mathrm{c,ATES},t} \quad \forall\, t \in T : t \neq t_0 \tag{158}$$

$$E_{\mathrm{cw},t} = E_{\mathrm{cw},t-1} - \dot{Q}_{\mathrm{c,ATES},t} + \dot{Q}_{\mathrm{h,ATES},t} \quad \forall\, t \in T : t \neq t_0 \tag{159}$$

Furthermore, thermal balancing of the ATES system is ensured is ensured by the constraint:

$$\sum_{t \in T} \dot{Q}_{\mathrm{h,ATES},t} = \sum_{t \in T} \dot{Q}_{\mathrm{c,ATES},t} \tag{160}$$

In the conventional DH system, heat can only be charged into the ATES at times that the temperature of the surface water exceeds the temperature of the hot well. The minimum temperature differences across the heat exchangers of the ATES and SWTE systems should be taken into account here. This is described by the constraint:

$$\mathrm{T_{ATES,hw}} + 2\Delta\mathrm{T_{HEX,min}} - \mathrm{T_{SW},}_t \leq (1 - y_{\mathrm{ATES,c},t})\mathrm{M_{ATES,c}} \quad \forall\, t \in T \tag{161}$$

Here, $y_{\mathrm{ATES,c},t}$ is a binary variables that is forced to be 1 if heat can be charged into the ATES. $\mathrm{M_{ATES,c}}$ is a big-M coefficient.

The thermal heating and cooling power delivered by the ATES system is limited by its thermal capacity. Furthermore, the cooling power equals 0 at times when the binary variables equal zero. This is ensured by the constraints:

$$\dot{Q}_{\mathrm{h,ATES},t} \leq \mathrm{cap_{ATES}} \quad \forall\, t \in T \tag{162}$$

$$\dot{Q}_{\mathrm{c,ATES},t} \leq \mathrm{cap_{ATES}} y_{\mathrm{ATES,c},t} \quad \forall\, t \in T \tag{163}$$

Finally, the electricity demand of the ATES system is determined by the heating and cooling power of the system:

$$P_{\mathrm{ATES},t} = e_{\mathrm{ATES}}(\dot{Q}_{\mathrm{h,ATES},t} + \dot{Q}_{\mathrm{c,ATES},t}) \quad \forall\, t \in T \tag{164}$$

Heat losses

The thermal heat flow between the distribution pipes and the soil are determined using Eq. 4. The heat losses from the supply and return pipe are therefore calculated using:

$$\dot{Q}_{\mathrm{loss,sp},t} = \sum_{s \in S} \frac{(T_{\mathrm{netw,sp}} - \mathrm{T_{soil},}_t)}{\mathrm{R_{i},}_s + \mathrm{R_{s},}_s} \quad \forall\, t \in T \tag{165}$$

$$\dot{Q}_{\mathrm{loss,rp},t} = \sum_{s \in S} \frac{(T_{\mathrm{netw,rp}} - \mathrm{T_{soil},}_t)}{\mathrm{R_{i},}_s + \mathrm{R_{s},}_s} \quad \forall\, t \in T \tag{166}$$

As the network topology is defined prior the optimization, the thermal resistances of the distribution pipes and the soil of the network segments s are constants. An elaboration on the calculations is provided in Appendix C.3.

Costs calculation

The annualized costs for the BESs are dependent on the annualized investment costs and the annual operation and maintenance costs for the ACs, HIUs, internal distribution pipes (IDPs) and internal hydraulic pumps (IHPs). The annualized costs for the BESs is therefore expressed by the constraint:

$$\begin{aligned} C_{\mathrm{BES}} = I_{AC}(a_{\mathrm{inv,AC}} + f_{\mathrm{om,AC}}) + I_{\mathrm{IDP}}(a_{\mathrm{inv,IDP}} + f_{\mathrm{om,IDP}}) + I_{\mathrm{IHP}}(a_{\mathrm{inv,IHP}} + f_{\mathrm{om,IHP}}) + \\ I_{\mathrm{HIU}}(a_{\mathrm{inv,HIU}} + f_{\mathrm{om,HIU}}) \end{aligned} \tag{167}$$

An elaboration on the calculation of the investment costs for the ACs, HIUs, IDPs and IHPs is provided in Appendix D.2.

The annualized costs for the central HP, central TES, ATES and SWTE system are determined using the constraints:

$$C_k = I_k(a_{\text{inv,k}} + f_{\text{om,k}}) \quad \forall\, k \in K \tag{168}$$

$$I_k = i_k cap_k \quad \forall\, k \in K \tag{169}$$

For the central HP, ATES and SWTE, cap_k denotes the rated thermal power. For the central TES, cap_k represents the storage capacity.

The annualized costs for the network infrastructure consists of annualized costs for the distribution pipes, hydraulic pumps and a technical area. An elaboration on the calculation of the investment costs for the different components of the network infrastructure is provided in Appendix C.3.

Finally, the annual costs for gas (C_{gas}) is calculated by multiplying the total amount of gas imported from the grid by the gas price:

$$\text{C}_{\text{gas}} = \sum_{t \in T} \dot{G}_{\text{grid},t}\, p_{\text{gas}} \tag{170}$$

Accordingly, the annual costs for electricity is determined using:

$$\text{C}_{\text{el}} = \sum_{t \in T} P_{\text{el,grid},t}\, p_{\text{el}} \tag{171}$$

D.2 Input parameters assessment of techno-economic feasibility

The technical, economic and environmental input parameters used during the third research phase are presented in this section. Firstly, the input parameters used in the optimization model for the conventional DH system are provided. The input parameters used for the calculation of the performance indicators are provided next.

Input parameters optimization model conventional DH system

The COP of the central HP is determined using the model proposed by Jensen et al. (2018). The same pinch point temperature difference, isotropic efficiency and compressor heat losses are used a in the optimization model for 5GDHC system (see Table C.1). For the ACs installed in individual dwellings, a COP of 3.5 is used (PBL, 2021a). The minimum temperature difference across heat exchanger is assumed to be 1 K. Regarding the central HP, central TES, ATES and SWTE, the same economic and technical input parameters are used as in the optimization model for 5GDHC systems. Furthermore, the same electricity and natural gas prices are considered.

The investment costs for the IDPs in buildings were determined using investment costs of €500 per meter (Waternet database). It is assumed that each individual dwelling required 5 meters of IDPs. Furthermore, one IHP is required in each apartment building. Investment costs of €5000 per pump are considered (Waternet database). For the HIUs, investment costs of €1500 per individual dwelling are used (Waternet database). The services lives, capital recovery factors and shares for OM are presented in Table C.3. For the ACs in individual dwellings, investment costs of €1680 are used. The services live, capital recovery factor and share for OM for the ACs is presented in Table D.3.

Table D.2: Pipe geometries and costs conventional DH network.

DN	d_i (mm)	L (m)	V [m^3]	kA [$\frac{kW}{k}$]	I_{pipes} [k€]	C_{pipes} [$\frac{k€}{a}$]
40	43	264	0,4	0,4	133	5,8
50	55	12	0,0	0,0	6	0,3
65	70	36	0,1	0,1	18	0,8
80	83	400	2,1	0,7	206	9,1
100	107	12	0,1	0,0	6	0,3
125	133	184	2,5	0,4	99	4,4
150	160	662	13,4	1,5	370	16,2
200	210	1120	38,8	2,8	674	29,6
250	263	140	7,6	0,4	92	4,1
	SUM	2830	65,1	6,2	1606	70,5

The pipe geometries and costs for the conventional DH network are listed in Table D.2. The pipe diameters vary between 65 and 250 mm. The total network length is 2.8 km and the heat loss coefficient is 6.2 kW/K.

Input parameters used for calculation of performance indicators

In the reference scenario with stand-alone natural gas installations, each individual dwelling requires a GB and a AC. The investment costs for the devices were calculated by multiplying the specific investment costs by the number of individual dwellings. The specific investment costs, services lives, capital recovery factors and shares for O&M for the GBs and ACs are presented in Table D.3.

Table D.3: Economic parameters for GBs and ACs. Data retrieved from PBL (2021a).

Parameter	Symbol	GB	AC	Unit
Specific investment costs	i	1780	1680	€/dwelling
Service life	T_L	15	15	years
Capital recovery factor	a_{inv}	8.38	8.38	%
Share for O&M	f_{om}	4.00	7.00	%

For the calculation of the PER for the three heating and cooling concepts, PEF of 0.65 and 1.10 GJ_{pr}/GJ_{final} were used for electricity and natural gas respectively (Blok & Nieuwlaar, 2016; PBL, 2020). Furthermore, an EF of 0.12 $kg\ CO_2/kWh$ was used for electricity (PBL, 2020). For natural gas, an EF of 56.40 $kg\ CO_2/GJ$ was considered.